The study of MxB subcellular localization at different stages of cell cycle

Yishi Lin

Lady Davis Institute at Jewish General Hospital

Department of Microbiology and Immunology

McGill University

August 2021

A thesis submitted to McGill University in partial fulfillment

of the requirements of the degree of *Master of Science*

TABLE OF CONTENT

LIST OF FIGURES

Abstract

Human myxovirus resistance protein B (MxB, also known as Mx2) is a member of the dynamin-like GTPase family, induced by type-I interferon, and inhibits both DNA (e.g. Herpesviruses) and RNA viruses (e.g., HIV-1). MxB was reported to localize to the nuclear pore complex (NPC) on the nuclear envelope, in the cytoplasm, and shuttle between the nucleus and the cytoplasm. Recently, MxB was reported to localize in the mitochondria and play an essential role in mitochondria DNA stability, suggesting that MxB performs multiple functions. The aim of my project is to elucidate the dynamics of MxB localization during mitosis when the nuclear envelope breaks down. We hypothesize that MxB may maintain its association with components of NPC during mitosis and return to the NPC when the nuclear envelope is re-assembled at the end of mitosis. To test this hypothesis, we used the CRISPR-Cas9 technology to generate MxB-RFP knock-in cell clones, to facilitate the tracking of endogenous MxB in live cells during mitosis. The results of confocal microscopy confirmed MxB localization to the nuclear envelope at interphase. MxB begins to aggregate in the late prophase likely when the centrosome also starts to form. While NPC proteins NUP98, NUP214 and NUP358 have been reported to associate with MxB, none of these three nucleoporins co-localize with MxB during mitosis, suggesting that MxB is recruited to centrosome by a centrosome factor to be identified. To investigate whether MxB modulates centrosome function, we knocked down MxB with siRNA and observed abnormal alignment of chromosomes at metaphase. We have therefore discovered an important function of MxB during mitosis to ensure proper alignment and eventual faithful segregation of chromosomes by localizing to the centrosome during mitosis.

Résumé

La protéine B de résistance au myxovirus humain (MxB, également connue sous le nom de Mx2) est un membre de la famille des GTPases de type dynamine, induite par l'interféron de type I, et inhibe à la fois les virus à ADN (par exemple, les virus de l'herpès) et les virus à ARN (par exemple, le VIH-1). Il a été rapporté que MxB se localisait dans le complexe de pores nucléaires (NPC) sur l'enveloppe nucléaire, dans le cytoplasme, et faisait la navette entre le noyau et le cytoplasme. Récemment, il a été rapporté que MxB se localisait dans les mitochondries et jouait un rôle essentiel dans la stabilité de l'ADN des mitochondries, suggérant que MxB remplit de multiples fonctions. Le but de mon projet est d'élucider la dynamique de localisation de MxB au cours de la mitose lorsque l'enveloppe nucléaire se rompt. Nous émettons l'hypothèse que MxB peut maintenir son association avec les composants du NPC pendant la mitose et revenir au NPC lorsque l'enveloppe nucléaire est réassemblée à la fin de la mitose. Pour tester cette hypothèse, nous avons utilisé la technologie CRISPR-Cas9 pour générer des clones de cellules knock-in MxB-RFP, afin de faciliter le suivi du MxB endogène dans les cellules vivantes pendant la mitose. Les résultats de la microscopie confocale ont confirmé la localisation de MxB dans l'enveloppe nucléaire à l'interphase. MxB commence à s'agréger à la fin de la prophase, probablement lorsque le centrosome commence également à se former. Alors qu'il a été rapporté que les protéines NPC NUP98, NUP214 et NUP358 s'associent à MxB, aucune de ces trois nucléoporines ne co-localise avec la -tubuline ni Aurora A pendant la mitose, ce qui suggère que MxB est recruté dans le centrosome par un facteur centrosome à identifier. Pour déterminer si MxB module la fonction centrosome, nous avons renversé MxB avec siRNA et observé un alignement anormal des chromosomes à la métaphase. Nous avons donc découvert une fonction importante de MxB pendant la mitose pour assurer un alignement correct et une éventuelle ségrégation fidèle des chromosomes en se localisant dans le centrosome pendant la mitose.

ACKNOWLEDGMENTS

My graduate study is full of challenges and exciting findings. The challenges start with the language barrier. Although I have taken the English IELTS test and gained a desirable score, it is still a big challenge in terms of listening and understanding in courses or seminars and ordinary writing. I like Canada and enjoy my graduate study here for its respect for others and our diversity. I made quite a lot of lovely friends from different countries or nations. Most importantly, I gain access to work and study with many talented people.

Firstly, I would like to thank my supervisor Dr. Chen Liang for having me in the lab where I can work with people with enthusiasm in viral research and have the chance to gain access to state-of-the-art facilities. I will never forget Dr. Chen Liang's guidance and support throughout the project. He encourages me to read the literature and do experiments independently. I am particularly impressed by his dedication to the research. He takes research seriously in the design of experiments, data collection and analysis, etc. Under Dr. Chen Liang's supervision, I developed critical thinking skills in research and took research more seriously, which will benefit my whole life.

Secondly, I would like to acknowledge the committee members, Dr. Andrew J Mouland and Dr. Rongtuan Lin, who gave me lots of suggestions in the experiment and help me gain insight into my project.

I got to work with many awesome people here, but it is impossible to list all of them here. I would like to especially appreciate Zhen Wang, Qinghua Pan, and Myles McLean, who answered numerous questions without reservation and help me a lot in daily life. Zhen Wang also designed and performed parts of the project.

Meanwhile, I would like to acknowledge the Department of Microbiology & Immunology, McGill University, and Mitacs and Ministère de l'Éducation for financial support. Without these supports, I won't be able to finish the project and get the degree.

WITH THANKS

To my advisory committee Dr. Liang, Dr. Andrew Mouland and Dr. Rongtuan Lin

To all past and present lab members in Dr. Chen Liang's lab including Zhen Wang, Saina Beitari, Myles McLean, Qinghua Pan, Zhenlong Liu, Magan Solomon, Ariana Arduini, Cynthia McMahan, Yimeng Wang and Cesar Collazos for experiments support, especially Zhen Wang.

To Cynthia McMahan for the precious result of the live-cell imaging

To Mathew Duguay and Christian Young for the training and technical support of confocal and flow cytometry.

To Myles McLean, Magan Solomon, Ariana Arduini and Chuhan Feng for advising and correction of the thesis and daily life correction of writing documents.

To Cesar Collazos for ordering reagents and daily maintaining of the daily work.

To my friend Xianglong Li, Jianbin Chen, Ziyang Zhang for the initial financial support.

Lastly to my friends, my brother, and my mother for their constant encouragement.

PREFACE

All of the work presented was conducted in Lady Davis Institute at Jewish General Hospital, McGill University. The thesis has followed the Library and Archives Canada requirement under the guidelines of Graduate and Postdoctoral Studies of McGill.

AUTHOR CONTRIBUTIONS

Dr. Chen Liang conceived the experiments and gave support to the candidate to design specific assays. The candidate performed the experiments, collected, and analyzed the data. Cynthia McMahan observed the phenotype of MxB localization to the centrosome. She and Zhen Wang performed immunofluorescence and live-cell image to confirm exogenously expressed MxB is localized at the centrosome. In the CRISPR-Cas9 experiments, Zhen Wang designed the gRNAs and donor DNA plasmids and generated WM115 RFP knock-in clones. The candidate generated HeLa RFP knock-in clone

LITTERATURE REVIEW AND INTRODUCTION

Since the discovery of HIV in the early 1990s, AIDS has claimed 34.7 million lives across the world, and 37.6 million people are still living with HIV-1. Instead of being a deadly acute disease, AIDS has become a manageable chronic health condition under systematic antiretroviral therapy (ART). Understanding the host and HIV-1 interaction is essential in developing vaccines and novel drugs for the control of AIDS. Innate immunity is the body's first line of defense against pathogens. HIV-1 infection initiates the signaling pathway to activate interferon production, which in return induces numerous ISGs some of which restrict HIV-1 infection. MxB was reported in 2013 to recognize HIV-1 capsid and inhibits the nuclear import of HIV-1 DNA. MxB is localized on the cytoplasmic face of the NPC. Recently, MxB was reported to localize in the mitochondria and play an essential role in mitochondria DNA stability. My project is to characterize the subcellular distribution of MxB during mitosis, with the goal of generating insights into its cellular and antiviral functions. As an introduction to my project, I will review the biology of HIV-1, host restriction factors including MxB, cell cycle including the centrosome and nuclear pore complexes.

1 HIV-1

1.1 History of HIV-1 discovery

AIDS was first reported in 1981 in San Francisco and New York City, where doctors found more than twenty previous healthy homosexual men contracted pneumonia, cancer (Kaposi's sarcoma), and multiple viral infections [1, 2]. They developed immune deficiency with no lymphocyte proliferative responses to antigens and it was not clear why this illness was preferentially developed in homosexuals [1, 2]. Three patients died in 1982, just a couple of months after these symptoms, and a decreasing number of T-lymphocytes and the occurrence of T-lymphocytes abnormalities were observed in two patients [3].

In most instances, patients were the first cases in their cities or states and had no

common medications or antecedent history of personal or family illness relevant to immune deficiency. The limited data posed a challenge for physicians to identify the agent responsible for the illness [4]. In 1982, a transfusion acquired case was reported in which an infant received blood products from 19 donors, who appeared well after discharge in hospital. Still, several months later, he developed AIDS-related symptoms with decreased number of T-lymphocytes and impaired T-cell function and finally died in August 1982. One of the 19 blood donors was diagnosed with AIDS, suggesting the cause underlying AIDS could be an infectious agent [4].

In 1983, L Montagnier's team at the Pasteur Institute in Paris identified a novel retrovirus distinct from each previous isolate as the causative pathogen of AIDS [5]. They cultured cells of biopsied lymph nodes from a 33-year-old homosexual man who developed AIDS-like symptoms, and reverse transcriptase activity was tested in supernatants after 15 days in the supernatants. It was the first study to report a virus as the infectious agent of AIDS. L Montagnier and his team member F Barré-Sinoussi (the first author) were awarded the 2008 Nobel Prize in Physiology or Medicine for their contribution to isolating the AIDS-causing pathogen.

In 1984, Robert Gallo's team at the National Cancer Institute in Bethesda, Maryland, isolated retroviruses belonging to the HTLV family from 48 patients with pre-AIDS, mothers of juveniles with AIDS, but no HTLV isolation from heterosexual individuals. In the same year, the third group, JA Levy et al., isolated infectious retroviruses from patients with AIDS in San Francisco. They detected HIV-1 specific antibodies in all AIDS patients and a high percentage in homosexual men [6]. In a short time, three independent research groups identified retroviruses as the AIDS-causing pathogen by different methods, suggesting the causal link between AIDS and retroviruses, and in 1986 the pathogen was named HIV-1.

AIDS has claimed 34.7 million lives across the world so far, according to WHO (https://www.who.int/news-room/fact-sheets/detail/hiv-aids) with an estimated 37.6 million people, especially in the African region, living with HIV-1. Under antiretroviral

therapy (ART), HIV-1 infection has become a manageable chronic health condition that is still a major global public issue.

1.2 HIV-1 evolution and classification

Human immunodeficiency virus (HIV) belongs to the genus Lentivirus, family Retrovirus. It has two types, HIV-1 and HIV-2, both of which result from multiple cross-species transmission of simian immunodeficiency viruses (SIV) from primates to humans [7, 8]. SIVs infect a wide range of monkeys or apes in South Africa, but most of them are nonpathogenic to their natural hosts [8]. HIV-2 was closely related to SIVsm isolated from sooty mangabey in the late 1980s [9, 10]. In 1999, Feng Gao et al. identified HIV-1 is closely related to SIVcpz isolated from common chimpanzees (Pan troglodytes) in West Africa [11]. Further research found that SIVcpz originated from recombination of SIVrcm, infecting red-capped mangabeys (Cercocebus torquatus), and SIVgsn, infecting greater spot-nosed monkeys (Cercopithecus nictitans) on which Chimpanzees prey [12]. SIVcpz was transferred to humans from the blood and/or body fluids of chimpanzees killed by humans or kept as pets in west-central Africa [8, 13].

HIV-1 is classified into four distinct groups, including M, N, O, and P, and each group resulted from different cross-species transmission events [8]. Group M was the first one discovered and has driven the global pandemic. The other groups account for less than 1% of infection and are restricted to specific regions [8]. Group M is further divided into 9 subtypes, A, B, C, D, F, G, H, J, and K. Subtypes A and D were discovered in central Africa, but it spread to eastern Africa. Subtype C was introduced to Asian countries, whereas subtype B accounts for most infections in Europe and America[8, 14].

1.3 Epidemiology

As of 2020, 76 million people have been infected with HIV, with approximately 36 million deaths across the world according to WHO (https://www.who.int/teams/global-hiv-hepatitis-and-stis-programmes/hiv/strategic-

information/hiv-data-and-statistics).

37.6 million people are still living with HIV at the end of 2020, with 1.5 million newly infected cases in 2020 globally. To end the HIV/AIDS epidemic, in December 2013, the UNAIDS Programmer Coordinating Board called on UNAIDS to launch an initiative: by 2020, 90% of the people living with HIV know their status, 90% of the people diagnosed with HIV receive sustained antiretroviral therapy, 90% of the people who received antiretroviral therapy will have viral suppression (https://www.unaids.org/en/resources/909090).

It is estimated that 84% of people living with HIV received the diagnosis and know their status; 73% of people with confirmed HIV infection received ART; 90% of those who received ART were virally suppressed. The newly infected cases fell by 30% between 2010 and 2020, and the AIDS-related deaths fell by 42%, showing the effectiveness of HIV treatment. HIV/AIDS was considered as a global pandemic [15], but currently, the WHO uses the term epidemic because this illness is manageable and has developed into a chronic health condition in which people can live long and healthy lives with HIV

The transmission routes of HIV include sexual contact, maternal-infant exposure, and percutaneous inoculation into blood [16]. Sexual contact transmission is achieved across mucosal or body fluids such as anal, rectal, vaginal, semen, or pre-semen fluids. Heterosexual spread is the main route of transmission in sub-Saharan Africa, while men's sex with men (MSM) contributes to most cases in other regions [16, 17]. Maternal-infant transmission is the primary transmission route. Children can get infected with HIV during pregnancy, childbirth, or breastfeeding through breast milk [18-20]. Percutaneous inoculation is another important transmission route that results from transfusion from donors infected with HIV or shared needles between drug users [21, 22].

1.4 Clinical symptoms, diagnosis and treatment.

The symptoms depend on the stage of infection. It was reported that almost one-fifth of people didn't have symptoms in primary infection, based on a study that attempted to systematically examine symptoms of acute HIV infection [23]. Therefore, many patients are unaware of their infection status until later stages when the immune system has been severely weakened. Most of those with clinical presentations develop influenza-like symptoms like fever, headache, and fatigue at the first stage because a burst of viral replication often occurs 2 to 4 weeks following infection [24]. At the second stage of disease, HIV still multiplies, but at a low level; thus, only minor symptoms are presented. At the third stage, also the last stage, the immune system is damaged. The symptoms may include fever, headache, swollen lymph nodes, tuberculosis, severe bacterial infections, and cancer like Kaposi's sarcoma [1].

HIV antibodies, HIV antigens, HIV RNA, and CD4 cells have been used in HIV diagnosis. Five generations of enzyme-linked immunosorbent assays (ELIAs) have been developed since the mid-1980s, and the fifth-generation allows the diagnosis to distinguish HIV-1 and HIV-2 based on p24 antigen, but ELIA-based test technologies have high false positivity. Therefore, a further test following the positive result of ELIAs is required. Several rapid tests have been developed, which only take 20 to 30 minutes. Nonlaboratory workers can perform these tests with standard training. To achieve the goal of 90% of people living with HIV knowing their status, WHO prequalified three rapid tests for people to do HIV Self-Testing, which enable people who do not have access to test services to know their status [25].

There is no cure for HIV infection, but the viral load can be reduced to an extremely low level by a combination of several antiretroviral drugs. ART allows patients living with HIV to live a long and relatively healthy life. Numerous drugs have been approved by FDA which inhibit different stages of HIV infection [26]. Nucleoside reverse transcriptase inhibitors (NRTIs) are deoxynucleoside triphosphate analogs which once are incorporated into viral DNA in the reverse transcription step, DNA synthesis is terminated. The approved NRTIs include azidothymidine (AZT), disoproxil

fumarate (TDF), Lamivudine (3TC) and many others [27-29]. Non-nucleoside reverse transcriptase inhibitors (NNRTIs) are another type of drugs that inhibits the enzymatic activity of reverse transcriptase (RT), such as Etravirine (ETR), Rilpivirine (RPV), and Doravirine (DOR) [30-32]. Protease Inhibitors (PIs) include Atazanavir (ATV), Darunavir (DRV), Fosamprenavir (FPV) and others, which inhibit enzymatic activities of HIV protease that cleaves viral polyproteins Gag and Gag-Pol for virus maturation [33-35]. Fusion inhibitors prevent HIV entry, such as Enfuvirtide (T-20) and Maraviroc (MVC) [36, 37]. Integrase strand-transfer inhibitors (INSTIs) like Dolutegravir (DTG) and Raltegravir (RAL), bind and inhibit HIV integrase, thus reduce HIV DNA integration to the host genome [38, 39]. HIV treatment regimens are composed of a combination of three drugs to prevent the development of viral resistance and improve effectiveness. An estimated of 73% of people living with HIV received ART at the end of 2020 globally. To achieve the goal of 90% people receiving ART, more efforts are needed.

1.5 Genome structure

HIV-1 packages two identical copies of single-stranded viral RNA which is 9.7kb in length and is flanked at both ends by long terminal repeat (LTR) [7, 40]. The 5' LTR is the promoter for cellular RNA polymerase II to synthesize viral RNA. The 5' LTR region is followed by the gag gene, which encodes the Gag polyprotein consisting of the matrix protein (MA, p17) on the outer face of the core, the capsid protein (CA, p24), the nucleocapsid (NC, p7), p6, and two spacer peptides p1 and p2 [7, 41]. The gag gene is followed by the pol gene, which encodes viral protease (PR), reverse transcriptase (RT) and integrase (IN). Env encodes envelope glycoprotein (gp)160, which is processed to gp41 (transmembrane protein) and gp120 (surface protein). In addition to the structural proteins, HIV-1 also encodes two regulatory proteins Tat and Rev, four accessory proteins Vif, Vpr, Vpu, and Nef. Tat acts as an activation protein of HIV-1 gene transcription. Rev is responsible for the nuclear export of non-spliced or partially spliced viral RNA. Accessory proteins promote viral replication, enhance viral

pathogenesis and viral budding.

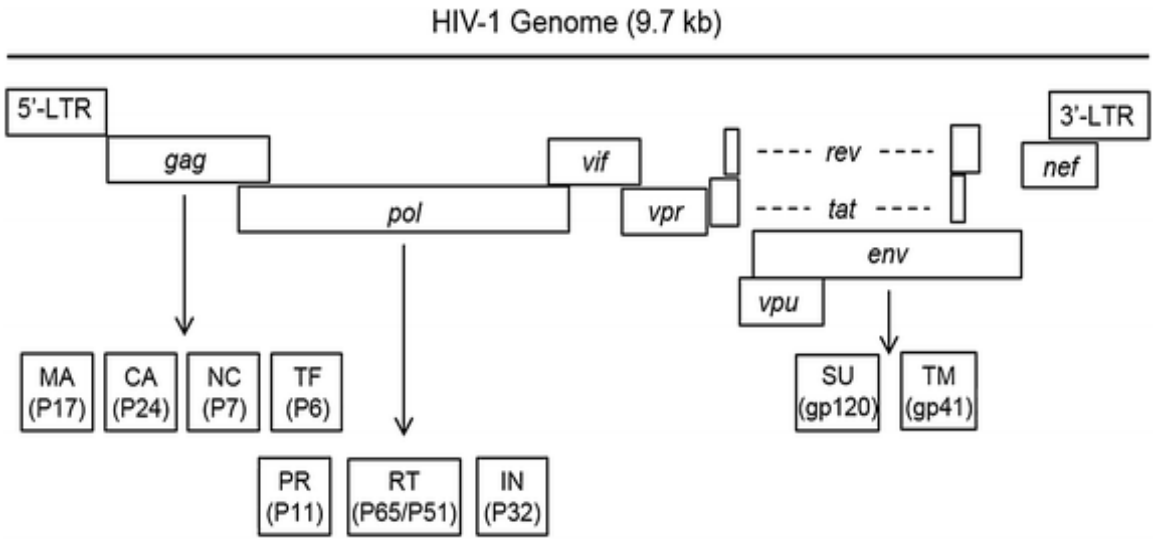

Fig. 1 HIV-1 genome. HIV-1 genome has two copies of identical RNA with each approximately 9.7 kilobase pairs (kb) in size. 5' and 3' ends are flanked by the long terminal repeat (LTR) promotor region. RNA splicing produces 9 gene products including 3 structure proteins (Gag, Pol and Env) and 6 accessory proteins (Tat, Rev, Vif, Vpr, Vpu, nef). The figure was obtained from Nkeze, Joseph, et al. "Molecular characterization of HIV-1 genome in fission yeast Schizosaccharomyces pombe." Cell & bioscience 5.1 (2015): 1-13.

1.6 Life cycle

1.6.1 Viral Entry

HIV-1 primarily targets CD4+ cells, including CD4 T-lymphocyte cells, macrophages, and dendritic cells [42]. The infection starts with the binding of HIV-1 envelope glycoprotein gp120 to CD4 [43, 44]. HIV-1 gp120/gp41 forms a trimer [45]. Upon binding to the CD4 receptor, gp120 undergoes conformational changes, which exposes the variable 3 (V3) domain and allows binding to co-receptor C-X-C chemokine receptor type 4 (CXCR4) or the C-C chemokine receptor type 5 (CCR5) to complete viral entry [46-48].

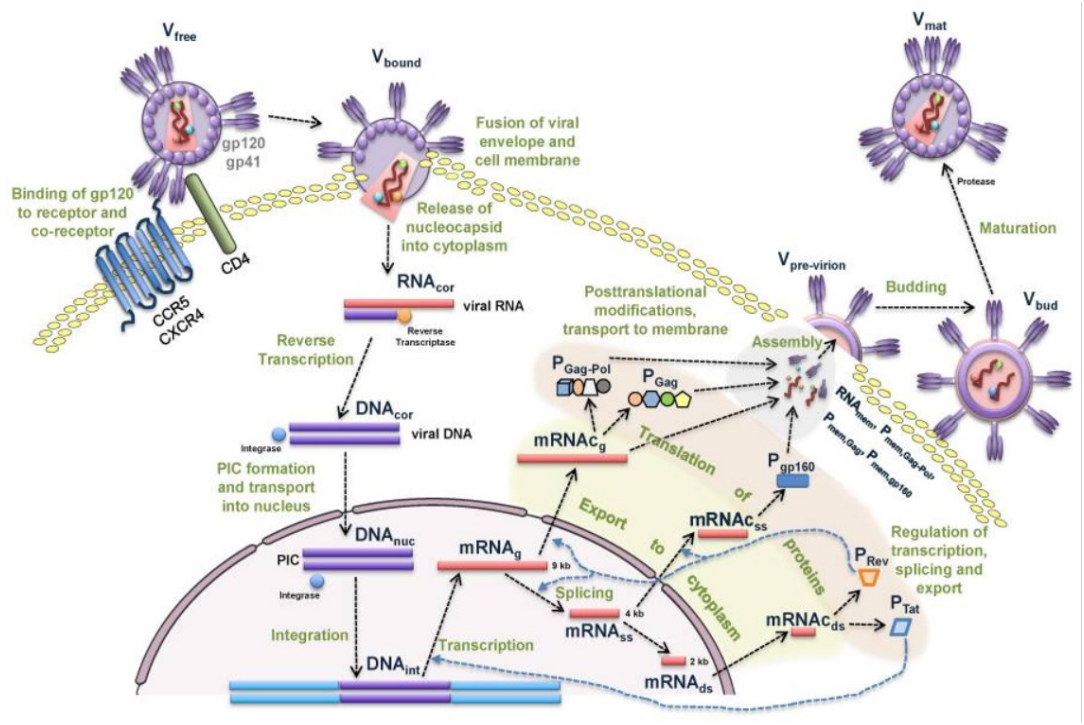

Fig. 2 HIV-1 life cycle. The HIV-1 fusion to the cell membrane starts with the binding of HIV-1 Env gp120 to CD4 receptor presenting on the cell surface. This binding results in the conformational change of gp120 in the V3 domain, which in return binds to the co-receptors CCR5 or CXCR4. Following viral fusion, the HIV-1core is injected into the cytoplasm and undergoes the process of uncoating. RT (Reverse Trancriptase) is activated and mediates the synthesis of viral DNA from the viral RNA. Once the double-stranded DNA is synthesized, IN (Integrase) and other proteins bind to the DNA to form pre-integration complex (PIC), which is transported into the nucleus for subsequent integration into the host genome. This integration is catalyzed by IN (Integrase). Upon receiving transcription signals, HIV-1 transcripts viral mRNAs which are transported to the cytoplasm for translation. The translated viral proteins undergo several modifications such as folding, glycosylation, phosphorylation and oligomerization and transportation to the plasma membrane where they package with the full-length viral genome to form virions. The virions are released from the plasma membrane and start the maturation process to form infectious HIV-1. The figure was obtained from Shcherbatova, Olga, et al. "Modeling of the HIV-1 life cycle in productively infected cells to predict novel therapeutic targets." Pathogens 9.4 (2020): 255.

1.6.2 Uncoating and reverse transcription

Following viral fusion to the plasm membrane, the HIV-1 core is release into the cytoplasm. Meanwhile, the reverse transcriptase is activated to synthesize HIV-1 DNA. Viral core is composed of viral capsid protein (CA), which protects the two copies of viral RNA tightly associated with nucleocapsid (NC), RT and integrase (IN) [49]. RT first synthesizes the minus-strand DNA using viral RNA as the template, followed by the synthesis of plus-strand DNA [44]. In addition to the polymerase activity, RT has RNase H activity which degrades the RNA in the RNA/DNA hybrid [50]. Recent studies captured the intact viral cores that cross the nuclear pore complex and enter the nucleus, this indicates that viral uncoating can occur within the nucleus [51].

1.6.3 Nuclear import and Integration

After the synthesis of HIV-1 DNA, integrase and other proteins bind to viral DNA and form a large molecule complex, termed pre-integration complex (PIC) [44]. Modification of HIV-1 DNA is required for integration to occur, which is achieved by cleaving two nucleotides from each 3' end of viral DNA. This generates a free hydroxyl group on each end, facilitating DNA integration to the host genome [52]. The nuclear import of PIC involves interaction between PIC and nucleoporins. The PIC can attack the host genome DNA and integrate viral DNA into cellular DNA to form a provirus [53].

1.6.4 Transcription

HIV-1 provirus starts transcription upon receiving activation signals. Once synthesized, HIV-1 RNA first undergoes complete splicing, forms multiply spiced viral RNA that is exported into the cytoplasm to produce viral Tat, Rev and Nef proteins. Tat acts as a transcription activator by binding the trans-activation response (TAR) element and hijacking RNA polymerase II elongation control machinery of the host cell to dramatically elevate HIV-1 transcription [54]. Rev binds to the Rev response element (RRE) in the env gene and enables the export of the full-length viral RNA and singly

spliced viral RNA into the cytoplasm to produce viral structural proteins and accessary proteins [44, 55, 56]. Rev hijacks the host Crm1/RanGTP nuclear export machinery to export viral RNA [57].

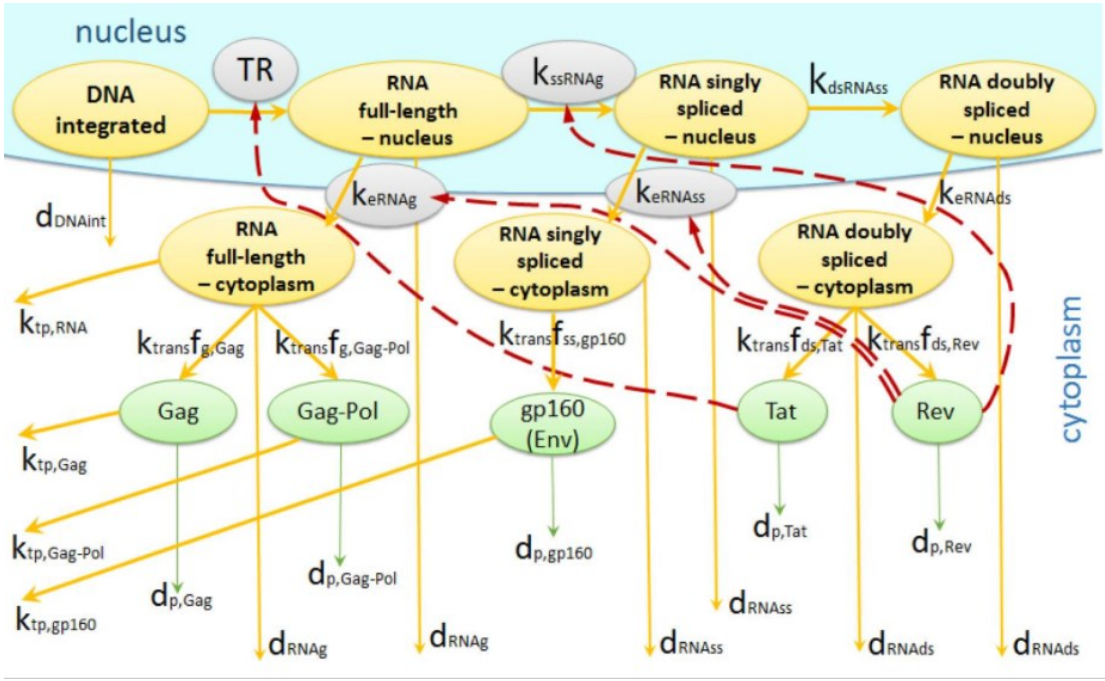

Fig. 3 HIV-1 transcription and translation. HIV-1 transcription and translation occur in a complex but highly organized manner. Upon receiving transcription signals, HIV-1 starts to transcribe mRNAs encoding Tat and Rev. Tat acts as a transcription activator that takes advantage of the host transcription machinery to facilitate HIV-1 transcription. There are three types of mRNAs: Completely unspliced approximately 9.2kb encoding Gag and Gag-Pol, incompletely spliced approximately 4.5kb encoding Env, Vpu, Vif, and Vpr and completely spliced approximately 2kb encoding Tat, Rev, and Nef. Rev binds to the RRE (Rev response element) of the intron-containing full-length viral mRNA to mediate the nuclear export of viral mRNA. The Env precursor protein gp160 is translated and trimerized in the ER and cleaved by protease in Golgi apparatus into gp120 and gp41 before being transported to the plasma membrane. Gag and Gag-Pol are synthesized at the ration of 20:1 and transported to the plasma membrane for assembly. Other accessory proteins are translated and essential in pathogenesis. The figure was obtained from Shcherbatova, Olga, et al. "Modeling of the HIV-1 life cycle in productively infected cells to predict novel therapeutic targets." Pathogens 9.4 (2020): 255.

1.6.5 Translation

The viral envelope (Env) precursor protein gp160 is synthesize at the ER, trimerizes before trafficking to the Golgi apparatus, where it undergoes glycosylation and is cleaved by furin into mature gp120 and gp41[58-60]. Gp120/gp41 trimer then transports to the plasma membrane to participate in virus assembly. Viral Gag and Gag-Pol are synthesized at the ratio of 20:1 due to the frequency of ribosome frameshift [61]. Gag and Gag-Pol form virus particles in the multivesicular bodies (MVBs) or at the plasma membrane [62-64].

1.6.6 Assembly, Budding and Maturation

Assembly is the process when essential viral components, including two copies of full-length viral RNA, Env, Gag, Pol (RT, PR, IN) and accessory proteins, come together at cellular membrane domains to form virus particles [65, 66]. The formed virus particles then egress and detach from the cellular membrane. HIV-1 particles also undergo a maturation process during which viral protease cleaves Gag and Pol into mature proteins so that the virus particles become infectious [66]. Viral assembly begins with the binding of Gag to the microdomains in the plasma membrane [67]. MA recruits Env into the particles through interaction with gp41 [68]. CA is the center domain of Gag, which multimerizes to form the conical shell in the mature virus particles. The NC domain of Gag captures HIV-1 RNA and is responsible for viral genome packaging. P6 domain harbors the binding sites of viral protein Vpr and cellular protein such as TSG101 and Alx1 that are essential for virus budding. Two spacer peptides SP1 and SP2 regulate virus particle maturation [66]. As the virions bud from the plasma membrane, PR is activated and cleaves Gag to MA, CA, NC and p6 proteins, cleaves Pol into PR, RT and IN. This maturation process enables HIV-1 virions to be infectious [66].

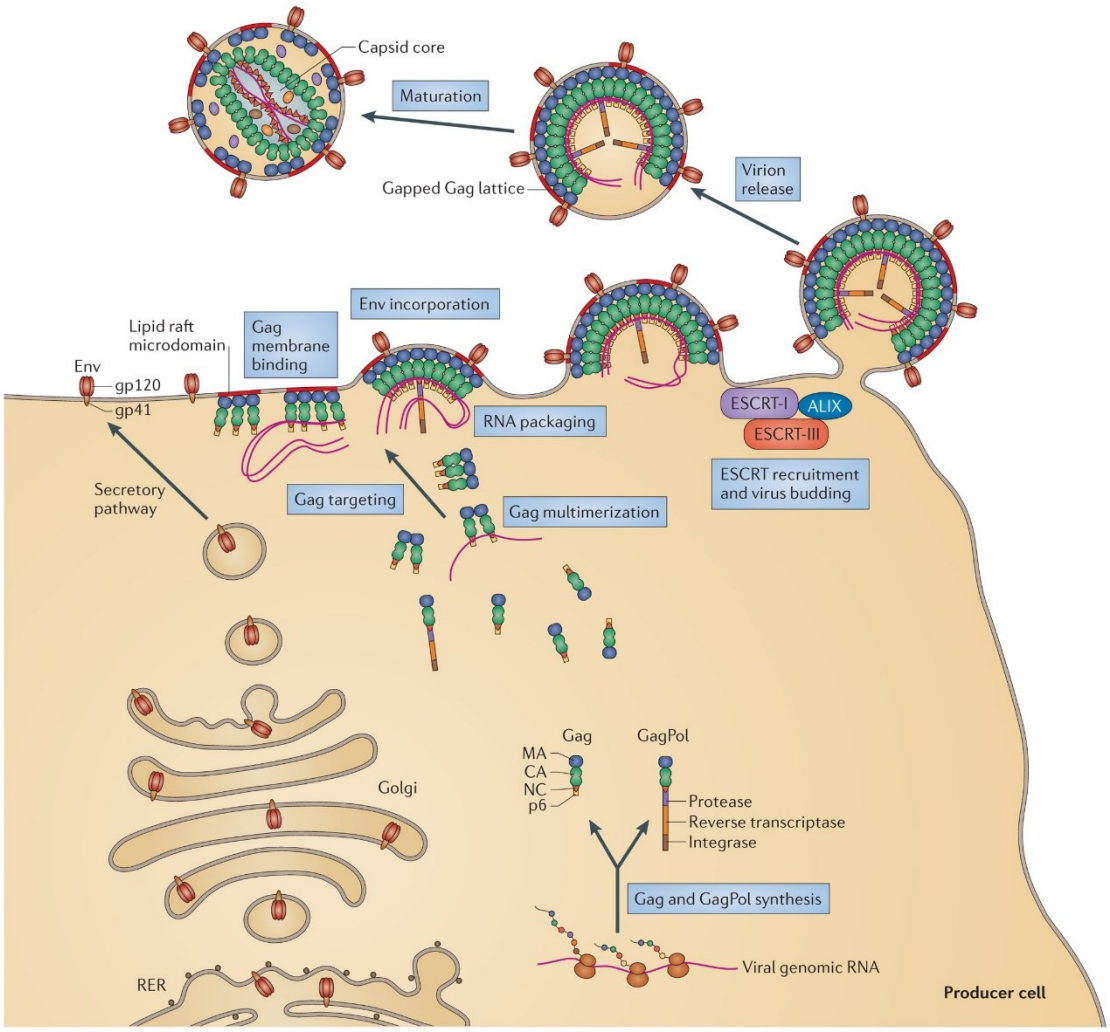

Fig. 4 Schematic diagram of HIV-1 assembly, budding and maturation. The Gag protein consists of matrix (MA), capid (CA), nucleocapsid (NC) and p6 proteins. The Gag-Pol protein consists of MA, CA, NC, protease (PR), reverse transcriptase (RT) and integrase (IN) domains. The Env gp120 and gp41 are transported to the plasma membrane. Gag is anchored to the plasma membrane and recruits viral genomic RNA. The Env is inserted into the assembling particles and the Gag multimerizes. The assembled particles are released from the plasma membrane and undergo the maturation process, which is achieved by protease mediated cleavage of Gag and Gag-Pol into mature proteins. The figure was obtained from Freed, Eric O. "HIV-1 assembly, release and maturation." Nature Reviews Microbiology 13.8 (2015): 484-496.

2 Innate immunity and restriction factors

2.1 Overall perspective

During HIV-1 infection, the innate immune response starts with the recognition of pathogen-associated molecular patterns (PAMPs) by pattern recognition receptors (PRRs) of the host cells, initiating a series of signaling pathways that often lead to interferon production [69]. These signaling pathways activate and produce soluble factors including Interferons (IFNs) which induces hundreds of interferon-stimulated genes (ISGs) to restrict replication and spread of HIV-1, as well as proinflammatory cytokines and chemokines which recruits innate immune cells such as macrophages, neutrophils, NK cells and dendritic cells to the site of infection [70, 71]. Meanwhile, HIV-1 has evolved strategies to evade host immune responses. The battle between host immune responses, including innate immunity and adaptive immunity, and HIV-1 evasion strategies often directs the course of viral infection [71, 72].

2.2 Sensing of HIV-1 infection

HIV-1 infection has been reported to be sensed by host PRRs, including Toll-like receptor (TLRs), RIG-I-like receptors, DNA sensors IFI16 and cGAS, as well as TRIM5α and tetherin, which act as restriction factor as well [73].

Toll-like receptors (TLRs): TLR2 and TLR4 recognize HIV-1 envelope glycoprotein gp120 in the human female genital epithelium [74]. This interaction leads to the production of proinflammatory cytokines by activation of the NF-κB pathway. TLR7 and TLR8 are genetically and functionally related to TLR2 and TLR4, but TLR7/8 is localized in the endosome and recognizes the incoming HIV-1 single-stranded RNA (ssRNA) [75]. Activation of TLR7/8 results in MyD88-dependent phosphorylation of interferon regulatory factors7 (IRF7), leading to the production of cytokines including IFNα, TNFα, and interleukins (ILs), which varies from one cell type to another [76-79].

RIG-I-like receptors: RLRs are important sensors of virus infection. RIG-I, but not MDA5, binds to the HIV-1 genome and induces the production of type I interferon [80]. After activation, RIG-1 interacts with the downstream adaptor protein, mitochondrial antiviral signaling protein (MAVS), which activates IKK-related kinases TBK1 and IKKε, leading to the phosphorylation of IRF3 and IRF7, which together with NFκB binds to virus responsive elements in IFN promotors to induce IFN expression[81-83]. RIG-I senses both dimeric and monomeric forms of the HIV-1 genome; however, HIV-1 inhibits RIG-I sensor by using viral protease (PR) to inhibit phosphorylation of IRF3 [80].

IFI16 and cGAS: In addition to TLRs and RIG-1-like receptors, IFI16 and cGAS have been reported to recognize HIV-1 DNA and elicit robust innate immune responses [70, 84-86]. IFI16 protein is interferon-inducible, and localizes to the nucleus and cytoplasm [87]. IFI16 protein can recognize viral dsDNA and ssDNA, and colocalizes with STING adaptor. Recognition of HIV-1 DNA by IFI16 results in activating the IFI16-STING-TBK1-IRF3/7 pathway, inducing the production of IFN and proinflammatory cytokines to defend against virus infection. IFI16 knockdown impairs IFN response and increases HIV-1 replication [84]. cyclic GMP-AMP synthase (cGAS) is another cytosolic DNA sensor that recognizes both viral and host DNA [86]. cGAS has a DNA binding domain for DNA sensing and nucleotidyltransferase domain which triggers the conversion of GMP and AMP to cyclic-di-GMP-AMP (cGAMP). cGAMP acts as the second messenger through binding to and activating STING to induce type I IFN production [70, 73, 86]. Meanwhile, cGAMP can be transferred to neighboring cells via gap junction to stimulate innate immune response [88].

TRIM5α and tetherin: The α isoform of Tripartite motif-containing protein 5 (TRIM5α) is a restriction factor of HIV-1, which recognizes HIV-1 core and inhibits reverse transcription [89, 90]. In addition to being a restriction factor, TRIM5α acts as a sensor of HIV-1 infection to promote innate immunity signaling. Specifically, TRIM5α is a RING domain E3 ubiquitin ligase that cooperates with heterodimeric E2

and UBC13 to stimulate the synthesis of K63-linked ubiquitin chains that activate TAK1 kinase, NF-κB, and AP-1 signaling, leading to the innate immune responses [90, 91]. Tetherin is also a restriction factor, which inhibits the release of HIV-1 and other retroviruses [92]. Besides, tethering HIV-1 particles at the cell surface, tetherin recruits TRAF6 and TAK1 and activates the production of IFN and other cytokines, thus acting as a sensor of HIV-1 infection [93].

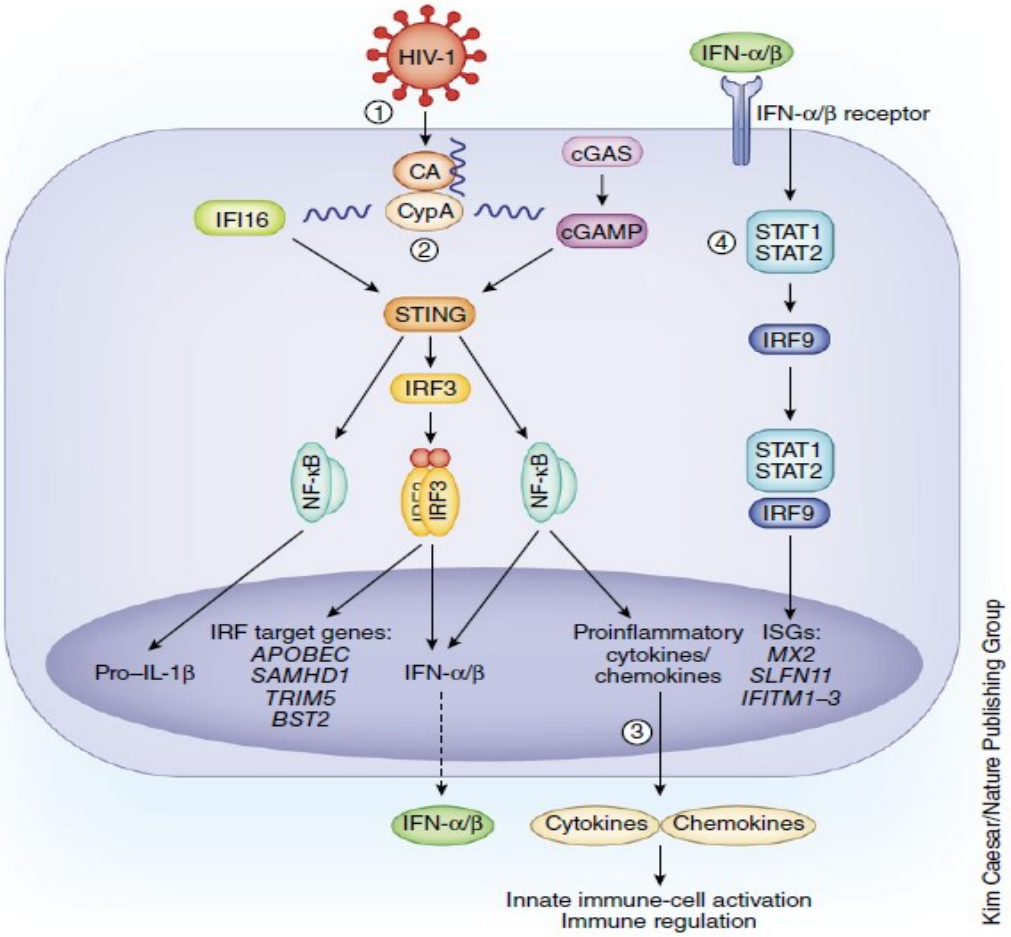

Fig. 5 Schematic diagram of HIV-1 innate immunity. Pathogen-associated molecular patterns (PAMPs) of HIV-1 are recognized by pattern recognition receptors (PRRs), including Toll-like receptor (TLRs), RIG-I-like receptors, IFI16 and cGAS, as well as TRIM5α and tetherin. These signaling pathways produce interferons (IFNs), proinflammatory cytokines as well as chemokines to inhibit HIV-1 infection and assist adaptive immunity.

2.3 Type-I interferon pathway

Interferon (IFN) was discovered for its inhibition of the influenza virus in 1957 [94]. After recognition of HIV-1 PAMPs by cellular PRRs, many types of the host cells were shown to produce IFN to inhibit HIV-1 replication and spread. However, HIV-1 has multiple strategies to subvert the IFN response by interfering with essential proteins in IFN pathways to evade host innate immune defense [95]. Type-I IFN interacts with the interferon receptor (IFNAR, including IFNAR1 and IFNAR2 subunits), and induces the expression of IFN-stimulated genes (ISGs) by activating the receptor-associated protein tyrosine kinases Janus kinase 1 (JAK1) and tyrosine kinase 2 (TYK2), which in turn phosphorylate the cytoplasmic transcription factors signal transducer and activator of transcription (STAT1 and STAT2). The phosphorylated STAT1 and STAT2 form a dimer, translocate to the nucleus and associate with IFN-regulatory factor 9 (IRF9) to form IFN-stimulated gene factor 3 (ISGF3), which binds to IFN-stimulated response elements (ISREs) to activate the expression of ISGs [96].

HIV-1 has evolved multiple mechanisms to curb IFN response. For example, the HIV Vif protein targets STAT1 and STAT3 in the JAK/STAT pathway and mediates the degradation of STAT1 and STAT3 to inhibit ISG production [97]. HIV-1 proteins Vpu and Nef are able to inhibit the phosphorylation of STAT1 [98]. HIV-1 proteins Vif and Vpr bind to TBK1 and inhibit TBK1 autophosphorylation in dendritic cells and macrophages, while Vpu and Nef can cause the degradation of IPS-1 which is an adaptor protein of RIG-I-like receptors [99, 100].

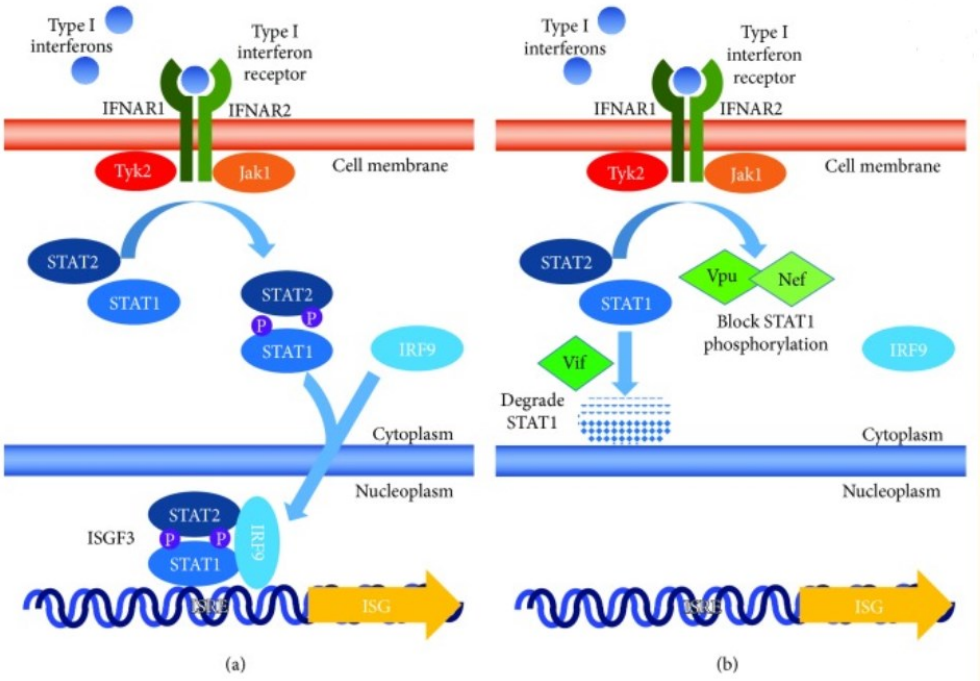

Fig. 6 Comparison of interferon induction between normal and HIV-1 infection. Secreted IFNs bind to IFN receptors to activate Janus kinase 1 (JAK1) and tyrosine kinase 2 (TYK2), which phosphorylate signal transducer and activator of transcription (STAT1 and STAT2). STAT1 and STAT2 translocate to the nucleus and bind to IRF9 to form ISGF3, which activates the expression of ISGs. Viral protein vif degrades STAT1. Vpu and Nef inhibit the phosphorylation of STAT1. The figure was obtained from He, Buyuan, James T. Tran, and David Jesse Sanchez. "Manipulation of Type I interferon signaling by HIV and AIDS-associated viruses." Journal of immunology research 2019 (2019).

2.4 HIV-1 restriction factors

Restriction factors constitute an important arm of innate host immunity against HIV-1 infection. They are cellular proteins, often IFN inducible, inhibit different stages of HIV-1 infection, including entry, uncoating, reverse transcription, nuclear import, integration, assemble, and virus release [70, 73]. In return, HIV-1 has various strategies to counteract these restriction factors, to promote HIV-1 replication and spread.

In 2002, APOBEC3G (also called CEM15) was reported to potently inhibit HIV-1 infection, and HIV-1 Vif counters APOBEC3G by causing ubiquitination and degradation of APOBEC3G [101]. APOBEC3G is a member of the Apolipoprotein B mRNA-editing enzyme catalytic polypeptide-like 3 (APOBEC3) family, including A3A, A3B, A3C, A3DE, A3F, A3G, and A3H [102].

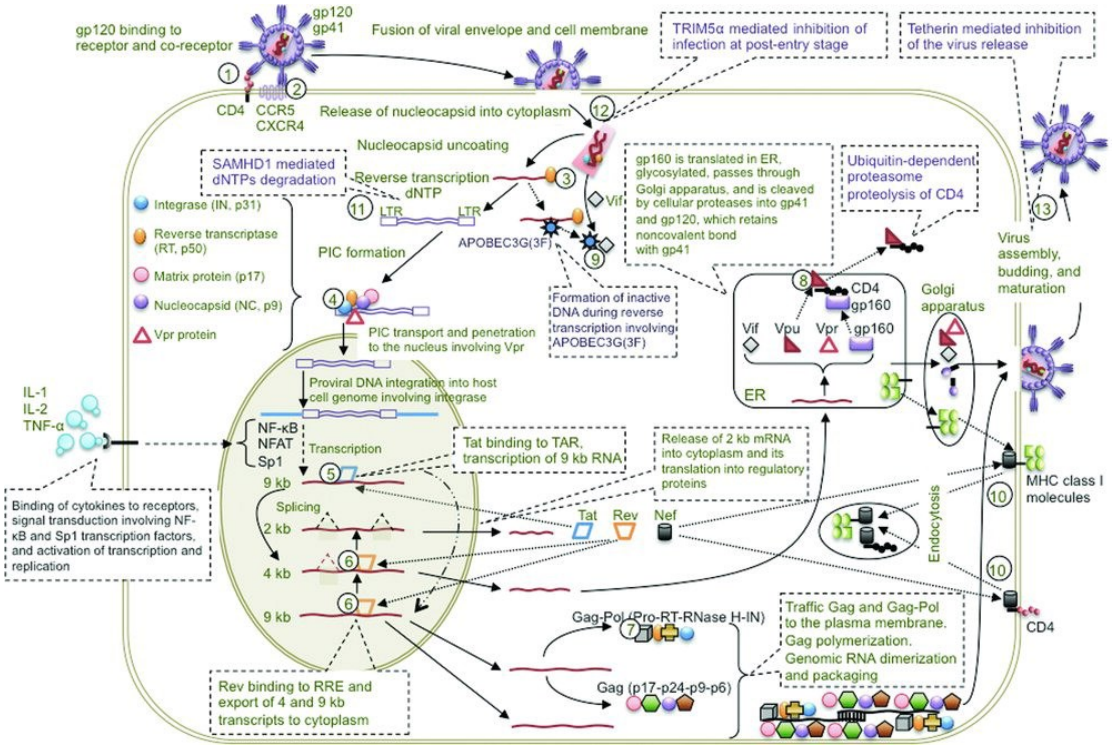

Fig. 7 HIV-1 life cycle and interaction with host restriction factors. Host restriction factors inhibit different steps of the HIV-1 life cycle. In return, the accessory proteins of HIV-1 counteract restriction factors to facilitate viral replication, persistence and transmission. This figure was obtained from Chereshnev, V. A., et al. "Pathogenesis and treatment of HIV infection: the cellular, the immune system and the neuroendocrine systems perspective." International reviews of immunology 32.3 (2013): 282-306.

APOBEC3 proteins exhibit broad antiviral activities against retroviruses and DNA viruses [103, 104]. The underlying antiviral mechanism is that APOBEC3G causes hypermutation from G to A in the newly synthesized HIV-1 DNA during reverse transcription, leading to the synthesis of defective viral DNA. The discovery of APOBEC3G restriction of HIV-1 infection marks the beginning of the HIV-1 restriction factor research era.

In 2004, rhesus monkey TRIM5α was found to inhibit HIV-1 infection by targeting the viral core, causing premature uncoating, and impairing viral reverse transcription. Human TRIM5α exhibits only weak inhibition of HIV-1 infection because HIV-1 capsid protein has adapted to avoid targeting by human TRIM5α. In addition to being a restriction factor, by recognizing the HIV-1 core structure, TRIM5α also functions as a

PRR and activates TAK1 kinase, NF-κB, and AP-1 signaling [90, 91].

In 2008, tetherin, also known as CD317, BST2 or HM1.24, was reported to inhibit the release of nascent HIV-1 particles. This anti-HIV-1 activity of tetherin is antagonized by HIV-1 protein Vpu through interaction with tetherin via their transmembrane domains and downregulation of tetherin from the cell surface so that HIV-1 can efficiently release from the plasma membrane. Like TRIM5α, tetherin also acts as a PRR when it blocks HIV-1 release and activates the TRAF6 and TAK1 signaling pathways [105].

In 2011, SAMHD1, sterile alpha motif and histidine-aspartic acid domain containing protein 1, was reported to inhibit HIV-1 DNA production in macrophages and dendritic cells. SAMHD1 is a deoxynucleoside triphosphate triphosphohydrolase (dNTPase), it hydrolyses dNTPs, thus lowers the cellular dNTP pool and suppress the synthesis of HIV-1 cDNA. Compared to HIV-1, which does not have a mechanism to antagonize SAMHD1, HIV-2 and simian immunodeficiency viruses (SIVsm/mac) encode accessory protein Vpx, which mediates the degradation of SAMHD1 [106]. In the same year, our group reported the inhibition of HIV-1 entry by IFITM proteins, the interferon-induced transmembrane proteins, including IFITM1, IFITM2, and IFITM3 [107]. IFITM3 was subsequently shown to increase the membrane rigidity and inhibits the fusion between the viral membrane and cellular membrane. HIV-1 can evade IFITM inhibition by changing the sequence of the viral envelope protein. IFITM proteins were also reported to suppress HIV-1 RNA translation, and HIV-1 Nef protein can counter IFITM inhibition [108]. Yiping Zhu et al. reported that ZAP, the zinc-finger antiviral protein, also targets HIV-1 RNA due to its high CpG content and mediates viral RNA degradation in a KHNYN protein dependent manner [109, 110].

In 2012, SLFN11, or schlafen protein 11, an interferon-inducible protein, was shown to be a potent restriction factor of HIV-1 in the late stages of the HIV-1 life cycle. SLFN11 restricts HIV-1 infection by binding transfer RNA (tRNA) required to synthesize viral proteins [111].

In 2013, three groups, including ours, reported that human myxovirus resistance protein B (MxB, also called Mx2) inhibits HIV-1 infection by impeding the nuclear import of viral DNA by targeting viral capsid. In turn, HIV-1 can change capsid protein sequence to escape MxB restriction, an evasion strategy similar to that against TRIM5α.

In 2015, transmembrane proteins serine incorporator 3 (SERINC3) and SERINC5 were shown to be incorporated into HIV-1 particles and thereby decrease viral infectivity. HIV-1 protein Nef curbs this host restriction by preventing the incorporation of SERINC3 and SERINC5 to virions [112].

In 2019, PSGL-1, P-selectin glycoprotein ligand 1, was identified to inhibit HIV-1 infection by incorporating into virus particles and impairing reverse transcription, HIV-1 Vpu is able to binds and mediates the degradation of PSGL-1 [113].

3 Myxovirus resistance protein

3.1 The Mx discovery history

The myxovirus resistance (Mx) genes include MxA (Mx1) and MxB (Mx2), both of which are restriction factors of a variety of DNA and RNA viruses. The story of the discovery of Mx antiviral activity went back to the 1960s in Bern, Switzerland, where Dr. Lindenmann found a rare inbred mouse strain, named A2G that is naturally resistant to neurotropic influenza virus infection, suggesting A2G mice have an unknown mechanism to suppress influenza virus infection specifically. The cellular protein behind this mechanism was only discovered two decades later [114, 115]. Lindenmann then moved to the University of Florida in Gainesville where his group found a single autosomal dominant locus responsible for influenza virus resistance, but A2G mice are also susceptible to other pathogens [115-117]. In 1987 and 1988, the underlying gene was mapped to mouse chromosome 16, and its cDNA was cloned [118-120]. In 1988, another Mx gene, Mx2, was identified, which is closely related to Mx1 [121].

In mice, the expression of Mx genes is inducible by type I and type III interferon. Mx1 and Mx2 have different subcellular localization and restrict other groups of viruses. In humans, the two Mx proteins, MxA and MxB, are encoded by the genes on the long arm of chromosome 21 [122]. In 2010, Gao et al. solved the crystal structure of MxA protein, and Jennifer et al. solved MxB structure in 2014 [123, 124]. MxA has been known for its broad antiviral activities toward DNA and RNA viruses including influenza virus, Thogoto virus (THOV), measles morbillivirus (MV), human parainfluenza viruses 3 (HPIV-3), Rift Valley fever virus (RVFV), La Crosse encephalitis virus (LACV), Crimean-Congo hemorrhagic fever virus (CCHFV), hantavirus (HNTV), Coxsackie B virus (CVB), vesicular stomatitis virus (VSV), Semliki Forest virus (SFV), hepatitis B virus (HBV), infectious bursal disease virus (IBDV) and African swine fever virus (ASFV) [125]. MxB was thought to be non-antiviral until 2013, when three groups independently reported that MxB is a potent restriction factor of HIV-1 [126-128]. After this discovery, MxB was shown to also

inhibit hepatitis C virus (HCV) and herpesviruses [129, 130].

3.2 The structure of human MxA and MxB proteins

Human MxA and MxB proteins are closely related with 63% similarity in sequence. Mouse Mx1 and Mx2 proteins are homologs of human MxA. Mice lost the MxB homolog during evolution [122]. MxA is an interferon-induced, dynamin-like GTPase [125]. MxA has three domains, the amino-terminal GTPase domain, the stalk domain and the central bundle signaling element (BSE) (Fig. 8) [131].

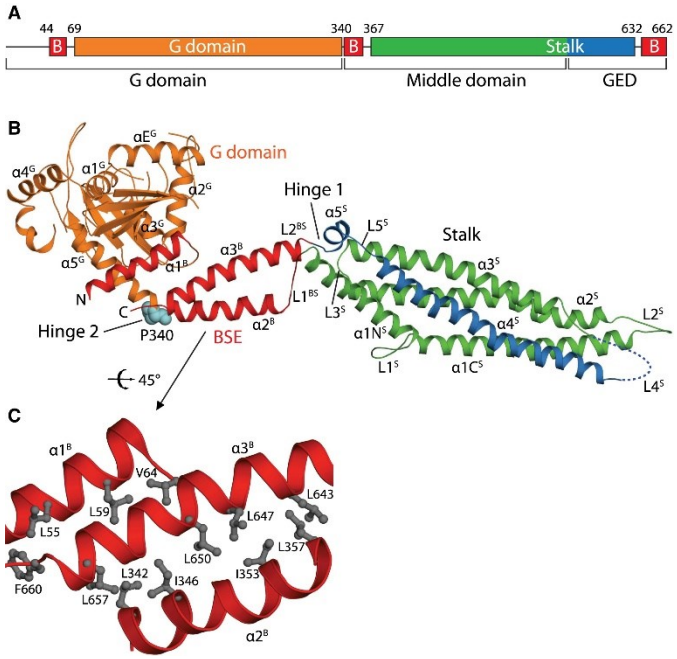

Fig. 8 Structure of the MxA monomer. (A) MxA structure based on the sequence. B is short for BSE. The GTPase domain and stalk domain are connected by BSE. (B) The secondary structure is labelled. (C) The details of BSE. The figure was obtained from Gao, Song, et al. "Structure of myxovirus resistance protein a reveals intra-and intermolecular domain interactions required for the antiviral function." Immunity 35.4 (2011): 514-525.

Mutagenesis analysis has shown that hinge 1 in the BSE regulates oligomerization of MxA and is essential for the antiviral activity. For example, the nucleoprotein (N) of La Crosse virus (LACV) can be sequestered to the perinuclear region in MxA-expressing cells [132]. The R640A mutation in hinge 1 caused the diffusion of the mutated MxA into the cytoplasm and failed to sequester the viral nucleoprotein, supporting hinge 1 in the antiviral function MxA [131]. MxA can assemble into oligomers through BSE-stalk interactions. A model of the MxA oligomeric ring composed of 16 MxA dimers was proposed, which is believed to be able to sequester viral nucleoprotein complexes [131].

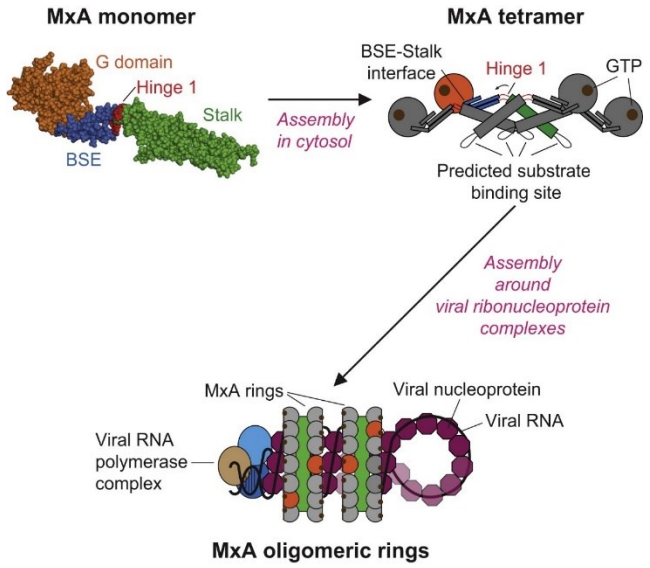

Fig. 9 Structural Model of MxA monomer and Oligomeric Rings. The MxA oligomeric ring is composed of 16 MxA dimers. This ring structure is essential in antiviral function of MxA. The figure is obtained from Gao, Song, et al. "Structure of myxovirus resistance protein a reveals intra-and

One year after discovering MxB restriction of HIV-1 in 2013, the crystal structure of MxB was reported. MxB has two isoforms of 76 kDa or 78 kDa due to an alternative start codon at position 26. The longer isoform, or the full-length MxB, has a nuclear localization signal (NLS) in the first 25 amino acids essential for its localization to the nuclear envelope, while the short isoform is observed in the cytoplasm [133].

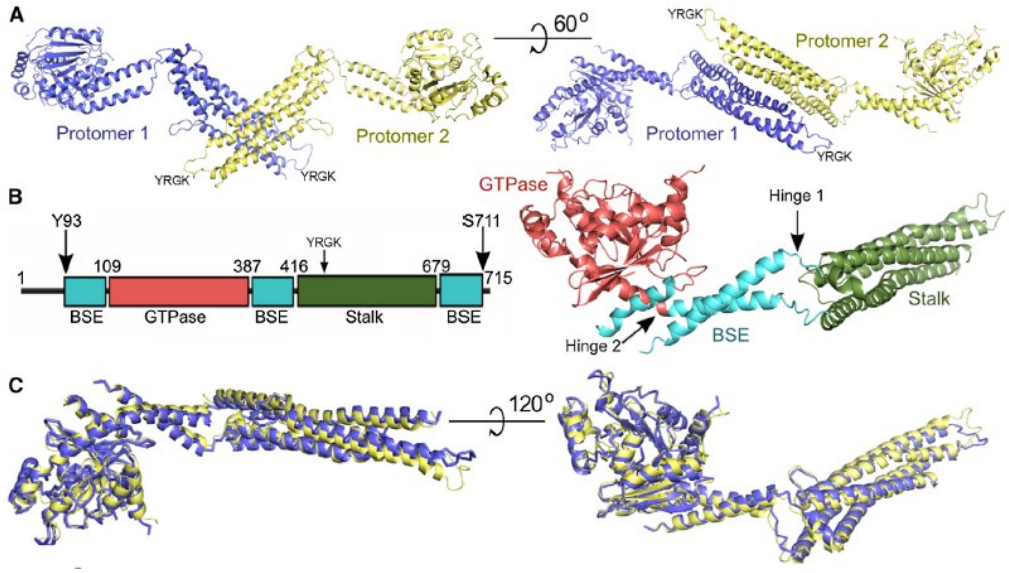

Fig. 10 Structure of MxB_{84YRGK} dimer and monomers. (A) Structure of MxB dimers composed of two monomers in two orientations. (B) MxB is composed of GTPase domain and stalk domain connected by BSE. (C) Superposition of two monomers in two views. The figure was obtained from Fribourgh J L, Nguyen H C, Matreyek K A, et al. Structural insight into HIV-1 restriction by MxB[J]. Cell host & microbe, 2014, 16(5): 627-638.

To form MxB crystals, the first 83 amino acids had to be removed and 4 mutations in the stalk domain at position 487-490 (YRGK-AAAA) called MxB_{84YRGK} were introduced. The first 91 amino acids amino-terminal domain (NTD) which includes NLS is predicted to be unstructured. The overall structure of MxB is similar to that of MxA, consisting of a GTPase domain and a stalk domain connected by BSE via two hinge regions [123]. The GTPase function of MxB, binding and hydrolyzing GTP, seems to be dispensable for restricting HIV-1, which is contrary to MxA. In addition, the hinge region of MxB is not required for HIV-1 restriction. The hinge mutation E681A and R689A mutants didn't abolish the anti-HIV-1 activity of MxB [123]. Interestingly, MxB dimerization has an essential role in this regard. Mutations M574D, Y651D, and M567D/L570D destabilize MxB dimer and do not affect HIV-1 infection. MxB forms high-order oligomers which contribute to its anti-HIV-1 function.

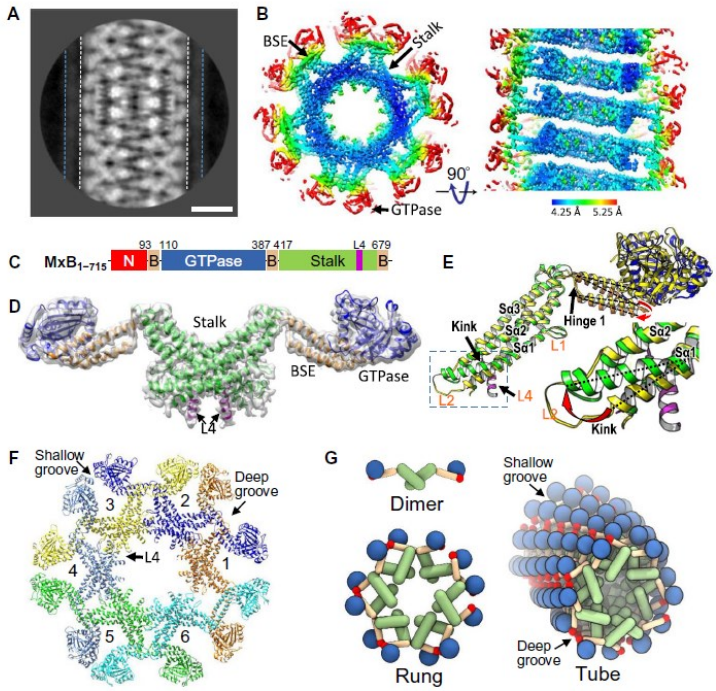

Fig. 11 High-order oligomerization of MxB. MxB dimers are essential in the antiviral activity. Six MxB dimer units go hand in hand via stalk and BSE domains to form a tube structure. The figure was obtained from Alvarez, Frances JD, et al. "CryoEM structure of MxB reveals a novel oligomerization interface critical for HIV restriction." Science advances 3.9 (2017): e1701264.

3.3 The antiviral mechanism by MxB

MxB was thought to not have antiviral properties and instead function in cellular processes such as cell cycle progression and nuclear import [134]. This was challenged by Su-Yang Liu et al., who reported that MxB inhibited replication of MHV-68 and VSV [135]. In 2013, MxB was shown to be a potent restriction factor of HIV-1[126-128]. MxB was found to decrease viral 2-LTR circles, which serve as a marker of viral DNA nuclear import [127, 136]. HIV-1 capsid mutations CA88, P90A, P89A, and N57S confer resistance to MxB inhibition, and it was subsequently reported that MxB associates with HIV-1 capsid, confirming viral capsid is the target of MxB [126, 128]. MxB recognition of HIV-1 capsid is cyclophilin A (CypA)-dependent [128]. Further biochemical and structural studies showed that MxB recognizes the tri-hexamer interface of HIV-1 capsid to impede viral nuclear import [137]. Recently, our lab reported that MxB also targets HIV-1 Rev protein and blocks the nuclear import of Rev, thus impairing the nuclear export of HIV-1 RNA.

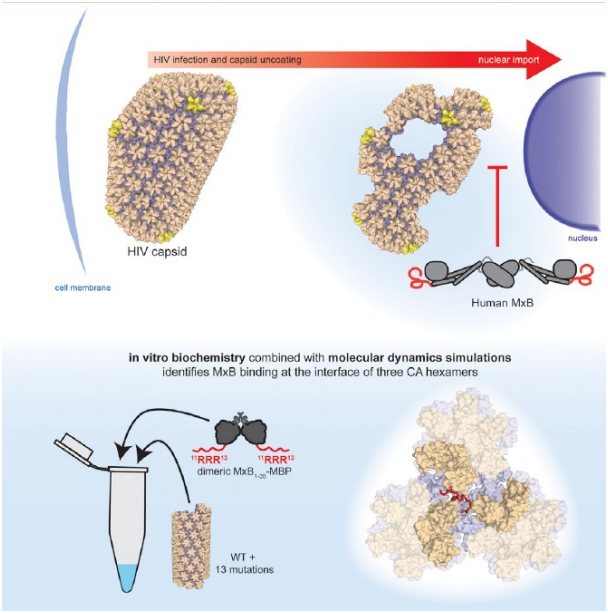

Fig. 12 A model of MxB interaction with HIV-1 capsid. MxB binds to the intersection of c and inhibits HIV-1 uncoating process. The figure was obtained from Fricke, Thomas, et al. "MxB binds to the HIV-1 core and prevents the uncoating process of HIV-1." Retrovirology 11.1 (2014): 1-14.

4 Cell cycle and nuclear envelope

4.1 Cell cycle

The cell cycle is divided into two main phases, interphase and mitotic phase (including mitosis and cytokinesis). Interphase is further divided into G1 (gap1), S (DNA synthesis) and G2 (gap2), while mitosis is divided into prophase, prometaphase, metaphase, anaphase and telophase, followed by cytokinesis [138, 139]. During interphase, the cell synthesizes proteins, duplicates DNA, and replicates organelles such as mitochondria and centrosomes. During mitosis, the cell uses microtubules (MTs) that are nucleated from the centrosome to anchor the duplicated chromosomes and segregates the two copies of chromosomes to two daughter cells. This process allows the faithful transfer of genetic materials from mother cells to the next generation. This process is highly regulated by cell cycle checkpoints to ensure successful cell division [138, 140].

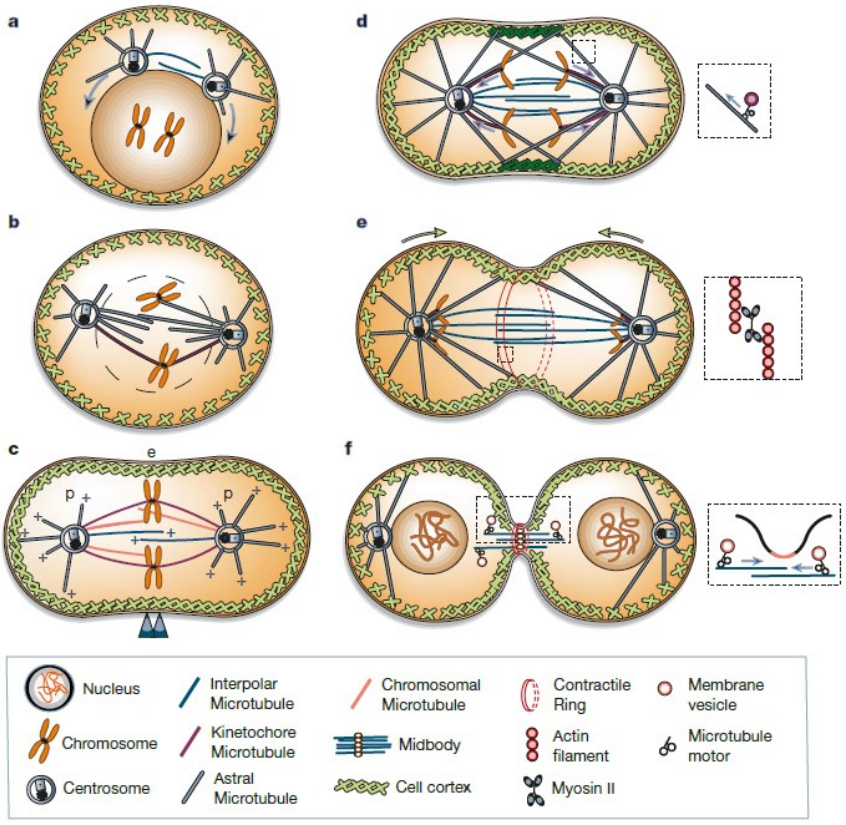

Fig. 13 scheme of mitosis and cytokinesis.
a prophase
b prometaphase
c metaphase
d anaphase
e telophase
f cytokinesis
The figure was obtained from Scholey et al. "Cell division." Nature 422.6933 (2003): 746-752.

4.1.1 Interphase

G1 is the gap between mitosis and the onset of the S phase. When the cell is exposed to stimulation by mitogens (a peptide or small protein that can induce the cell to begin division) or growth factor such as the TGF-β family, the cell starts DNA synthesis and enters the S phase. Centrosomes replicate in G1 and S phases but only mature in G2. G2 is the interval between the S phase and the onset of mitosis. Cellular organelles such as mitochondria, lysosomes also multiply in G2 [139, 141]. The interphase typically occupies more than 23 hours in human cell lines, while the mitosis lasts less than 1 hour.

4.1.2 Mitosis

Prophase marks the beginning of mitosis when chromosomes become visible as the chromatin condenses and compacts to form individual chromosomes. Each chromosome consists of two genetically identical chromatids. Meanwhile, the duplicated centrosomes move away from each other around the nucleus until reaching the opposite poles. Prometaphase, also known as late prophase or early metaphase, is characterized by nuclear envelope breakdown (NEBD). The nuclear envelope comprises two lipid bilayer membranes, inner and outer membranes, separated by the perinuclear space. The nuclear envelope has numerous holes occupied by nuclear pore complexes (NPC) which is comprised of more than 30 kinds of nucleoporins. NEBD results in the disassembly of NPCs and nuclear membranes [138, 142]. Upon NEBD, sister chromatids are exposed to the cytoplasm, allowing kinetochore MTs to anchor at the centromere. The MTs start pulling back and forth on the sister chromatids, driving them to the middle of the cells. In metaphase, all the chromosomes align to the middle of the cells called the equatorial plane. Chromosome alignment is essential in mitotic fidelity, misalignment results in spindle misorientation [143]. This phase has an important checkpoint to ensure that chromosomes are evenly distributed and aligned well in the equatorial plane. In anaphase, sister chromatids detach from each other and start moving to the opposite poles of the cells by the force of microtubules. During

anaphase, the chromosomal condensation level reaches its maximum, and this process ensures the daughter cells receive identical copies of DNA from the mother cell. Telophase is the last stage of mitosis when the nuclear envelope starts to re-assemble. The interpolar MTs form mid-zone body which separated the two daughter cells. Cytokinesis is the last stage of the cell cycle when two separate daughter cells are formed [138, 139].

4.2 Centrosome structure and biogenesis

The centrosome is an important microtubule organization center (MTOC), which regulates the nucleation and spatial organization of MTs. In mitosis, the centrosome drives the formation of mitotic spindles. Defective centrosome results in genome instability and aberrant cell division [144, 145]. In addition, the centrosome components, centrioles, act as basal bodies which nucleate microtubules to form cilia and flagella that regulate cell mobility [146].

The centrosome comprises two centrioles that are positioned at right angles to each other and a matrix of proteins called pericentriolar material (PCM). In animal cells, the centrosome is localized outside but near the nuclear envelope. The centriole is made of nine-triplet microtubules, and is around 0.2 μm in diameter and 0.2 to 0.4 μm in length depending on the species, cell type and the cell cycle phases, because the centrosome matures and enlarges as the cell cycle proceeds [147-149]. The mother and daughter centrioles vary in size, structure, and function. Compared to the immature daughter centriole, the mother centriole is bigger in size and has distal and subdistal appendages, so only the mother centriole can anchor MTs, but both centrioles are capable of nucleating MTs. The mother centrioles act as basal bodies in resting cells due to their ability to nucleate MTs at the distal appendage [150].

PCM is an amorphous, electron-dense material, which plays an important role in the formation of centrioles and centrosome maturation [151]. During centrosome maturation, PCM increases in size and the ability to nucleate more γ-Tubulin ring

complexes (γTuRCs) which is the microtubule nucleation centre. This process drives the maturation of centrosomes and mitotic spindles. PCM includes two main layers of proteins, PCM fibers and matrix. PCM fibers have pericentrin and Cep152, whose C-terminal end is closed to centrioles. PCM matrix includes cep192, cep215 and γTuRCs. During centrosome maturation, PCM expands to form a large layer of matrix [149].

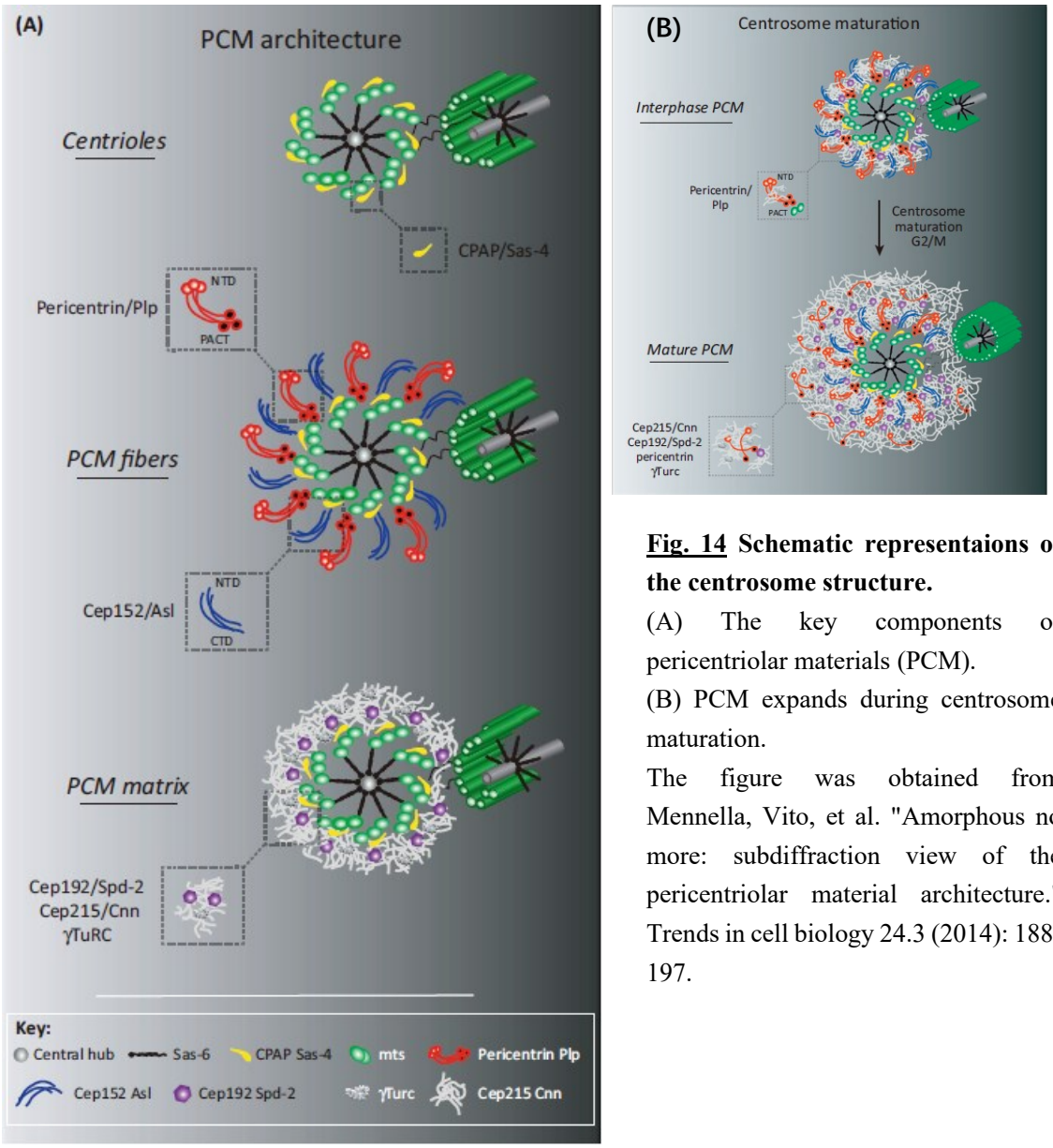

Fig. 14 Schematic representaions of the centrosome structure.
(A) The key components of pericentriolar materials (PCM).
(B) PCM expands during centrosome maturation.
The figure was obtained from Mennella, Vito, et al. "Amorphous no more: subdiffraction view of the pericentriolar material architecture." Trends in cell biology 24.3 (2014): 188-197.

4.3 Centrosome function

The centrosome functions as the microtubule organization center (MTOC). In interphase, the centrosome is localized outside the nuclear envelope. PCM nucleates and anchors MTs, especially γTuRC, which is a tetrameric complex, including two molecules of γ-tubulin and one molecule of DGRP84 and DGRP91 [152]. γ-tubulin is vital for microtubules nucleation. In addition, the centrosome is responsible for the formation and regulation of cilia and flagella, which facilitate the movement of some cells. Only the mother centriole can nucleate primary cilia because the mother centriole has the distal appendage [153, 154].

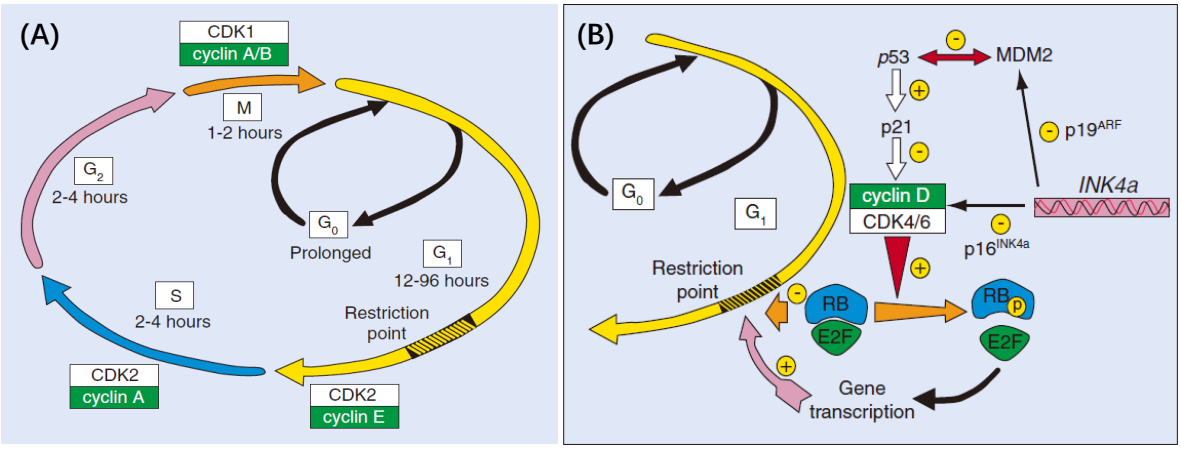

Fig. 15 Cell cycle time and the p53-RB axis in the regulation of the cell cycle.
(A) Cell cycle time. In human cell line, the interphase occupies normally more than 23 hours while the mitosis is less than 1 hour.
(B) Cell cycle is regulated by cyclins and cyclin-dependent kinases (CDKs)
The figure was obtained from Israels ED, Israels LG. The cell cycle. Oncologist. 2000;5(6):510-3. doi: 10.1634/theoncologist.5-6-510. PMID: 11110604.

In mitosis, the centrosome increases its size by recruiting a series of proteins to the PCM and MTs, including kinetochore MTs, chromosomal MT, astral MTs and interpolar MTs to form spindles. The centrosome proteins regulate the cell cycle during G1/S transition, G2/M transition, metaphase to anaphase transition (M/A) and cytokinesis [155]. Defective centrosomes act as acentriolar microtubule organizing centers (MTOCs), which can form mitotic spindles, but most cells fail to complete division [156, 157]. Change in centrosome proteins can lead to G1 arrest. For example, depletion of a mother centriole component results in an extended period of time in cytokinesis, and these cells are arrested in the G1 phase. Overexpression of a PCM component AKAP450 results in mislocalizing endogenous AKAP450 and protein kinase A from the centrosome, leading to cytokinesis defect and G1 arrest [155].

The cell cycle is regulated by a group of protein kinases called cyclin-dependent kinases (CDKs). CDKs regulate the transition of the cell cycle from one phase to the next by phosphorylating key regulators [158]. In G1 phase, Cyclin D increases its level, then binds and activates CDK4/CDK6, which phosphorylates retinoblastoma (RB). The activated RB protein dissociates with E2F, allowing E2F to enhance the transcription of genes that are essential for the cell cycle progression, including cyclin E. In the late G1 phase, an increase in cyclin E expression and activation of CDK2 are essential for G1/S transition. At the G1/S transition, cyclin A increases and accumulates in S phase, which binds and phosphorylates CDK2. In late S phase, cyclin A binds CDK1 with a check point to ensure the completion of DNA synthesis. The transcription factor p53 is essential in monitoring DNA damage, which mediates DNA repair by inhibiting RB phosphorylation if the DNA synthesis is incomplete [159]. Recently, several research groups reported that cyclin A and cyclin E contain centrosome localization sequences which may target these cyclins to centrosome [160-162].

4.4 Nuclear envelope and nuclear pore complexes (NPCs)

4.4.1 Nuclear envelope

The nuclear envelope (NE) comprises two layers of lipid membranes, termed inner nuclear membrane (INM) and outer nuclear membrane, separated by the perinuclear space. The outer membrane is the extension of the endoplasmic reticulum (ER). They are similar in composition. The NE is perforated by holes occupied by nuclear core complexes (NPCs), which regulate the import and export of macromolecules [142]. The nuclear lamina is a dense fibrillar network consisting of intermediate filaments lamins (lamin A/B/C and lamin-associated proteins) close to the INM. Its structure is similar to the nuclear matrix. Lamin-associated proteins bind to the lamins and interact with chromatin, playing an important role in DNA replication and NE assembly [163].

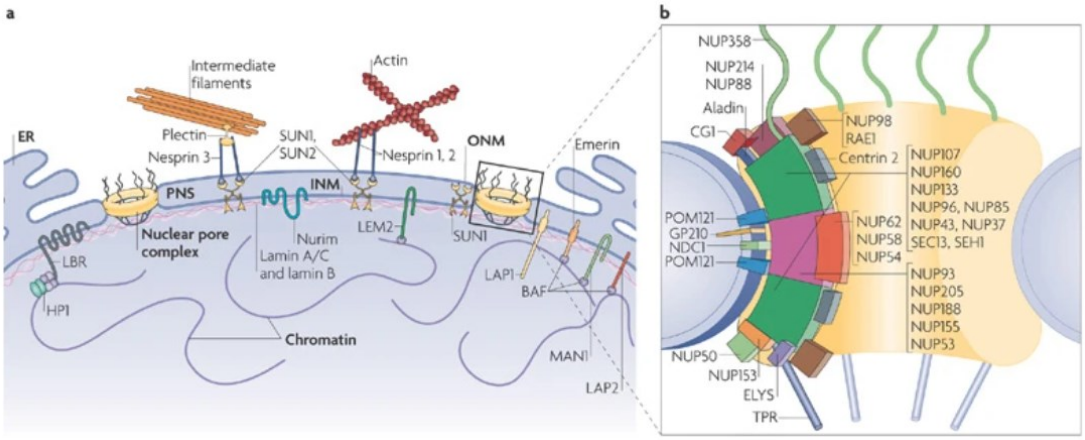

Fig. 16 Scheme of the nuclear envelope (NE) and Nuclear pore complexes (NPC) structure. The NE is composed of inner nuclear membrane (INM) and outer nuclear membrane (ONM) separated by the perinuclear space (PNS). The nuclear lamina consists of intermediate filaments lamins (laminA/B/C and lamin-associated proteins. The NE has numerous holes occupied by nuclear core complexes (NPC), which are composed of nucleoporins such as NUP358, NUP214 and NUP153. The figure was obtained from Güttinger, Stephan, Eva Laurell, and Ulrike Kutay. "Orchestrating nuclear envelope disassembly and reassembly during mitosis." Nature reviews Molecular cell biology 10.3 (2009): 178-191.

4.4.2 NE Assembly and disassembly

Nuclear envelope breakdown (NEBD) occurs at the late prophase. This process allows microtubules to anchor to the kinetochores of chromosomes. The NPCs and lamina also disassemble. NPCs are the first to disassemble, triggered by nucleoporin phosphorylation, including NUP98 [164, 165], [166]. In the late G2 phase, CDK1 is activated and advances G2 to mitosis. Chromosome condenses, the centrosomes moves away from each other and nucleate microtubules which attach to the NE. This process leads to NE invaginations around centrosomes.

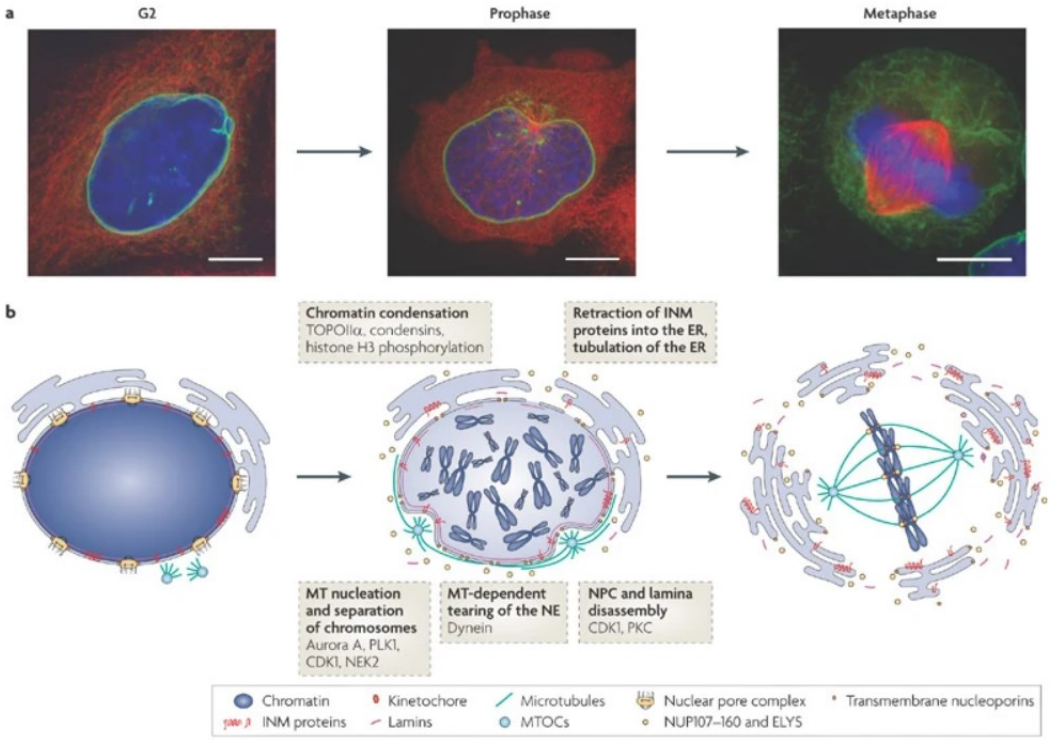

Fig. 17 Nuclear envelope breakdown (NEBD) during mitosis.

a: A HeLa cell with inner nuclear membrane stained by lamina-associated protein 2β(Green), DNA and microtubules in G2, prophase and metaphase.

b: Schematic representations of the nuclear envelope breakdown (NEBD). During the transition from G2 to prophase, the NEBD is characterized by chromatin condensation, NE invaginations around the centrosomes and NPCs disasembly. The figure was obtained from Güttinger, Stephan, Eva Laurell, and Ulrike Kutay. "Orchestrating nuclear envelope disassembly and reassembly during mitosis." Nature reviews Molecular cell biology 10.3 (2009): 178-191.

CDK1 and protein kinase C (PKC) mediate the phosphorylation of lamins and INM proteins, leading to the disassembly of the lamina. The NPCs dissemble in the late prophase within several minutes. Nucleoporins play an important role in spindle formation and kinetochore function. For example, RNA export 1 (RAE1) binds to microtubules, and depletion of RAE1 inhibits spindle formation [167]. The nucleoporin NUP107–160 complex localize to the spindle microtubules and help NUP358 localize to kinetochores [168]. Some nucleoporins have been reported to localize to the centrosome in mitosis, including NUP358, NUP58, NUP62, NUP188 and help chromosomal alignment [169-172]. The NE assembly starts in the late anaphase and finishes during telophase. This process includes the recruitment of membranes and NPCs to form the complete NE [173].

4.4.3 Nuclear pore complexes

The nuclear envelope is perforated by numerous nuclear pore complexes (NPCs). NPCs are large protein structures that mediate the nucleocytoplasmic transportation of macromolecules [174]. NPCs are eight-fold symmetry structures consisting of 30 different nucleoporins.

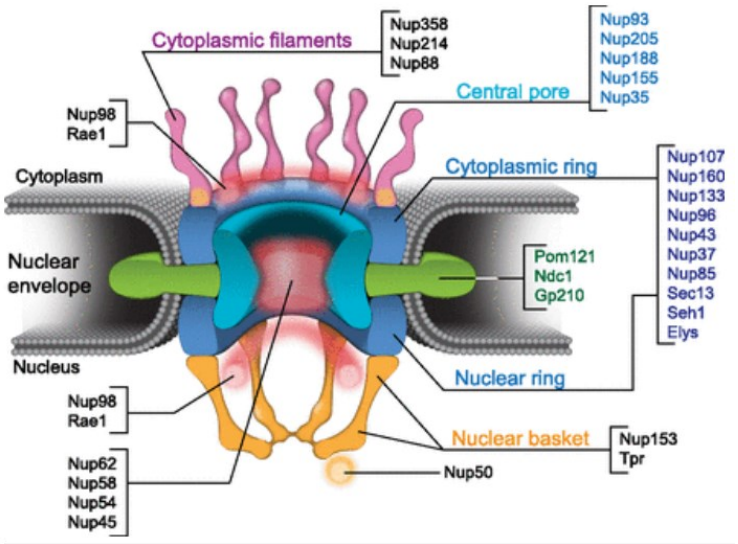

Fig. 18 Nuclear pore complexes (NPCs) structure: The NPCs are centered by a core scaffold, which surround the FG-containing nucleoporins. The core scaffold is surrounded by the cytoplasmic ring and the nuclear ring, both of which attach to eight filaments. The nuclear filaments are joined in a distal ring to fore a nuclear basket structure. The figure was obtained from Ibarra, Arkaitz, and Martin W. Hetzer. "Nuclear pore proteins and the control of genome functions." Genes & development 29.4 (2015): 337-349.

The backbone of the NPC is the three-ring structure, including a core scaffold surrounding a central transport channel, and the cytoplasmic ring and the nuclear ring, coupled with cytoplasmic filaments and the nuclear basket [175-177]. Two main protein subcomplexes form the core scaffold, the NUP93/NUP205 complex and the NUP107/NUP160 complex, attaching inner FG-containing nucleoporins such as NUP62 complex [177, 178]. Pom121, Ndc1, and Gp210 are transmembrane nucleoporins that link NPCs to the NE. The eight cytoplasmic filaments are composed of NUP358, NUP214 and NUP88, and have loose ends. The nuclear filaments are joined in a distal ring and form a nuclear basket composed of NUP153 and Tpr [177, 178].

5 Rationale and objectives

MxB has a nuclear localization sequence, which was defined as a cytoplasmic protein localizing at the cytoplasmic face of the nuclear envelope [179]. But, Bianca et al. reported MxB possesses the property to shuttle in and out the nucleus [180]. Recently, MxB was shown to localize in mitochondria and is essential for mitochondrial DNA stability [181]. However, the subcellular distribution of MxB during mitosis has not been investigated.

5.1 Determine the subcellular localization of MxB during mitosis

Our preliminary data showed that RFP-tagged MxB (MxB-RFP) formed two patches in the spindle region during mitosis. Therefore, we hypothesize MxB may associate with the centrosome in mitosis. We plan to use the anti-Aurora A and anti-gamma tubulin antibodies, two centrosome markers, to determine if exogenous MxB is localized at the centrosome. We also plan to use the anti-MxB antibody to determine if endogenous MxB is localized at the centrosome.

5.2 Determine how MxB goes to the centrosome

Mitosis is divided into prophase, metaphase, anaphase and telophase. To determine the dynamics of MxB throughout the cell cycle, we plan to transfect MxB-RFP in HeLa cells and perform live-cell imaging to determine MxB dynamics during the cell cycle. In addition, we plan to use CRISPR-Cas9 to knock in RFP to the C-terminus of MxB and generate cell clones to determine endogenous MxB dynamics during the cell cycle. By performing live-cell imaging with these cell clones, we expect to determine at which stage of mitosis MxB begins to associate with the centrosome. In addition, MxB is localized at the cytoplasmic face of the nuclear envelope and several nucleoporins at the cytoplasmic face of NE, including NUP358, NUP214, and NUP88, have been shown to associate with MxB [182]. Therefore, we hypothesize MxB may travel to the centrosome together with specific nucleoporins. We plan to transfect HeLa cells with MxB-RFP and GFP-tagged nucleoporins to determine if MxB colocalizes

with some of these nucleoporins at the centrosome in mitosis.

5.3 Determine the biological functions of MxB at the centrosome

The centrosome plays an important role in cell cycle regulation, the nucleation of microtubules, apoptosis and cancer. We plan to knock down MxB with siRNAs and examine the effect on spindle structure and chromosome segregation.

5.4 Determine whether MxB affects microtube acetylation during HIV-1 infection.

The centrosome is a microtubule organization center (MTOC). Although microtubules (MTs) are highly dynamic, subsets of these MTs are stabilized through acetylation [183]. Microtubule acetylation has been shown to facilitate HIV-1 uncoating process. Therefore, we plan to determine if MxB inhibits HIV-1-induced microtubule acetylation as one potential anti-HIV-1 mechanism.

MATERIALS AND METHODS

1. Cell culture

The adherent cell lines HeLa, TZM-bl and Huh7.5 were maintained in Dulbecco's Modified Eagle's medium (DMEM; Life Technologies) supplemented with 10% fetal bovine serum (FBS; Invitrogen). The TZM-bl cell line (NIH AIDS Reagent Program; #8129) was derived from HeLa cells, expressing CD4, CCR5, CXCR4 and HIV-1 LTR-Luc. The Huh7.5 cell (ATCC) was a generous gift from Dr. Rongtuan Lin's lab. The WM115 melanoma cell was a gift from Dr. Ian Watson's lab, maintained in RPMI supplemented with 10% FBS. All cells were maintained at 37℃ with 5% CO2.

2. Plasmid DNA

pMxB-RFP and pMxB-GFP DNA clones were generated in Dr. Chen Liang's lab [184]. pCS-H2B-cerulean (Addgene; #53748) was a generous gift from Dr. Suzanne Bechstedt's lab. The pHR_dSV40-Aurora A-GFP (#67924) was purchased from Addgene. pEGFP2-NUP58(P30483), pEGFP3-NUP153 (P30458), pPOM121-EGFP3 (P30459) were purchased from EUROSCARF. HIV-1 reporter virus construct NLENY1-IRES-ES was kindly provided by David Levy, which harbors a yellow fluorescent protein (YFP) sequence that is inserted in the *nef locus* [185].

3. Antibodies and reagents

The antibodies used include: anti-MxB produced by our lab [128], 1:100 in IF and 1:500 in WB; anti-Mx2 (NBP1-81018; Novus), 1:100 in IF and 1:500 in WB; anti-Aurora A (ab13824; Abcam), 1:1000 in IF; anti-gamma Tubulin (ab11316; Abcam), 1:200 in IF; anti-acetylated Tubulin (T7451; Sigma), 1:500 in IF and 1:2000 in WB; anti-alpha Tubulin (sc-23948; SANTA CRUZ BIOTECHNOLOGY), 1:100 in IF and 1:2000 in WB; anti-GAPDH (sc-32233; SANTA CRUZ BIOTECHNOLOGY), 1:10,000 in WB; anti-p24 (SAB3500946; Sigma), 1:5000 in WB. IFN-α-2b was obtained from Jewish General Hospital, Montreal, Canada. Western Lightning ECL Pro was purchased from

PerkinElmer (250-19371) Lipofectamine™ 3000 from Invitrogen (Lot 2067544).

4. Western blotting (WB)

Cells were lysed in RIPA buffer (50 mM Tris-HCl [pH 7.5], 150 mM NaCl, 1 mM EDTA, 1% Nonidet P-40, 0.1% SDS, and 1× protease inhibitor cocktail (Sigma)), centrifuged at 12,000 rpm for 15 min. The supernatant containing target proteins was separated on a 12% SDS/PAGE, then transferred to the PVDF membrane (Sigma). The membranes were blocked with 5% non-fat milk in 1X phosphate-buffered saline supplemented with 0.1% Tween 20 (PBST) for 1 h at room temperature. The membranes were incubated by primary antibodies in PBST supplemented with 2% BSA for 2 h at room temperature (RT), washed three times with PBST followed by anti-Mouse IgG (H+L) antibody (SeraCare; 5450-0011; 1:10000) or anti-Rabbit IgG (H+L) antibody (SeraCare; 5450-0010; 1:10000) secondary antibodies in PBST supplemented with 2% non-fat milk for 1 h at RT. Protein bands were visualized using ECL Lightning Pro by exposure to X-ray films.

5. Immunofluorescence (IF)

HeLa, Huh7.5 or WM115 cells at a density of 30, 000, 30, 000 and 40,000 cells/well respectively were seeded on the coverslip and transfected with 25 ng MxB-RFP or 25 ng MxB-GFP construct using Lipofectamine™ 3000 according to the manufacturer's directions. After 24 h, cells were treated with 5 μM RO3306 (SML0569; Sigma) for 16 h to synchronize cells at G2/M. Afterwards, RO3306 was washed off with the culture media, cells were maintained for 50 min to proceed into mitosis, before being fixed by ice-cold methanol for 15 min at -20°C and washed 3 times with PBS. Cells were blocked with 1X PBS containing 5% bovine serum and 0.3% Triton™ X-100 at RT for 1 h, then incubated with primary antibodies in 1X PBS with 2% BSA and 0.3% Triton™ X-100 at 4°C overnight. The coverslips were washed three times with PBS and incubated by Alexa Fluor 488-conjugated donkey anti-mouse secondary antibody (Invitrogen; A21202; 1:500), Alexa Fluor 594-goat anti-Rabbit secondary antibody

(Invitrogen; A21237; 1:500) or Alexa Fluor 647-goat anti-mouse secondary antibody (Invitrogen; A21237; 1:500) for an additional 40 min at RT, followed by three washes with PBS. Afterward, cellular DNA was stained with 1: 1000 DAPI(1mg/mL) for 10 min and mounted on slides. Images were acquired with Zeiss LSM800 laser scanning confocal microscope (LSM).

6. Live cell imaging

15,000 MxB-RFP knockin HeLa cells were seeded into a u-Dish 35 mm high plate (Ibidi; 190820/4) for 24 h, before 1000 IU/ml IFN-α2b was added for an additional 24 h to induce endogenous MxB-RFP expression. Cells were then treated with 5 μM R03306 for 16 h to synchronize the cells at G2/M. The nucleus was stained with 0.2 μg /ml Hoechst33342 for 10 min and washed with DMEM supplemented with 5 μM RO3306. Images were recorded with a Quorum wave FX spinning disk (SD) confocal microscope. After locating the cells under the microscope, cells were washed with DMEM, and proceeded from the G2 phase to mitosis. Images were recorded every 3 minutes for each channel and DIC. The excitation lasers and filter wavelengths were used. Hoechst 33342, 405nm, 460/50; RFP, 640nm, 690/50; GFP, 488nm, 525/50;

7. siRNA interference

siRNAs targeting MxB (siMxB-1 (5'-GCACGAUUGAAGACAUAAA-3'); siMxB-3 (5'-GGAGAAUGAGACCCGUUUA-3')) were synthesized by Sigma. Cells were transfected with 50 pmol siRNAs using Lipofectamine™ 3000 for 24 h in a 12-well plate, followed by a second transfection for another 24 h to knock down MxB before 1000 IU/mL IFN treatment to induce IFN expression.

8. gRNA design

Two guide RNAs (gRNAs) targeting human MxB were designed using the Off-Spotter tool at Jefferson Computational Medicine Center(https://cm.jefferson.edu/Off-Spotter/). Each gRNA has a NGG PAM. The gRNAs were synthesized by Invitrogen.

Table.1 gRNAs characteristics

Target gene	gRNA	start site (bp)	strand	gRNA Sequence	Reverse Complement	Length (nt)	PAM
Mx2	G1	2144	-	CAGGCATCGCCGCCCTTCAG	CTGAAGGGCGGCGATGCCTG	20	CGG
2148bp	G2	2129	+	CCAGCAAAGAGATCCACTGA	TCAGTGGATCTCTTTGCTGG	20	AGG

9. Use CRISPR-Cas9 to knock in RFP to the C-terminus of MxB in HeLa and WM115 cells

To generate cell clones expressing the fusion protein MxB-RFP under IFN stimulation, two guide RNAs were cloned into the CRISPR v2 vector (Addgene plasmid #52961), which expresses a mammalian Cas9 protein and confers resistance to puromycin and ampicillin. The donor DNA has a inserted sequence containing 1000 bp left homology arm followed by 711bp tRFP and 1000 bp right homology arm of MxB in the pUC57 vector, which was generated and purchased from BIOMATIK.

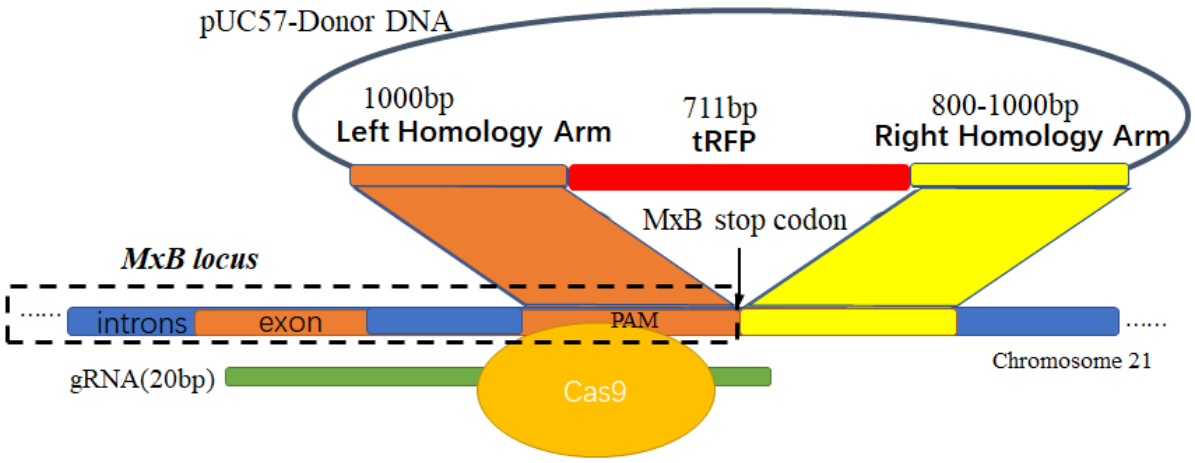

Fig. 19 Schematic of CRISPR-Cas9 MxB RFP knockin. Dotted frame represents *MxB locus* in chromosome 21; The guide RNA (green bar) recognizes the target sequence, and the CRISPR-associated endonuclease (Cas) cuts the targeted sequence. PAM is a short DNA sequence usually 2-6 base pairs, required for a Cas nuclease to cleave the DNA, and PAM is generally found 3-4 nucleotides downstream from the cut site.

HeLa and WM115 cells were seeded at a density of 1.0×10^5 cells/well and 2.0×10^5 cells/well respectively in a 6-well plate for 24 h and co-transfected with 1μg donor DNA and 1μg guide RNA (G1 or G2) with Lipofectamine™ 3000 (Invitrogen; Lot 2067544) for 48 h. Next, HeLa and WM115 cells were selected by puromycin (Invivogen) at 1 μg/mL and 2 μg/mL respectively for two weeks. The selected G1 and G2 pools were treated with 1000 IU/ml IFN-α-2b to induce MxB-RFP expression. After 24 h, the pools were trypsinized, suspended with PBS supplemented with 2% FBS and centrifuged at 1,500 rpm twice, 5 min each. The pools were re-suspended and filtered through 40 μm filter into the polystyrene round-bottom BD Falcon tubes to generate single-cell suspension. The RFP expressing cells were sorted into the 96-well-plate. Prepare conditioned medium and add medium into the 96-well-plate before single cell sorting. The conditioned medium is composed of cell culture supernatant and MEM medium (Gibco, Lot 1930003) supplemented with 20 % FBS at the ratio of 1:1. Cell culture supernatant contains growth factors that stimulate the growth of the single cell. The cell sorting process was performed with BD FACSAria Fusion by Christian Young. The insertion of RFP to the C-terminal end of MxB was confirmed by sequencing.

10. Flow cytometry

The HeLa and WM115 MxB-RFP knock-in cell clones were seeded at a density of 2.0×10^5 cells/well and 5.0×10^5 cells/well respectively in the 6-well plate. After 24h, these cells were either treated with 1000 IU/mL IFN for another 24 h to induce MxB-RFP expression or no IFN treatment as the control. The wild-type HeLa and WM115 cells were used as the negative control. After 24 h, the cells were trypsinized, washed with PBS supplemented with 2% FBS by centrifuging at 1,500 rpm twice and fixed by 500 μL 2% paraformaldehyde (PFA) at 4°C for 10 min. The percentage of RPF expression cells was scored by flow cytometry by counting 20,000 cells with LSRFortessa.

11. HIV-1 infection

HIV-1 reporter virus was produced by transfecting HEK293T cells with proviral DNA clone NLENY1-ES-IRES. The pVSV-G plasmid was cotransfected to produce HIV-1 particles that carry the VSV glycoprotein required for viral entry. The amounts of VSV-G pseudotyped HIV-1 reporter virus produced were determined by measuring HIV-1 capsid/p24 by enzyme-linked immunosorbent assay. TZM-bl cells at a density of 30 000 cells/well for IF and 60,000 cells/well for WB were seeded on the 12-well-plate. After 24 h, the cells were transfected with MxB or mock-transfected for 24 h and then infected with VSV-G pseudotyped NLEY1-ES-IRES viruses at an amount of virus equivalent to 50 ng p24. After 2 h or 6 h post-infection, the cells were washed three times with DMEM and lysed by RIPA lysis buffer for WB or fixed by methanol for IF.

12. Statistical analysis

The colocalization analysis was performed in ZEN 3.3 (blue edition). All values are expressed at means±SD.

RESULTS:

1 MxB localizes to the centrosome in mitosis.

1.1 MxB-RFP and MxB-GFP localized to the centrosome.

MxB is localized to the nuclear pore complexes (NPCs) in the cytoplasmic face of the nuclear envelope and shuttles between the nucleus and the cytoplasm [114, 130, 133, 134]. Localization to the NPC facilitates MxB inhibiting the nuclear import of HIV-1 DNA and proteins since NPCs mediate the nuclear transport of macromolecules [126-128]. Recently, MxB was reported to localize at the mitochondria and plays an important role in mitochondria DNA stability, suggesting MxB has other cellular functions [181]. However, the subcellular localization of MxB during mitosis is unknown. To test this, we transfected HeLa cells with plasmid DNA pMxB-RFP and performed a live-cell imaging assay. RO3306, a CDK1 inhibitor, was used to synchronize cells at G2/M. After localizing the cells under the confocal microscope, RO3306 was washed off with the culture media, allowing the cells to process into mitosis. At interphase, we found that the majority of MxB-RFP was mainly localized at the nuclear envelope, with minute amount in the cytoplasm and the nucleus. During mitosis, when the nuclear envelope broke down, MxB-RFP first associated with the condensed chromosomes, then enriched to form two patches as chromosomes are aligned along the equatorial plane (Fig. 20).

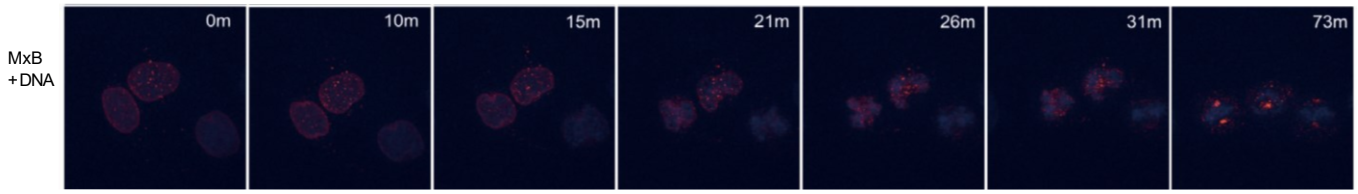

Fig. 20 Live-cell imaging of exogenous MxB. HeLa cells were transfected with pMxB-RFP. After 24 h post transfection, the cells were treated with 5 μM RO3306, a CDK1 inhibit to synchronize the cells in G2/M for 16 h. Nucleus was stained with 0.2 μg/ml Hoechst33342. After localizing the cells under confocal microscope, RO3306 was washed off with the culture media supplemented with 0.2 μg/ml Hoechst33342. Images were recorded every 5 minutes for each channel and DIC. The data was obtained with permission from Cynthia McMahan, a previous honor student.

Based on the position of two MxB-RFP patches at metaphase, we suspected that MxB are localized to the centrosomes which occupy the two poles and form spindles at metaphase. To test this possibility, we performed immunofluorescence to stain two centrosome markers, Aurora A and gamma tubulin. At metaphase, MxB was colocalized with Aurora A and gamma tubulin (Fig. 21 A and B). The same observation was made in both HeLa cells and Huh7.5 cells but not in WM115 cells, which suggests that MxB-RFP localization to the centrosome at metaphase is cell type-dependent.

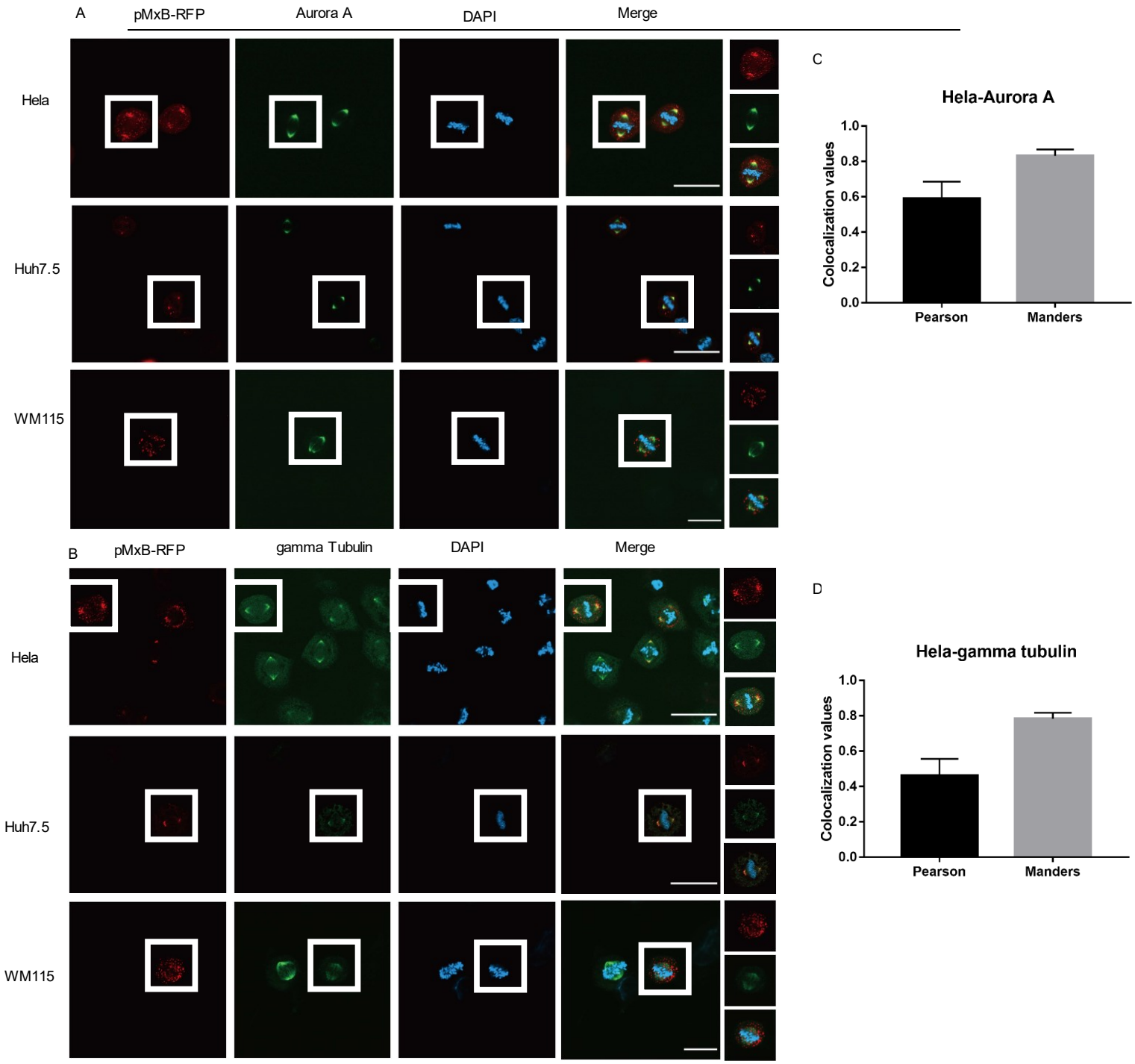

Fig. 21 MxB-RFP localizes to the centrosome in mitosis. HeLa, Huh7.5 or WM115 cells were transfected with 25 ng pMxB-RFP. After 24 h post transfection, the cells were treated with 5 μM RO3306 to synchronize the cells in G2/M for 16 h. Afterwards, RO3306 was washed off with the culture media, cells were maintained for 50 min to proceed into mitosis, before being fixed by ice-cold methanol and stained with anti-Aurora A or anti-gamma Tubulin antibodies. Nucleus was stained with DAPI. (A) MxB localizes to the centrosome with Aurora A in HeLa, Huh7.5, but not in WM115 cells. (B) MxB localizes to the centrosome with gamma tubulin in HeLa, Huh7.5, but not in WM115 cells. Colocalization coefficients (Pearson and Manders coefficient values) of MxB-RFP with AuroraA (C) or gamma Tubulin (D) in HeLa cells were determined by randomly selecting 20 cells and analyzed with ZEN 3.3 (blue edition). Data are representative of at least three independent experiments, and values are expressed at means±SD.

To rule out the possible effect of RFP on the observation, we tested MxB-EGFP in HeLa cells, and again observed co-localization of MxB-EGFP with Aurora A at metaphase (Fig. 22).

We next examined whether MxB is already colocalized with gamma tubulin at interphase. Gamma tubulin marks the location of MTOC at interphase (Fig. 23), whereas Aurora A is mostly dispersed in the nucleus and only co-localizes with gamma tubulin during mitosis to form the centrosome. The majority of MxB-RFP is localized at the nuclear envelope, but not co-localized with gamma tubulin (Fig. 23). Therefore, MxB is not localized to MTOC at interphase but is recruited to centrosome during mitosis together with other centrosome proteins.

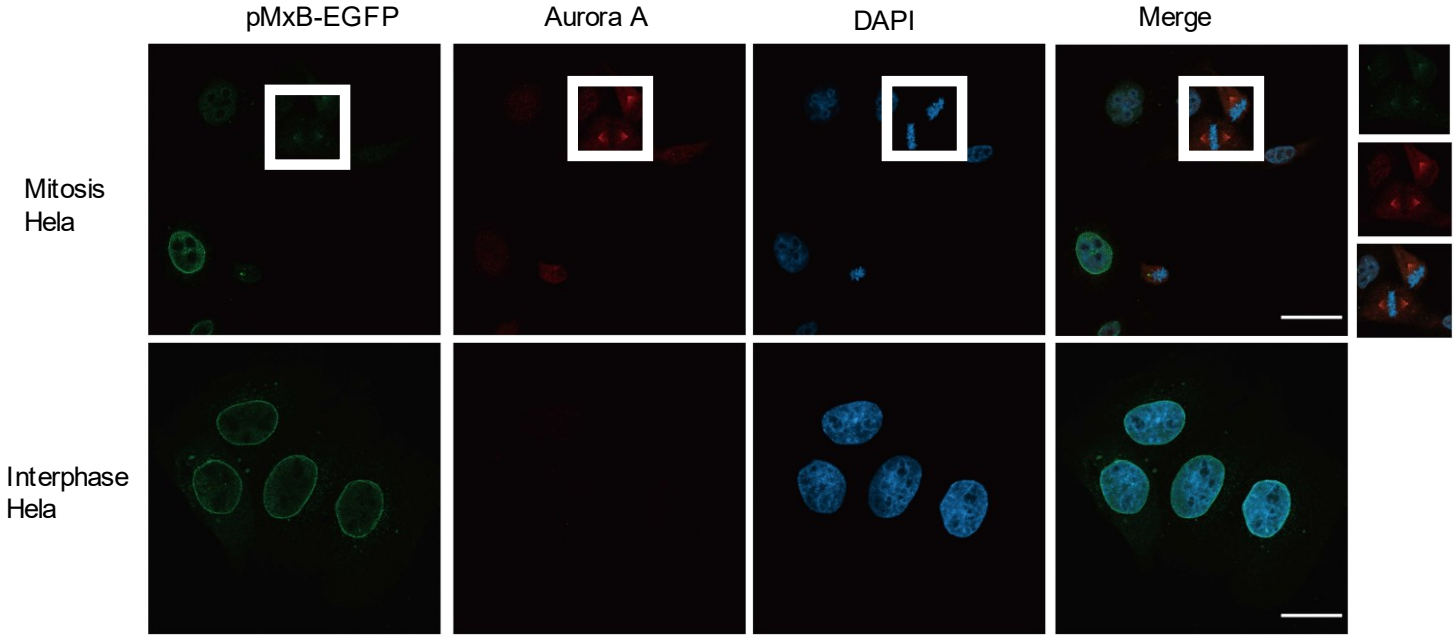

Fig. 22 MxB-EGFP localizes to the centrosome in mitosis. HeLa cells were transfected with 25 ng pMxB-RFP. After 24 h post transfection, the cells were treated with 5 μM RO3306 to synchronize the cells in G2/M for 16 h. Afterwards, RO3306 was washed off with the culture media, cells were maintained for 50 min to proceed into mitosis, before being fixed by ice-cold methanol and stained with anti-Aurora. Nucleus was stained with DAPI. As predicted, MxB-EGFP localized to the nuclear envelope in interphase and distributed in the cytoplasm in puncta, while MxB-eGFP formed two patches and colocalized to the centrosome with Aurora A in mitosis.

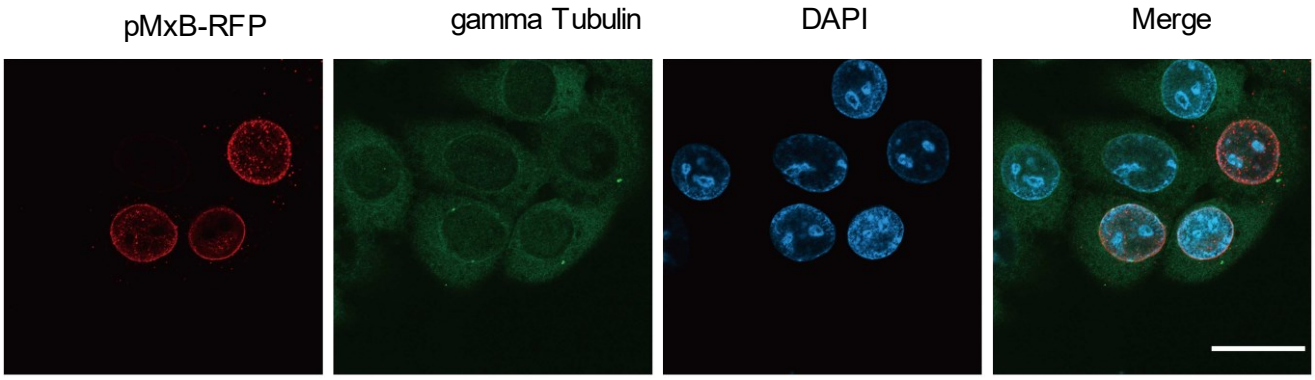

Fig. 23 MxB-RFP is not localized to the centrosome at interpahse. HeLa cells were transfected with 25 ng pMxB-RFP. After 24 h post transfection, the cells were treated with 5 μM RO3306 to synchronize the cells in G2/M for 16 h and fixed by ice-cold methanol and stained with anti-gamma Tubulin. Nucleus was stained with DAPI. As predicted, MxB-EGFP localized to the nuclear envelope in interphase and distributed in the cytoplasm in puncta, while MxB-EGFP formed two patches and colocalized to the centrosome with gamma Tubulin in mitosis.

1.2 The knock-in MxB-RFP is localized at the centrosome

We next asked whether endogenous MxB is localized at the centrosome. We first treated HeLa cells and Huh7.5 cells with IFN-α-2b (1000 IU/ml) for 24 hours to induce MxB expression and performed immunofluorescence microscopy using the anti-MxB (CL) generated from us [128]. With anti-MxB (CL), IF showed that endogenous MxB is localized at the nuclear envelope, the cytoplasm and the nucleus in interphase, and colocalized with Aurora A and gamma tubulin in mitosis with IFN treatment (Fig. 24 A-D).

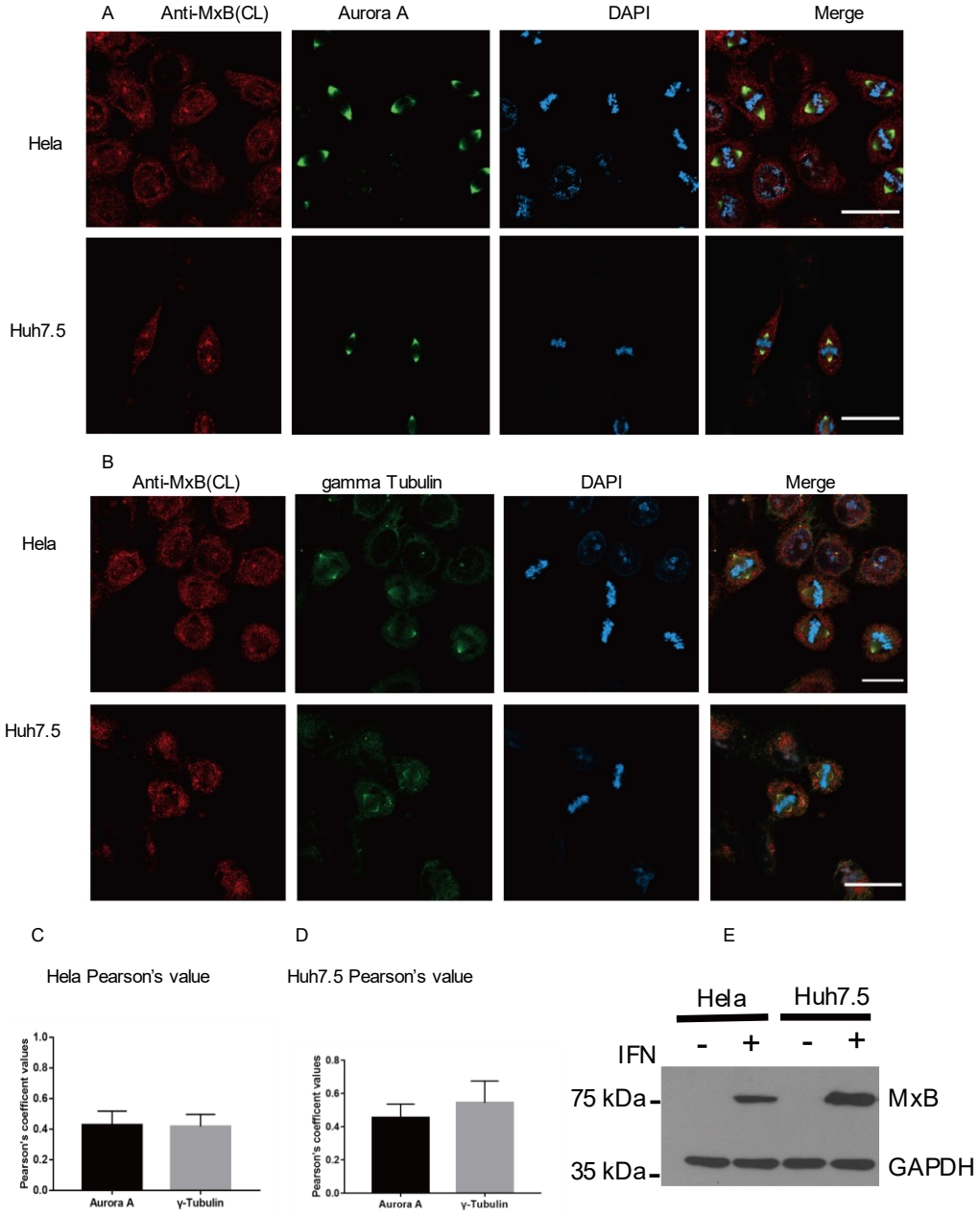

Fig. 24 Endogenous MxB localization. (A) Immunofluorescence images of HeLa and Huh7.5 cells stained by the Anti-MxB (CL) antibody with Aurora A (A) or gamma Tubulin (B). The cells were treated with 1000 IU/ml IFN-α-2b for 24 h to induce MxB expression before synchronization by RO3306 for 16 h. Endogenously expressed MxB is localized at the centrosome in HeLa and Huh7.5 cells. Colocalization coefficients (Pearson and Manders coefficient values) of MxB (Red) with AuroraA (C) or gamma Tubulin (D) were determined by randomly selecting 20 cells and analyzed with ZEN 3.3 (blue edition). (E) WB result of the cells treated with 1000 IU/ml IFN-α-2b with anti-Mx2(Novus Biologicals)

We next sought to examine the dynamics of MxB in the cell cycle in live cells to determine when MxB goes to and leaves the centrosome and determine the localization of endogenous MxB in mitosis. We used CRISPR-Cas9 technology to knock in RFP to the C-terminus of MxB in HeLa and WM115 cells. The WM115 cell is a melanoma cell line with an appreciable basal level of endogenous MxB [186]. Two guide RNAs targeting the MxB gene and the donor DNA were co-transfected to the cells, and the cells were selected by puromycin. The G1 and G2 pools were treated with 1000 IU/ml IFN to induce MxB expression and sorted into single cell clones. These RFP knock-in cell clones endogenously express the MxB-RFP fusion protein in the presence of IFN. In HeLa cells, we generated 5 clones based on G1, and 3 clones based on G2. In WM115 cells, we generated 2 clones in both guide RNAs. The MxB-RFP knockin cell clones were identified by flow cytometry (Fig. 25A), and further verified by Western blotting (Fig 25B). The knocked in RFP sequence was confirmed by sequencing (see Appendix). In WM115 cell clones, we found MxB has a basal level expression of MxB, with approximately 60%-70% of the two G1 WM115 cell clones expressing RFP without IFN treatment, although only around 1% in the two G2 clones. When IFN was added to induce MxB expression, more than 97% of WM115 cells expressed RFP in all four clones. In HeLa cell clones, there was no RFP expression without IFN treatment, which is consistent with the WB result. When IFN was added, the five G1 HeLa clones expressed RFP with a percentage ranging from 64% to 87%. The G2 HeLa clones showed a similar pattern, but two cell clones showed an MxB knockout effect. Those two G2 clones failed to express MxB under IFN treatment based on WB and IF (Fig. 25A and 25B). In addition, we observed two bands in WB with the size ranging from wild-type MxB and MxB-RFP. We hypothesize it is the result of alternative translation initiation.

Next, we used the cell clones to test RFP knock-in MxB localization during the cell cycle. We used IFN to induce MxB expression.

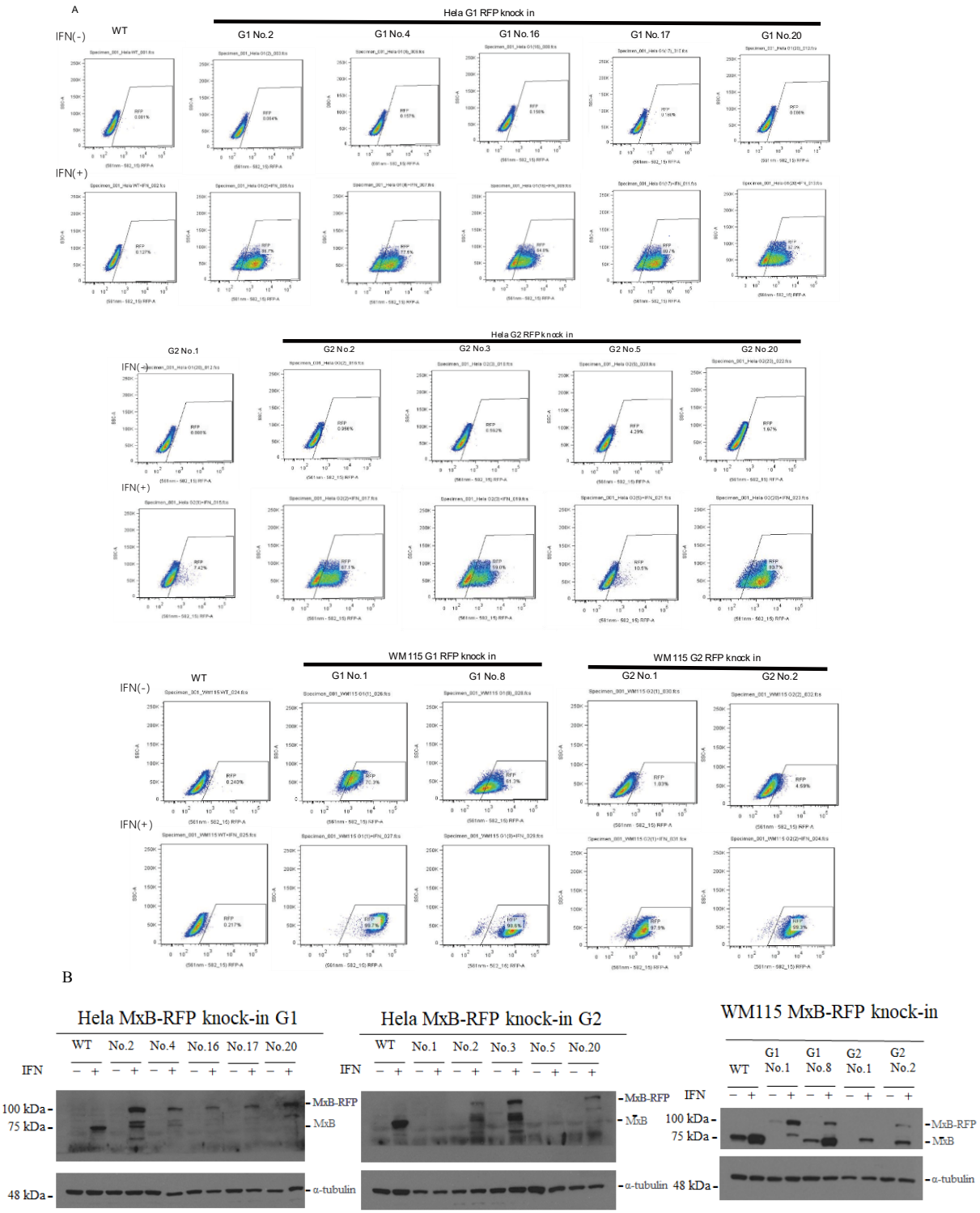

Fig. 25 tRFP was knockin to the C-terminus of MxB. (A) Flow cytometry analysis of 10 HeLa clones (5 G1 and 5 G2) and 4 WM115 clones (2 G1 and 2 G2). (B) Western blotting analysis of 10 HeLa clones (5 G1 and 5 G2) and 4 WM115 clones (2 G1 and 2 G2).

Confocal images showed that most endogenously expressed MxB-RFP is localized at the nuclear envelope, with minute amount in the cytoplasm and the nucleus (Fig. 26A). In addition, we stained the cells with the centrosome marker Aurora A and found MxB formed two patches and colocalized with Aurora A at the centrosome in mitosis in HeLa cells, while MxB diffused into the cytoplasm in WM115 cells (Fig. 26B and 26C). This result is consistent with the localization of exogenous MxB (Fig. 26D), supporting the localization of MxB to the centrosome is cell type-dependent. In conclusion, both the exogenous and endogenous MxB are localized to the centrosome during mitosis.

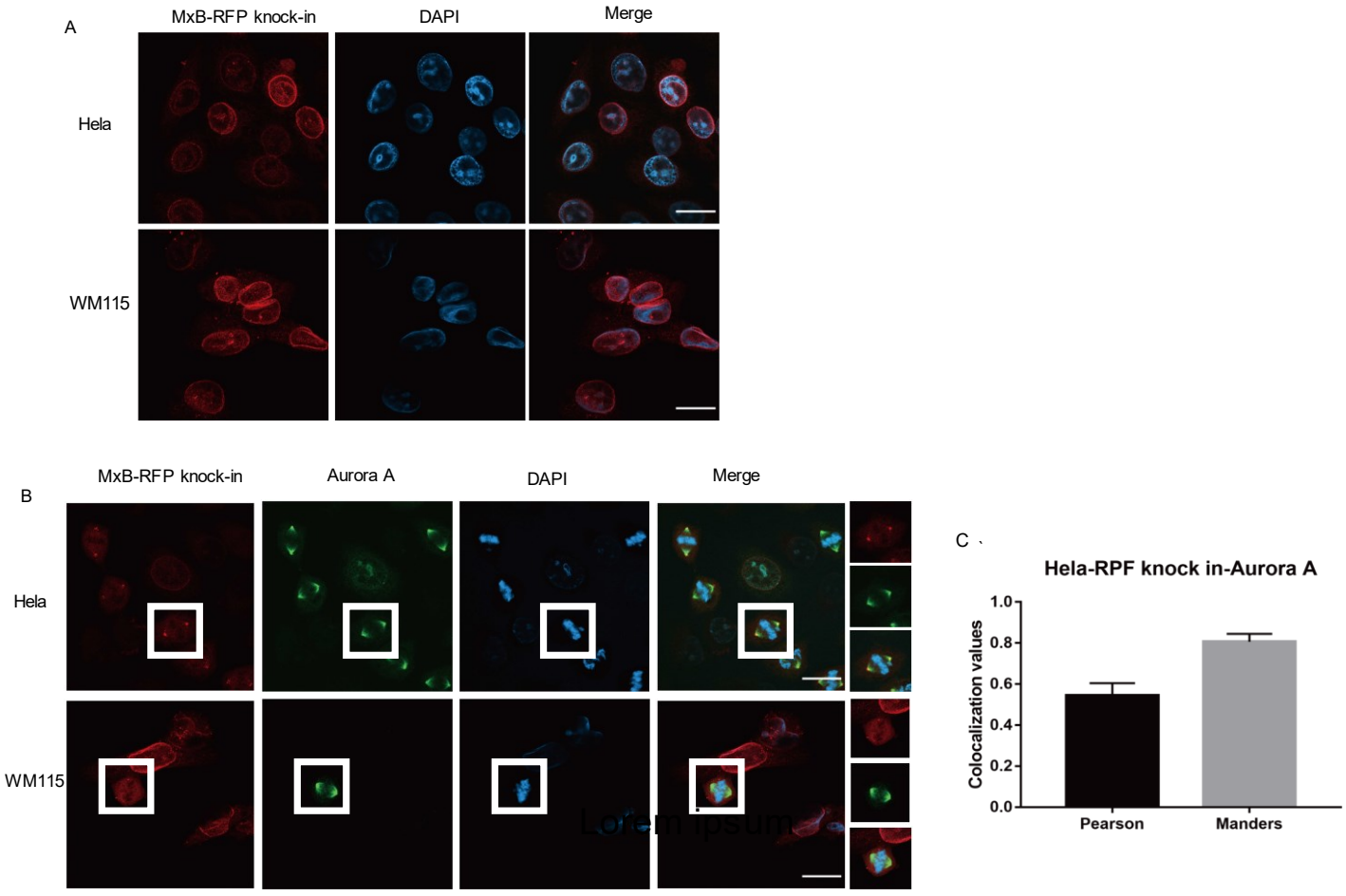

Fig. 25 MxB is localized at the centrosome in the CRISPER-Cas9 knock-in cell. (A) With IFN treatment, MxB is induced in HeLa and WM115 cell clones, which is localized at the nuclear envelope. (B) IF images of HeLa G1 no.20 and WM115 G1 no.8 stained by Aurora A. MxB is localized at the centrosome in mitosis in HeLa cells, but not in WM115 cells. (C) Colocalization coefficients (Pearson and Manders coefficient values) of MxB-RFP with AuroraA were determined by randomly selecting 20 cells and analyzed with ZEN 3.3 (blue edition).

MxB is not associated with gamma tubulin at interphase. To determine at which stage of mitosis MxB begins to associate with the centrosome, we recorded the dynamic of endogenous MxB during mitosis by live-cell imaging. The HeLa G1 No.2 was used due to its high expression of MxB-RFP based on the data of western blotting and flow cytometry. The cells were transfected with the plasmid DNA pHR_dSV40-Aurora A-GFP to indicate the centrosome formation. After 24 h, the cells were treated with 1000 IU/ml IFN for another 24 h to induce MxB-RFP expression before being synchronized with RO3306. The cells were washed with DMEM to free the inhibition of RO3306, allowing the cells to transit through G2/M. Unfortunately, plasmid DNA seemed to interfere with endogenous MxB-RFP expression. Therefore, we only used IFN to induce MxB-RFP expression. In interphase, MxB is localized at the nuclear envelope. At 30 min after the drug was washed off, the nuclear envelope began to break down (NEBD), resulting in nuclear envelope invaginations (Fig. 27). MxB is enriched in the invagination regions. MxB accumulated as the cell cycle progresses and forms two big patches at metaphase, but it dispersed into the cytoplasm in early anaphase and re-localized to the NE in late anaphase when the cells began to assemble the NE (Fig. 27). These data suggest that MxB begins to aggregate in the late prophase, likely when the centrosome also starts to form.

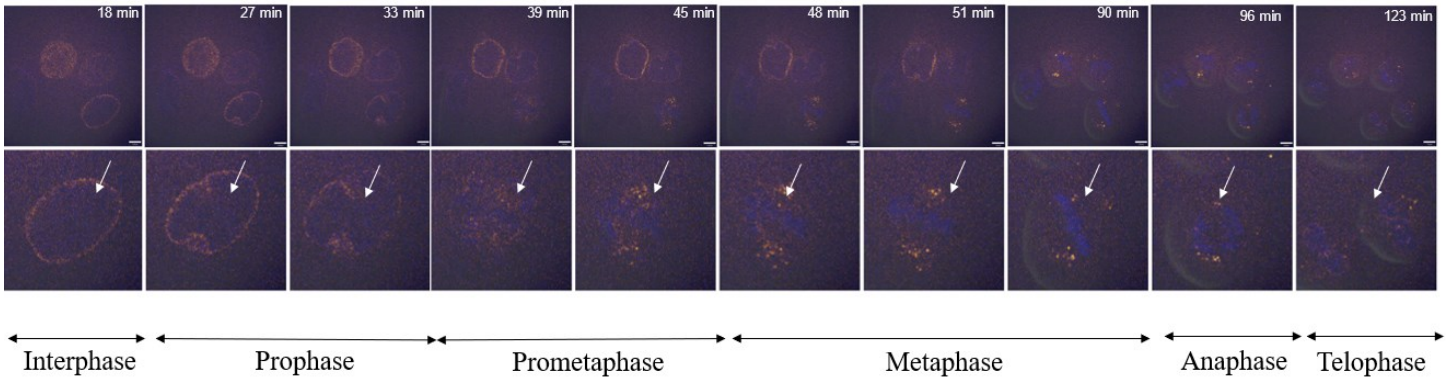

Fig. 27 Live cell-imaging of CRISPR-Cas9 knock-in HeLa G1 no. 2 cell. The cells were treated with 1000IU/ml IFN for 24 h to induce MxB-RFP expression and the cell was synchronized with RO3306 for 16 h. The nucleus was visualized with Hoechst33342.

2 Investigating the colocalization of MxB and nucleoporins during mitosis.

The nuclear envelope is occupied by NPCs consisting of several copies of 30 different nucleoporins [178]. NUP58 is one of the FG-NUPs, a component of the NUP62 complex that is attached to the inner side of the core scaffold [178, 187]. NUP58 and NUP62 were reported to localize at the centrosome in mitosis and are essential in centrosome homeostasis [170]. The eight cytoplasmic filaments are composed of NUP358, NUP214 and NUP88, and have loose ends. The nuclear filaments are jointed in a distal ring and form a nuclear basket composed of NUP153 and Tpr [177, 178]. In addition, multiple components of nuclear pore complexes (NPCs) interact with the amino-terminal of MxB, including NUP358, NUP214, NUP98 in the nuclear envelope [182]. The localization of NUP358 to the centrosome is essential in chromosomal alignment [169]. We hypothesized MxB might maintain association with specific nucleoporins to the centrosome to regulate the centrosome functions. To test this, we co-transfected HeLa cells with MxB-RFP and EGFP-tagged nucleoporins, including pNUP58-GFP, pNUP153-GFP, NUP358-GFP and pNUP121-GFP to examine whether they colocalize at the centrosome in mitosis.

The result showed that these nucleoporins were localized at the nuclear envelope in interphase, although some NUP358 appeared diffused in the cytoplasm (Fig. 28A). In mitosis, MxB formed two patches. NUP58, pNUP153 and pNUP121 appeared diffuse in the cytoplasm and NUP358 was not detected (Fig. 28B). Further experiments are warranted to characterize the localization of nucleoporins in mitosis to verify the reports in the literature [169, 170, 188].

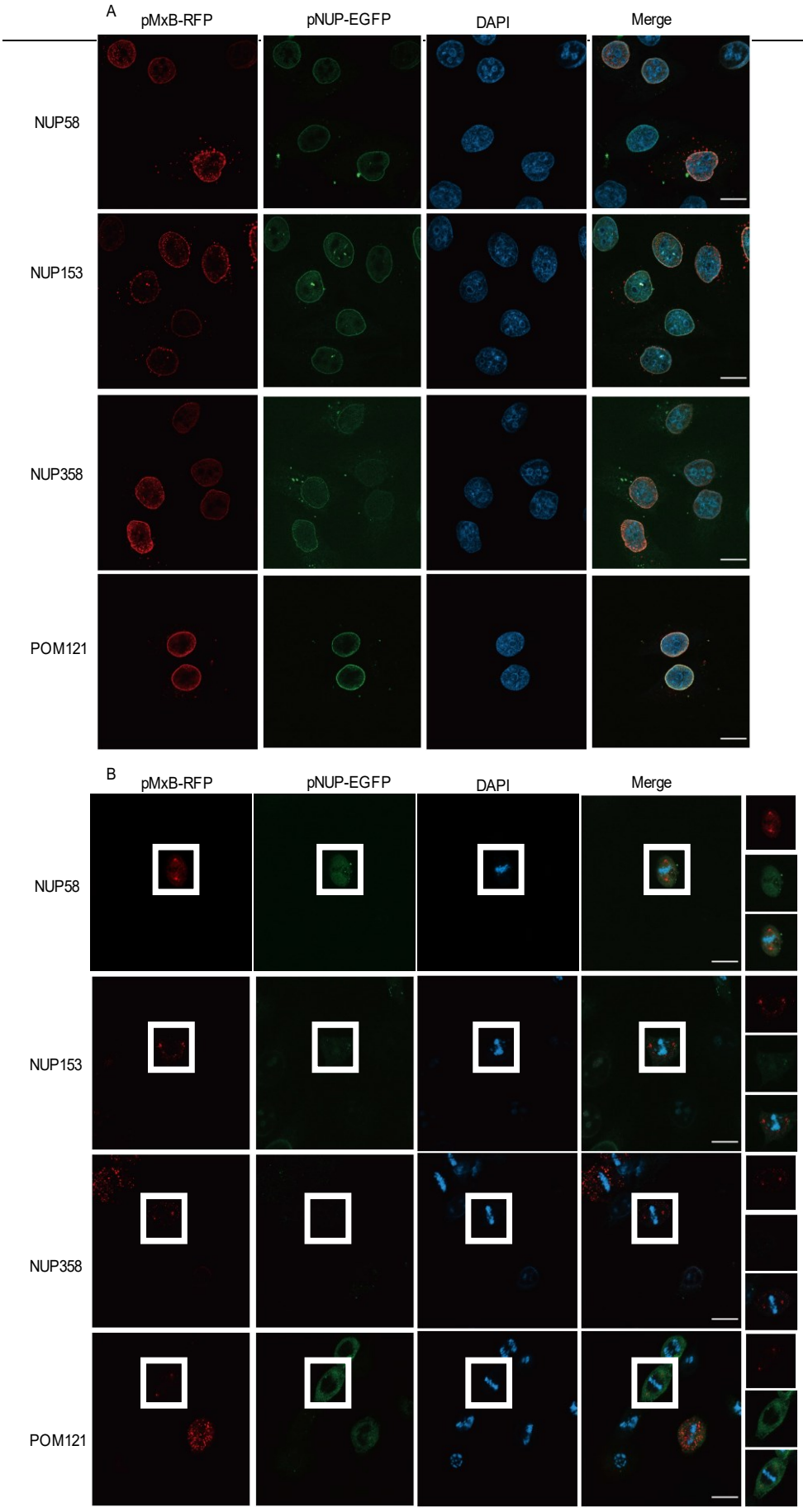

Fig. 28 MxB does not localize to the centrosome with nucleoporins. Representative images of HeLa cells transfected with MxB-RFP and pNUP58-GFP, pNUP153-GFP, pNUP358-GFP or pPOM121-GFP for 24 h followed by RO3306 treatment for 16 h. The nucleus was visualized by DAPI. (A） MxB and the four nucleoporins tested were localized at the nuclear envelope. (B) MxB was localized at the centrosome in mitosis, but the four nucleoporins diffused into cytoplasm.

3 MxB KD is associated with chromosome misalignment

The centrosome has a central role in the formation of spindles and faithful segregation of chromosomes into two daughter cells [147-149]. We, therefore, examined whether MxB has an impact on the spindle structure. We used two small interference RNAs (siRNA) to knock down MxB in the HeLa MxB-RFP knock-in cell line and stained the spindle with alpha Tubulin. HeLa G1 No. 20 cells were treated with siMxB-1, siMxB-3 or control. After 24 h, the cells were re-transfected with siRNAs for another 24 h before 1000 IU/mL IFN to induce endogenous MxB expression. In the control group, MxB-RFP fusion protein was induced and localized at the nuclear envelope, while in the two siRNA groups, we did not observe MxB-RFP signal, suggesting MxB was knocked down (Fig. 29A). The spindle is a steady-state structure, and the key feature is the bipolar and antiparallel MTs [189]. MxB KD seemed to have no impact on spindle structure, which maintained twofold symmetry (Fig. 29B), although we observed abnormal alpha tubulin in the siMxB-3 group (Fig. 29A). This abnormal alpha Tubulin could result from different Z-stack when I acquired the image data, and only one image was recorded here. Therefore, I will repeat the experiment. As metaphase begins, the centrosome aligns along the equatorial plane and the kinetochore MTs from the spindle poles attach to the kinetochore of the centrosome. Our result shows that the chromosomes align well in the control group and approximately half of the MxB KD mitotic cells had a 5-fold increase in chromosome misalignment compared to the control group (Fig. 29B and 29C), suggesting MxB is involved in ensuring proper chromosome alignment and eventual segregation of chromosomes. We also examined whether MxB knockdown can cause chromosome misalignment in HeLa cells in the absence of IFN treatment because HeLa cells have been shown to have a basal level of MxB expression [134, 181]. Indeed, MxB KD led to chromosome misalignment but had no impact on the spindle structure (Fig. 29D and 29E). Our data suggest a functional role of MxB in mitosis as a result of its localization to the centrosome.

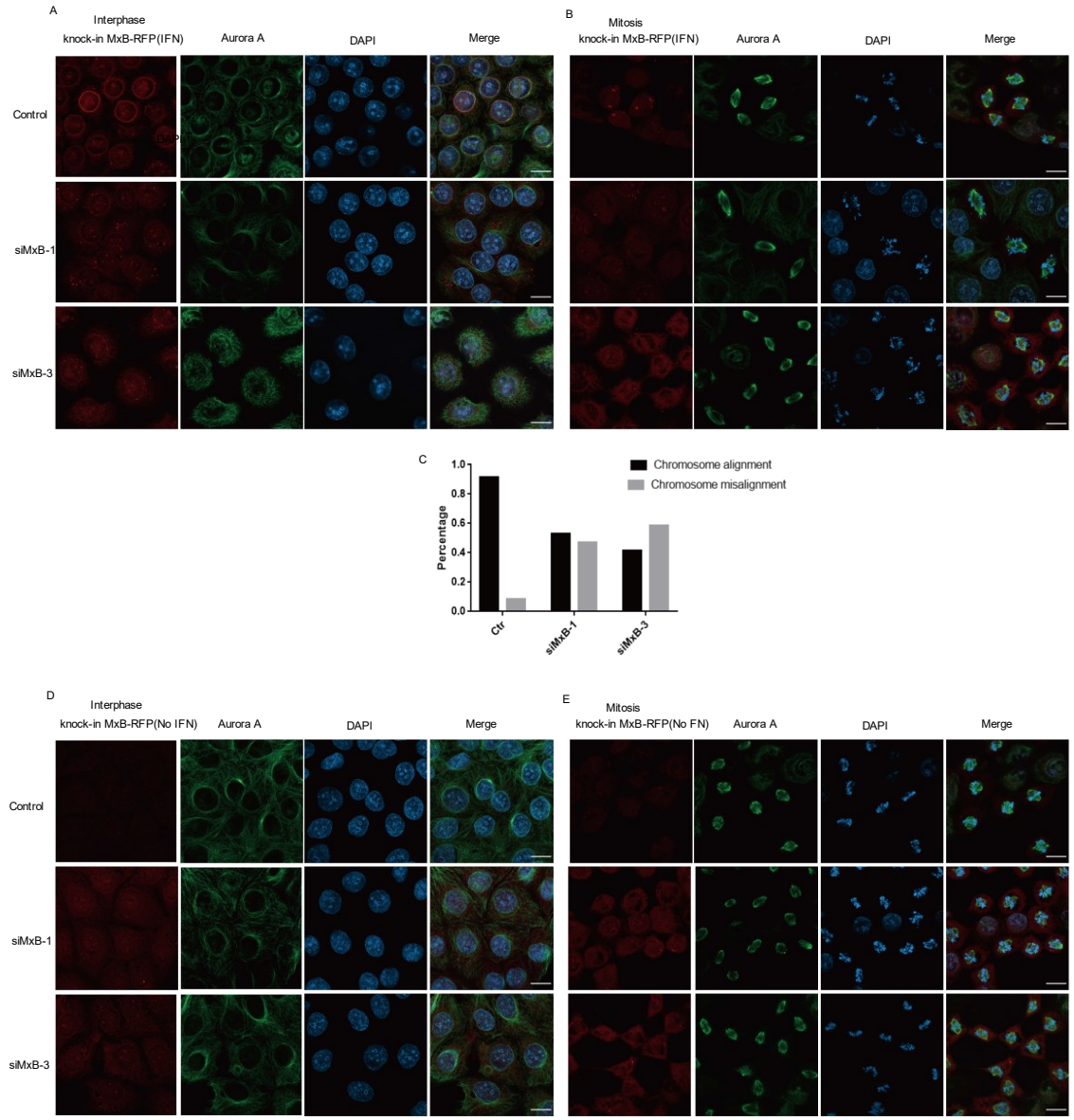

Fig. 29 MxB KD is associated with chromosome misalignment. Representative images of a HeLa RFP knock-in clone stained by alpha Tubulin (Green) and the nucleus was visualized by DAPI. The cell clone was treated with siRNAs or mock transfection before 1000IU/ml IFN treatment to induce MxB-RFP expression. MxB is induced in the mock transfection group, but not in the two siMxB groups (A). Chromosome alignment was observed in the mock transfection group, while MxB KD leads to chromosome misalignment in the metaphase (B). (C) The percentage of the cells with chromosome misalignment was calculated by randomly selecting > 90 cells. (D and E) representative images of the cells without IFN treatment. Chromosome misalignment was observed in the cell without IFN treatment

4 The impact of MxB and HIV-1 infection on MTs acetylation.

Although microtubules (MTs) are highly dynamic, subsets of these MTs are stabilized through the process of acetylation or tyrosination and basal level expression of acetylated microtubules (Ac-MTs) was observed by WB and IF [183]. Microtubule stabilization has been shown to facilitate HIV-1 uncoating. HIV-1 infection dramatically increases the expression of Ac-MTs [183]. Transfected with pGag-HA and pMA-HA can also show this phenotype, which indicates MA plays a critical role in the acetylation of microtubules. Therefore, we hypothesize MxB associate with unknown MTs associated proteins and inhibit MTs acetylation to restrict HIV-1 infection. To test this hypothesis, we transfected TZM-bl cells with MxB and used HIV-1 to infect the cells to examine if MxB can counteract HIV-1 induced Ac-MTs. The HIV-1 used is a reporter virus called NLEY1-ES-IRES, which harbors a yellow fluorescent protein (YFP) sequence inserted into Nef [185]. However, we failed to repeat the result, which showed HIV-1 infection upregulated Ac-MTs. Our result showed no detectable differences in Ac-MTs between HIV-1 infected cells (2h and 4h infection) and uninfected cells, and the expression of MxB has no detectable impact on the Ac-MTs (Fig. 30A). The WB result is consistent with the IF result that HIV-1 infection didn't upregulate the expression of Ac-MTs (Fig. 30B). MxB seems to downregulate α-tubulin and HIV-1 infection seems to downregulate α-tubulin in the 2h group. We noticed that the cell line we used was different. HIV-1-VSV infection was shown to increase the expression of Ac-MTs in NHDFs, CHME3 cells and primary human macrophages [183]. We used TZM-bl cells, which is derived from HeLa cells, although harboring the receptors required for HIV-1 infection. It is possible that HIV-1-induced MTs acetylation may be cell type-dependent.

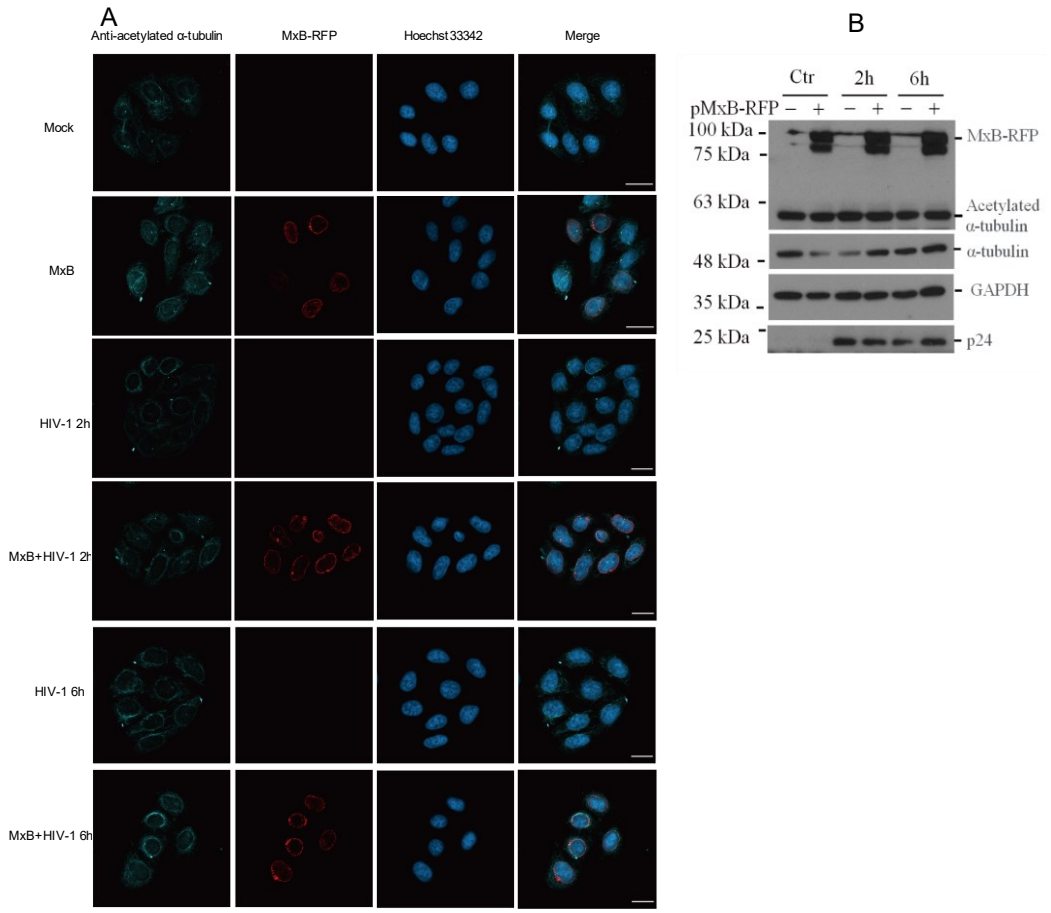

Fig. 30 The impact of MxB and HIV-1 infection on MTs acetylation. (A) Representative images of TZM-bl cells stained by anti-acetylated microtubules antibody. MxB-RFP was transfected for 24 h before HIV-1 infection for 2 h or 6 h. A basal level expression of acetylated microtubules was observed. The first second line images showed that MxB has no impact on acetylated microtubules, which is consistent with the WB result (B). MxB seems to downregulate α-tubulin expression. HIV-1 infection was confirmed by WB, but HIV-1 infection didn't show to influence the level of acetylated microtubules, although HIV-1 infection for 2 h seems to downregulate α-tubulin expression.

DISCUSSION

This study reported an unexpected MxB subcellular localization to the centrosome during mitosis, and MxB plays an essential role in chromosome alignment. It is the first study to demonstrate the dynamics of endogenous MxB throughout the cell cycle by generating MxB-RFP knockin cell clones. Most exogenous MxB was shown to localize at the cytoplasmic face of the nuclear envelope [130, 133, 134]. Recently, MxB was shown to be localized at the mitochondria and played an important role in the stability of mitochondria DNA [181]. Here we found MxB localizes to the centrosome in mitosis, and MxB KD results in chromosome misalignment, suggesting MxB has a broad subcellular localization in the cytoplasm and performed other unknown essential cellular functions. Hong Cao et al. failed to generate viable HeLa MxB-knockout clones, which further strengthened the essential function of MxB within the cells. We identified the localization of MxB to the centrosome is cell type-dependent. MxB has 76 kDa or 78 kDa isoforms due to an alternative start codon at position 26. The longer isoform has a nuclear localization signal (NLS) in the first 25 amino acids essential for localization to the nuclear envelope and antiviral activity. In contrast, the short isoform is observed in the cytoplasm [133]. But this opinion is challenged by Hong Cao et al., who found MxB varied its expression patterns in different tissues and cell lines[181]. A high endogenous MxB expression was observed in the human liver, lymph node, testis, and tonsil, while no endogenous MxB expression in the human brain, lung, and spleen tissues. Of those human tissues expressing endogenous MxB, lymph node and tonsil have two bands, while others have a single band [181]. Similarly, compared to HeLa and Huh7.0 cells, primary hepatocytes and melanoma cells have the basal level expression of endogenous MxB, although MxB band was observed with longer exposure [181, 186]. Under IFN induction, HeLa and primary hepatocytes have two MxB bands, while melanoma and Huh7.0 has single band [181, 186]. This observation showed that MxB expression pattern varied in cell types, which strengthens the idea that MxB's localization to the centrosome is cell type-dependent.

MxB has been shown to localize to at least two organelles. Hong Cao et al. showed a fusiform and linear staining pattern in HeLa cells with three different anti-MxB antibodies, including the one produced in our lab. However, we didn't observe the fusiform and linear staining patterns. Instead, we found MxB diffused into the cytoplasm with the anti-MxB (CL) antibody. With the MxB-RFP knockin cell clones, we observed most endogenous MxB localized to the nuclear envelope with minute amount of puncta MxB near the nuclear envelope, which is approximately the localization of ER. Indeed, exogenous MxB was reported to partially localize to the ER and inhibits Hepatitis C virus (HCV) replication by preventing the localization of HCV nonstructural protein 5A (NS5A) to ER and downregulating nonstructural protein 3 (NS3) [130]. NS3 and NS5A are essential components of the HCV replication complex. NSP5 interacts with other viral proteins (NS4B, NS5B) and host proteins (cyclophilin A, kinases, etc.) to mediate HCV replication and assembly[190, 191]. Our study suggests endogenous MxB might localize to the ER and restrict HCV replication. Human MxA is accumulated in the cytoplasm under IFN treatment and inhibits a variety of DNA and RNA viruses. The subcellular localization determines that MxA has a broader antiviral activity compared to MxB [192]. MxA was shown to inhibit the influenza A virus (IAV), but MxB did not as MxB has an NLS targeting the nuclear envelope. Replacing the N terminus of MxB with that of MxA redirects MxB to the cytoplasm and enables MxB to inhibit IAV infection, suggesting the significance of MxB localization in antiviral activity [192]. The unexpected subcellular localization of MxB to the centrosome can contribute to discovering the novel antiviral mechanism of MxB to pathogens.

The centrosome comprises two centrioles positioned at right angles and a matrix of proteins called pericentriolar material (PCM). PCM nucleates and anchors MTs, especially γTuRC, a tetrameric complex, including two molecules of γ-tubulin and one molecule of DGRP84 and DGRP91 [152]. In this study, we determined MxB colocalized with γ-tubulin, suggesting MxB localized to PCM in mitosis, but it is

unknown the interaction map of MxB to centrosome proteins, which would be vital in figuring out MxB's function at the centrosome. Meanwhile, in our MxB-RFP cell clones, in addition to MxB-RFP bands, we observed the band between MxB and MxB-RFP. It could result from alternative splicing, but we do not understand its impact on the cells.

Another objective of this project is to determine how MxB goes to the centrosome. Localization of proteins to specific compartments contributes to different regulatory processes. Many proteins harbor a nuclear localization sequence (NLS), a short amino acids sequence responsible for the nuclear import of these proteins. Cyclin A and Cyclin E have been shown to have a centrosome localization sequence (CLS) responsible for its localization to the centrosome [161, 162, 193, 194]. In addition, Cyclin E interacts and recruits DNA replication factor MCM5 to the centrosome to regulate centrosome duplication in a CLS-dependent manner [195]. Cyclin A recruits DNA replication factors MCM5 and Orc1 to regulate centrosome duplication in a CLS-dependent manner [162, 194]. Expression of wild-type CLS peptides was shown to localize at the centrosome and prevent endogenous cyclin A and cyclin E from targeting the centrosome, suggesting the significance of CLS in cell cycle regulation [161, 193]. To figure out how MxB goes to the centrosome, we aligned the protein sequence of MxB with CLS of Cylin A and E. A short protein sequence in the stalk domain of MxB shows high similarity with the CLS of Cyclin A, suggesting MxB may harbor a CLS targeting the centrosome. It would be interesting to determine if MxB harbors a CLS. In addition, figuring out the proteins that interact with MxB at the centrosome would help to decipher the function of MxB at the centrosome. We hypothesized that MxB maintains an association with specific nucleoporins to the centrosome. Still, our results showed that none of the NUPs tested targeting the centrosome in mitosis, including NUP358 and NUP58, both of which were shown to localize at the centrosome in mitosis [169, 188], suggesting MxB is recruited to the centrosome by other unknown cellular proteins. Notably, we did not observe a NUP358 signal in mitosis. Thus, further experiments are warranted to characterize the localization of nucleoporins in mitosis to coincide with the reports in the literature.

Our results showed that MxB KD led to chromosome misalignment. Chromosome alignment is a highly conserved step in mammalian cells [196]. Proper chromosome alignment promotes equal chromosome segregation [197, 198]. However, the mammalian cells can still complete cell division with chromosome misalignment [199]. Although chromosome misalignment was observed in MxB KD cells, it is unknown if chromosome misalignment affects chromosome segregation during metaphase. We observed MxB has no impact on the spindle structure. More studies are warranted to further determine how MxB regulates chromosome alignment at metaphase.

Cyclin A and cyclin E have CLS, and they are essential in the centrosome duplication and cell-cycle progression by recruiting DNA replication factors [161]. Marina et al. previously showed that MxB is a new regulator of the cell cycle in melanoma cells and MxB downregulation is associated with cell cycle arrest [186]. Our data further support the function of MxB in cell cycle regulation. However, it was still largely unknown how MxB contributes to the cell cycle regulation in HIV-1 infection. But there are some interesting clues. HIV-1 Vpr facilitates the nuclear import of HIV-1 PIC [200], and MxB inhibits the nuclear import of PIC. It would be interesting to determine the correlation between MxB, Vpr and the cell cycle, which may lead to the discovery of a new antiviral mechanism of MxB towards HIV-1

To determine the antiviral mechanism of MxB based on the phenotype that we observed, we hypothesized that MxB may interfere with microtubules to influence the trafficking of the viral particles because MxB is localized at the centrosome, which is the microtubule organization center (MTOC) from which the microtubule emerge (MTs) [201]. Apart from the nuclear envelope, MxB is localized in the cytoplasm based on live-cell imaging results in RFP-MxB knock-in line and transfected MxB-RFP HeLa cell. MxB may interact with MAPs to mediate MTs acetylation or tyrosination to restrict HIV-1 replication as MTs stabilization has been shown to facilitate the uncoating process [202, 203]. However, when we used HIV-1 to infect TZM-bl cells, the microtubule acetylation was not affected. It is possible that HIV-1-induced MTs

acetylation may be cell type-dependent. It would be interesting to further examine the correlation between the localization of MxB to the centrosome and the antiviral mechanism.

SUMMARY AND CONCLUSION

In summary, we took the CRISPR-Cas9 tool to generate MxB-RFP knock-in cell clones and found MxB is localized at the centrosome in mitosis in a cell-type dependent manner. Live-cell imaging showed that endogenous MxB begins to aggregate in the late prophase, likely when the centrosome also starts to form, diffuse into the cytoplasm in the early anaphase and return to the NPC when the nuclear envelope is re-assembled at the end of mitosis. By aligning MxB sequence with CLS of other proteins, we found MxB might harbor a centrosome localization sequence responsible for its localization to the centrosome in an ill-defined manner. MxB is recruited by other unknown centrosome factors instead of maintaining association with the nucleoporins. The spindle remains its bipolar dynamic steady-state structure in MxB KD cells, but MxB KD results in chromosome misalignment. It remains unknown whether MxB is essential in the proper segregation of the chromosome in anaphase. To investigate the potential antiviral mechanism associated with the special localization to the centrosome, we found MxB has no impact on microtubule acetylation, which HIV-1 takes advantage of to facilitate the trafficking of the viral particles. Collectively, our data is the first time to show MxB, an interferon-stimulated gene (ISG), is localized at the centrosome in mitosis and plays an important role in chromosome alignment by localizing to the centrosome during mitosis.

APPENDIX

Alignment of DNA sequence result with the template DNA was performed with NCBI blast https://blast.ncbi.nlm.nih.gov/Blast.cgi. The DNA template sequence (Top on each line) contains MxB left homology arm 1000 bp(1 to 1000), followed by tRFP sequence 711 bp (1001 to 1711) and MxB right homology arm 1000 bp (1712 to 2711). The bottom DNA sequence is the sequencing result from MCLAB. Due to the long DNA sequence, two promotors, SP6 and T7 were used to sequence in two sides. The black frame represents MxB left and right homology arms. The red frame represents part of the tRFP sequence.

1. HeLa MxB-RFP knockin clone G1. No 2 sequencing result. **Promotor SP6**

   Black frame, part of the MxB **left homology arm** (880 to 1000)

   Red frame, part of the tRFP sequence (1001 to 1419).

```
880   TTCCTGGCTGCTTCAAGAGCAGAGTGAGACCGCTACCAAGAGAAGAATCCTTAAGGAGAG   939
35    TTCCTGGCTGCTTCAAGAGCAGAGTGAGACCGCTACCAAGAGAAGAATCCTTAAGGAGAG   94
940   AATTTACCGGCTCACTCAGGCGCGACACGCACTCTGTCAATTCTCCAGCAAAGAGATCCA   999
95    AATTTACCGGCTCACTCAGGCGCGACACGCACTCTGTCAATTCTCCAGCAAAGAGATCCA   154
1000  CGTGTCTAAGGGCGAAGAGCTGATTAAGGAGAACATGCACATGAAGCTGTATATGGAGGG   1059
155   CGTGTCTAAGGGCGAAGAGCTGATTAAGGAGAACATGCACATGAAGCTGTATATGGAGGG   214
1060  CACCGTGAACAACCACCACTTCAAGTGCACATCCGAGGGCGAAGGCAAGCCCTACGAGGG   1119
215   CACCGTGAACAACCACCACTTCAAGTGCACATCCGAGGGCGAAGGCAAGCCCTACGAGGG   274
1120  CACCCAGACCATGAGAATCAAGGTGGTCGAGGGCGGCCCTCTCCCCTTCGCCTTCGACAT   1179
275   CACCCAGACCATGAGAATCAAGGTGGTCGAGGGCGGCCCTCTCCCCTTCGCCTTCGACAT   334
1180  CCTGGCTACCAGCTTCATGTACGGCAGCAGAACCTTCATCAACCACACCCAGGGCATCCC   1239
335   CCTGGCTACCAGCTTCATGTACGGCAGCAGAACCTTCATCAACCACACCCAGGGCATCCC   394
1240  CGACTTCTTTAAGCAGTCCTTCCCTGAGGGCTTCACATGGGAGAGAGTCACCACATACGA   1299
395   CGACTTCTTTAAGCAGTCCTTCCCTGAGGGCTTCACATGGGAGAGAGTCACCACATACGA   454
1300  AGACGGGGGCGTGCTGACCGCTACCCAGGACACCAGCCTCCAGGACGGCTGCCTCATCTA   1359
455   AGACGGGGGCGTGCTGACCGCTACCCAGGACACCAGCCTCCAGGACGGCTGCCTCATCTA   514
1360  CAACGTCAAGATCAGAGGGGTGAACTTCCCATCCAACGGCCCTGTGATGCAGAAGAAAAC   1419
515   CAACGTCAAGATCAGAGGGGTGAACTTCCCATCCAACGGCCCTGTGATGCAGAAGAAAAC   574
```

2. HeLa MxB-RFP knockin clone G1. No 2 sequencing result. **Promotor T7**

   Red frame, part of the tRFP sequence (1300 to 1711).

   Black frame, part of the MxB **right homology arm** (1712 to 1830)

3. WM115 MxB-RFP knockin clone G1. No 8 sequencing result. **Promotor SP6**

   Black frame, part of the MxB **left homology arm** (879 to 1000)

   Red frame, part of the tRFP sequence (1001 to 1418).

4. WM115 MxB-RFP knockin clone G1. No 8 sequencing result. **Promotor T7**

   Red frame, part of the tRFP sequence (1294 to 1711).

   Black frame, part of the MxB **right homology arm** (1712 to 1830)

BIBLIOGRAPHY

1. Gottlieb, M.S., et al., *Pneumocystis carinii pneumonia and mucosal candidiasis in previously healthy homosexual men: evidence of a new acquired cellular immunodeficiency.* New England Journal of Medicine, 1981. **305**(24): p. 1425-1431.
2. *Kaposi's sarcoma and Pneumocystis pneumonia among homosexual men--New York City and California.* MMWR Morb Mortal Wkly Rep, 1981. **30**(25): p. 305-8.
3. *Update on acquired immune deficiency syndrome (AIDS) among patients with hemophilia A.* MMWR Morb Mortal Wkly Rep, 1982. **31**(48): p. 644-6, 652.
4. *Possible transfusion-associated acquired immune deficiency syndrome (AIDS) - California.* MMWR Morb Mortal Wkly Rep, 1982. **31**(48): p. 652-4.
5. Barré-Sinoussi, F., et al., *Isolation of a T-lymphotropic retrovirus from a patient at risk for acquired immune deficiency syndrome (AIDS).* 1983. **220**(4599): p. 868-871.
6. Levy, J.A., et al., *Isolation of lymphocytopathic retroviruses from San Francisco patients with AIDS.* Science, 1984. **225**(4664): p. 840-842.
7. German Advisory Committee Blood, S.A.o.P.T.b.B., *Human Immunodeficiency Virus (HIV).* Transfusion medicine and hemotherapy : offizielles Organ der Deutschen Gesellschaft fur Transfusionsmedizin und Immunhamatologie, 2016. **43**(3): p. 203-222.
8. Sharp, P.M. and B.H. Hahn, *Origins of HIV and the AIDS pandemic.* Cold Spring Harbor perspectives in medicine, 2011. **1**(1): p. a006841-a006841.
9. Gao, F., et al., *Human infection by genetically diverse SIV SM-related HIV-2 in West Africa.* Nature, 1992. **358**(6386): p. 495-499.
10. Hirsch, V.M., et al., *An African primate lentivirus (SIV sm closely related to HIV-2.* Nature, 1989. **339**(6223): p. 389-392.
11. Gao, F., et al., *Origin of HIV-1 in the chimpanzee Pan troglodytes troglodytes.* 1999. **397**(6718): p. 436-441.
12. Bailes, E., et al., *Hybrid origin of SIV in chimpanzees.* Science, 2003. **300**(5626): p. 1713-1713.
13. Peeters, M., et al., *Risk to human health from a plethora of simian immunodeficiency viruses in primate bushmeat.* Emerging infectious diseases, 2002. **8**(5): p. 451-457.
14. Désiré, N., et al., *Characterization update of HIV-1 M subtypes diversity and proposal for subtypes A and D sub-subtypes reclassification.* Retrovirology, 2018. **15**(1): p. 80.
15. Cohen, M.S., et al., *The spread, treatment, and prevention of HIV-1: evolution of a global pandemic.* The Journal of clinical investigation, 2008. **118**(4): p. 1244-1254.
16. Shaw, G.M. and E. Hunter, *HIV transmission.* Cold Spring Harb Perspect Med, 2012. **2**(11).
17. Dosekun, O. and J. Fox, *An overview of the relative risks of different sexual behaviours on HIV transmission.* Curr Opin HIV AIDS, 2010. **5**(4): p. 291-7.
18. Connor, E.M., et al., *Reduction of maternal-infant transmission of human immunodeficiency virus type 1 with zidovudine treatment.* 1994. **331**(18): p. 1173-1180.
19. Ruff, A.J., et al., *Breast-feeding and maternal-infant transmission of human immunodeficiency virus type 1.* J Pediatr, 1992. **121**(2): p. 325-9.
20. Ioannidis, J.P.A., et al., *Perinatal transmission of human immunodeficiency virus type 1 by pregnant women with RNA virus loads< 1000 copies/ml.* The Journal of infectious diseases,

2001. **183**(4): p. 539-545.
21. Baggaley, R.F., et al., *Risk of HIV-1 transmission for parenteral exposure and blood transfusion: a systematic review and meta-analysis.* Aids, 2006. **20**(6): p. 805-812.
22. Des Jarlais, D.C., et al., *30 Years on Selected Issues in the Prevention of HIV among Persons Who Inject Drugs.* Advances in preventive medicine, 2013. **2013**: p. 346372-346372.
23. Daar, E.S., C.D. Pilcher, and F.M. Hecht, *Clinical presentation and diagnosis of primary HIV-1 infection.* Current Opinion in HIV and AIDS, 2008. **3**(1): p. 10-15.
24. Schacker, T., et al., *Clinical and epidemiologic features of primary HIV infection.* Ann Intern Med, 1996. **125**(4): p. 257-64.
25. Parekh, B.S., et al., *Diagnosis of Human Immunodeficiency Virus Infection.* Clinical microbiology reviews, 2018. **32**(1): p. e00064-18.
26. Cihlar, T. and M. Fordyce, *Current status and prospects of HIV treatment.* Current opinion in virology, 2016. **18**: p. 50-56.
27. Fischl, M.A., et al., *The efficacy of azidothymidine (AZT) in the treatment of patients with AIDS and AIDS-related complex.* New England Journal of Medicine, 1987. **317**(4): p. 185-191.
28. Sarafianos, S.G., et al., *Lamivudine (3TC) resistance in HIV-1 reverse transcriptase involves steric hindrance with beta-branched amino acids.* Proceedings of the National Academy of Sciences of the United States of America, 1999. **96**(18): p. 10027-10032.
29. Gomez, M., et al., *A retrospective analysis of weight changes in HIV-positive patients switching from a tenofovir disoproxil fumarate (TDF)- to a tenofovir alafenamide fumarate (TAF)-containing treatment regimen in one German university hospital in 2015–2017.* Infection, 2019. **47**(1): p. 95-102.
30. Côté, B., et al., *Discovery of MK-1439, an orally bioavailable non-nucleoside reverse transcriptase inhibitor potent against a wide range of resistant mutant HIV viruses.* Bioorganic & medicinal chemistry letters, 2014. **24**(3): p. 917-922.
31. Domingo, P. and E. Ribera, *Data on rilpivirine in treatment-naïve patients. Lessons from ECHO, THRIVE and STaR.* Enfermedades infecciosas y microbiologia clinica, 2013. **31**: p. 20-29.
32. Schiller, D.S. and M. Youssef-Bessler, *Etravirine: a second-generation nonnucleoside reverse transcriptase inhibitor (NNRTI) active against NNRTI-resistant strains of HIV.* Clinical therapeutics, 2009. **31**(4): p. 692-704.
33. Wire, M.B., M.J. Shelton, and S. Studenberg, *Fosamprenavir.* Clinical pharmacokinetics, 2006. **45**(2): p. 137-168.
34. Ghosh, A.K., Z.L. Dawson, and H. Mitsuya, *Darunavir, a conceptually new HIV-1 protease inhibitor for the treatment of drug-resistant HIV.* Bioorganic & medicinal chemistry, 2007. **15**(24): p. 7576-7580.
35. Colonno, R.J., et al., *Activities of atazanavir (BMS-232632) against a large panel of human immunodeficiency virus type 1 clinical isolates resistant to one or more approved protease inhibitors.* Antimicrobial agents and chemotherapy, 2003. **47**(4): p. 1324-1333.
36. Matthews, T., et al., *Enfuvirtide: the first therapy to inhibit the entry of HIV-1 into host CD4 lymphocytes.* Nature reviews Drug discovery, 2004. **3**(3): p. 215-225.
37. Veljkovic, N., et al., *Preclinical discovery and development of maraviroc for the treatment*

of HIV. Expert opinion on drug discovery, 2015. **10**(6): p. 671-684.
38. Lennox, J.L., et al., *Safety and efficacy of raltegravir-based versus efavirenz-based combination therapy in treatment-naive patients with HIV-1 infection: a multicentre, double-blind randomised controlled trial.* The Lancet, 2009. **374**(9692): p. 796-806.
39. Hazuda, D.J., et al., *Inhibitors of strand transfer that prevent integration and inhibit HIV-1 replication in cells.* Science, 2000. **287**(5453): p. 646-650.
40. Muesing, M.A., et al., *Nucleic acid structure and expression of the human AIDS/lymphadenopathy retrovirus.* Nature, 1985. **313**(6002): p. 450-458.
41. Gallo, R., et al., *HIV/HTLV gene nomenclature.* Nature, 1988. **333**(6173): p. 504-504.
42. Wu, H., P.D. Kwong, and W.A. Hendrickson, *Dimeric association and segmental variability in the structure of human CD4.* Nature, 1997. **387**(6632): p. 527-530.
43. Lu, M., S.C. Blacklow, and P.S. Kim, *A trimeric structural domain of the HIV-1 transmembrane glycoprotein.* Nature structural biology, 1995. **2**(12): p. 1075-1082.
44. Shcherbatova, O., et al., *Modeling of the HIV-1 life cycle in productively infected cells to predict novel therapeutic targets.* Pathogens, 2020. **9**(4): p. 255.
45. Pancera, M., et al., *Structure of HIV-1 gp120 with gp41-interactive region reveals layered envelope architecture and basis of conformational mobility.* Proc Natl Acad Sci U S A, 2010. **107**(3): p. 1166-71.
46. Pd, K., *Wyatt R. Robinson J. Sweet RW. Sodroski J. Hendrickson WA. Structure of an HIV gp120 envelope glycoprotein in complex with the CD4 receptor and a neutralizing human antibody.* Nature, 1998. **393**(6686): p. 648-659.
47. Starcich, B.R., et al., *Identification and characterization of conserved and variable regions in the envelope gene of HTLV-III/LAV, the retrovirus of AIDS.* Cell, 1986. **45**(5): p. 637-648.
48. Kozak, S.L., et al., *CD4, CXCR-4, and CCR-5 dependencies for infections by primary patient and laboratory-adapted isolates of human immunodeficiency virus type 1.* Journal of virology, 1997. **71**(2): p. 873-882.
49. Ambrose, Z. and C. Aiken, *HIV-1 uncoating: connection to nuclear entry and regulation by host proteins.* Virology, 2014. **454-455**: p. 371-9.
50. Tian, L., et al., *Structure of HIV-1 reverse transcriptase cleaving RNA in an RNA/DNA hybrid.* Proceedings of the National Academy of Sciences, 2018. **115**(3): p. 507-512.
51. Dharan, A., et al., *Nuclear pore blockade reveals that HIV-1 completes reverse transcription and uncoating in the nucleus.* Nature Microbiology, 2020. **5**(9): p. 1088-1095.
52. Fujiwara, T. and R. Craigie, *Integration of mini-retroviral DNA: a cell-free reaction for biochemical analysis of retroviral integration.* Proceedings of the National Academy of Sciences, 1989. **86**(9): p. 3065-3069.
53. Temin, H.M., *The DNA provirus hypothesis.* Science, 1976. **192**(4244): p. 1075-1080.
54. Tahirov, T.H., et al., *Crystal structure of HIV-1 Tat complexed with human P-TEFb.* Nature, 2010. **465**(7299): p. 747-751.
55. Borg, K.T., J.P. Favaro, and S.J. Arrigo, *Involvement of human immunodeficiency virus type-1 splice sites in the cytoplasmic accumulation of viral RNA.* Virology, 1997. **236**(1): p. 95-103.
56. Watts, J.M., et al., *Architecture and secondary structure of an entire HIV-1 RNA genome.*

Nature, 2009. **460**(7256): p. 711-716.
57. Fernandes, J., B. Jayaraman, and A. Frankel, *The HIV-1 Rev response element: an RNA scaffold that directs the cooperative assembly of a homo-oligomeric ribonucleoprotein complex.* RNA Biol, 2012. **9**(1): p. 6-11.
58. Swanson, C.M., N.M. Sherer, and M.H. Malim, *SRp40 and SRp55 promote the translation of unspliced human immunodeficiency virus type 1 RNA.* Journal of virology, 2010. **84**(13): p. 6748-6759.
59. Earl, P.L., R.W. Doms, and B. Moss, *Oligomeric structure of the human immunodeficiency virus type 1 envelope glycoprotein.* Proceedings of the National Academy of Sciences, 1990. **87**(2): p. 648-652.
60. Hallenberger, S., et al., *Inhibition of furin-mediated cleavage activation of HIV-1 glycoprotein gpl60.* Nature, 1992. **360**(6402): p. 358-361.
61. Jacks, T., et al., *Characterization of ribosomal frameshifting in HIV-1 gag-pol expression.* Nature, 1988. **331**(6153): p. 280-283.
62. Liu, Y. and X. Zou, *Mathematical modeling and quantitative analysis of HIV-1 Gag trafficking and polymerization.* PLoS Comput Biol, 2017. **13**(9): p. e1005733.
63. Molle, D., et al., *Endosomal trafficking of HIV-1 gag and genomic RNAs regulates viral egress.* Journal of Biological Chemistry, 2009. **284**(29): p. 19727-19743.
64. Nydegger, S., et al., *HIV-1 egress is gated through late endosomal membranes*. Traffic, 2003. **4**(12): p. 902-910.
65. Ono, A. and E.O. Freed, *Plasma membrane rafts play a critical role in HIV-1 assembly and release.* Proceedings of the National Academy of Sciences, 2001. **98**(24): p. 13925-13930.
66. Sundquist, W.I. and H.G. Kräusslich, *HIV-1 assembly, budding, and maturation.* Cold Spring Harb Perspect Med, 2012. **2**(7): p. a006924.
67. Saad, J.S., et al., *Structural basis for targeting HIV-1 Gag proteins to the plasma membrane for virus assembly.* Proceedings of the National Academy of Sciences, 2006. **103**(30): p. 11364-11369.
68. Yu, X., et al., *Mutations in the cytoplasmic domain of human immunodeficiency virus type 1 transmembrane protein impair the incorporation of Env proteins into mature virions.* Journal of virology, 1993. **67**(1): p. 213-221.
69. Rustagi, A. and M. Gale Jr, *Innate antiviral immune signaling, viral evasion and modulation by HIV-1.* Journal of molecular biology, 2014. **426**(6): p. 1161-1177.
70. Altfeld, M. and M. Gale Jr, *Innate immunity against HIV-1 infection.* Nature immunology, 2015. **16**(6): p. 554-562.
71. Towers, Greg J. and M. Noursadeghi, *Interactions between HIV-1 and the Cell-Autonomous Innate Immune System.* Cell Host & Microbe, 2014. **16**(1): p. 10-18.
72. Malim, M.H. and M. Emerman, *HIV-1 Accessory Proteins—Ensuring Viral Survival in a Hostile Environment.* Cell Host & Microbe, 2008. **3**(6): p. 388-398.
73. van Montfoort, N., D. Olagnier, and J. Hiscott, *Unmasking immune sensing of retroviruses: interplay between innate sensors and host effectors.* Cytokine & growth factor reviews, 2014. **25**(6): p. 657-668.
74. Nazli, A., et al., *HIV-1 gp120 induces TLR2-and TLR4-mediated innate immune activation in human female genital epithelium.* The Journal of Immunology, 2013. **191**(8): p. 4246-

4258.
75. Heil, F., et al., *Species-specific recognition of single-stranded RNA via toll-like receptor 7 and 8.* Science, 2004. **303**(5663): p. 1526-1529.
76. Colisson, R., et al., *Free HTLV-1 induces TLR7-dependent innate immune response and TRAIL relocalization in killer plasmacytoid dendritic cells.* Blood, 2010. **115**(11): p. 2177-2185.
77. Meier, A., et al., *Sex differences in the Toll-like receptor–mediated response of plasmacytoid dendritic cells to HIV-1.* Nature medicine, 2009. **15**(8): p. 955-959.
78. Cervantes, J.L., et al., *TLR8: the forgotten relative revindicated.* Cellular & molecular immunology, 2012. **9**(6): p. 434-438.
79. Honda, K., et al., *Spatiotemporal regulation of MyD88-IRF-7 signalling for robust type-I interferon induction.* Nature, 2005. **434**(7036): p. 1035-40.
80. Solis, M., et al., *RIG-I-mediated antiviral signaling is inhibited in HIV-1 infection by a protease-mediated sequestration of RIG-I.* Journal of virology, 2011. **85**(3): p. 1224-1236.
81. Ning, S., J.S. Pagano, and G.N. Barber, *IRF7: activation, regulation, modification and function.* Genes & Immunity, 2011. **12**(6): p. 399-414.
82. Honda, K. and T. Taniguchi, *IRFs: master regulators of signalling by Toll-like receptors and cytosolic pattern-recognition receptors.* Nature Reviews Immunology, 2006. **6**(9): p. 644-658.
83. Rehwinkel, J. and M.U. Gack, *RIG-I-like receptors: their regulation and roles in RNA sensing.* Nature Reviews Immunology, 2020. **20**(9): p. 537-551.
84. Jakobsen, M.R., et al., *IFI16 senses DNA forms of the lentiviral replication cycle and controls HIV-1 replication.* Proceedings of the National Academy of Sciences, 2013. **110**(48): p. E4571-E4580.
85. Li, X.-D., et al., *Pivotal roles of cGAS-cGAMP signaling in antiviral defense and immune adjuvant effects.* Science, 2013. **341**(6152): p. 1390-1394.
86. Gao, D., et al., *Cyclic GMP-AMP synthase is an innate immune sensor of HIV and other retroviruses.* Science, 2013. **341**(6148): p. 903-906.
87. Thompson, M.R., et al., *Interferon γ-inducible protein (IFI) 16 transcriptionally regulates type i interferons and other interferon-stimulated genes and controls the interferon response to both DNA and RNA viruses.* Journal of Biological Chemistry, 2014. **289**(34): p. 23568-23581.
88. Ablasser, A., et al., *Cell intrinsic immunity spreads to bystander cells via the intercellular transfer of cGAMP.* Nature, 2013. **503**(7477): p. 530-534.
89. Stremlau, M., et al., *The cytoplasmic body component TRIM5α restricts HIV-1 infection in Old World monkeys.* Nature, 2004. **427**(6977): p. 848-853.
90. Grütter, M.G. and J. Luban, *TRIM5 structure, HIV-1 capsid recognition, and innate immune signaling.* Current Opinion in Virology, 2012. **2**(2): p. 142-150.
91. Pertel, T., et al., *TRIM5 is an innate immune sensor for the retrovirus capsid lattice.* Nature, 2011. **472**(7343): p. 361-365.
92. Neil, S.J.D., T. Zang, and P.D. Bieniasz, *Tetherin inhibits retrovirus release and is antagonized by HIV-1 Vpu.* Nature, 2008. **451**(7177): p. 425-430.
93. Galão, Rui P., et al., *Innate Sensing of HIV-1 Assembly by Tetherin Induces NFκB-*

Dependent Proinflammatory Responses. Cell Host & Microbe, 2012. **12**(5): p. 633-644.
94. Isaacs, A., J. Lindenmann, and R.C. Valentine, *Virus interference. II. Some properties of interferon.* Proceedings of the Royal Society of London. Series B-Biological Sciences, 1957. **147**(927): p. 268-273.
95. He, B., J.T. Tran, and D.J. Sanchez, *Manipulation of Type I Interferon Signaling by HIV and AIDS-Associated Viruses*. Journal of immunology research, 2019. **2019**: p. 8685312-8685312.
96. Ivashkiv, L.B. and L.T. Donlin, *Regulation of type I interferon responses.* Nature Reviews Immunology, 2014. **14**(1): p. 36-49.
97. Gargan, S., et al., *HIV-1 promotes the degradation of components of the type 1 IFN JAK/STAT pathway and blocks anti-viral ISG induction.* EBioMedicine, 2018. **30**: p. 203-216.
98. Nguyen, N.V., J.T. Tran, and D.J. Sanchez, *HIV blocks Type I IFN signaling through disruption of STAT1 phosphorylation.* Innate immunity, 2018. **24**(8): p. 490-500.
99. Mlcochova, P., et al., *Immune evasion activities of accessory proteins Vpu, Nef and Vif are conserved in acute and chronic HIV-1 infection.* Virology, 2015. **482**: p. 72-8.
100. Harman, A.N., et al., *HIV blocks interferon induction in human dendritic cells and macrophages by dysregulation of TBK1.* Journal of virology, 2015. **89**(13): p. 6575-6584.
101. Sheehy, A.M., et al., *Isolation of a human gene that inhibits HIV-1 infection and is suppressed by the viral Vif protein.* Nature, 2002. **418**(6898): p. 646-650.
102. Jarmuz, A., et al., *An anthropoid-specific locus of orphan C to U RNA-editing enzymes on chromosome 22.* Genomics, 2002. **79**(3): p. 285-296.
103. Zheng, Y.-H., K.-T. Jeang, and K. Tokunaga, *Host restriction factors in retroviral infection: promises in virus-host interaction.* Retrovirology, 2012. **9**(1): p. 1-28.
104. Koning, F.A., et al., *Defining APOBEC3 expression patterns in human tissues and hematopoietic cell subsets.* Journal of virology, 2009. **83**(18): p. 9474-9485.
105. Galão, R.P., et al., *Innate sensing of HIV-1 assembly by Tetherin induces NFκB-dependent proinflammatory responses.* Cell host & microbe, 2012. **12**(5): p. 633-644.
106. Hrecka, K., et al., *Vpx relieves inhibition of HIV-1 infection of macrophages mediated by the SAMHD1 protein.* Nature, 2011. **474**(7353): p. 658-661.
107. Lu, J., et al., *The IFITM proteins inhibit HIV-1 infection.* Journal of virology, 2011. **85**(5): p. 2126-2137.
108. Lee, W.-Y.J., et al., *IFITM proteins inhibit HIV-1 protein synthesis.* Scientific reports, 2018. **8**(1): p. 1-15.
109. Ficarelli, M., et al., *KHNYN is essential for the zinc finger antiviral protein (ZAP) to restrict HIV-1 containing clustered CpG dinucleotides.* Elife, 2019. **8**: p. e46767.
110. Zhu, Y., et al., *Zinc-finger antiviral protein inhibits HIV-1 infection by selectively targeting multiply spliced viral mRNAs for degradation.* Proceedings of the National Academy of Sciences, 2011. **108**(38): p. 15834-15839.
111. Li, M., et al., *Codon-usage-based inhibition of HIV protein synthesis by human schlafen 11.* Nature, 2012. **491**(7422): p. 125-128.
112. Usami, Y., Y. Wu, and H.G. Göttlinger, *SERINC3 and SERINC5 restrict HIV-1 infectivity and are counteracted by Nef.* Nature, 2015. **526**(7572): p. 218-223.

113. Liu, Y., et al., *Proteomic profiling of HIV-1 infection of human CD4+ T cells identifies PSGL-1 as an HIV restriction factor.* Nature microbiology, 2019. **4**(5): p. 813-825.
114. Haller, O., et al., *The discovery of the antiviral resistance gene Mx: a story of great ideas, great failures, and some success.* Annual review of virology, 2018. **5**: p. 33-51.
115. Lindenmann, J., *Inheritance of resistance to influenza virus in mice.* Proceedings of the Society for Experimental Biology and Medicine, 1964. **116**(2): p. 506-509.
116. Lindenmann, J., C.A. Lane, and D. Hobson, *The resistance of A2G mice to myxoviruses.* The Journal of Immunology, 1963. **90**(6): p. 942-951.
117. Lindenmann, J. and P.A. Klein, *Further studies on the resistance of mice to myxoviruses.* Archiv für die gesamte Virusforschung, 1966. **19**(1): p. 1-12.
118. Staeheli, P., et al., *Interferon-regulated influenza virus resistance gene Mx is localized on mouse chromosome 16.* Journal of virology, 1986. **58**(3): p. 967-969.
119. Reeves, R.H., et al., *Genetic mapping of the Mx influenza virus resistance gene within the region of mouse chromosome 16 that is homologous to human chromosome 21.* Journal of virology, 1988. **62**(11): p. 4372-4375.
120. Staeheli, P., et al., *Influenza virus-susceptible mice carry Mx genes with a large deletion or a nonsense mutation.* Molecular and cellular biology, 1988. **8**(10): p. 4518-4523.
121. Staeheli, P. and J.G. Sutcliffe, *Identification of a second interferon-regulated murine Mx gene.* Molecular and cellular biology, 1988. **8**(10): p. 4524-4528.
122. Aebi, M., et al., *cDNA structures and regulation of two interferon-induced human Mx proteins.* Molecular and cellular biology, 1989. **9**(11): p. 5062-5072.
123. Fribourgh, J.L., et al., *Structural insight into HIV-1 restriction by MxB.* Cell host & microbe, 2014. **16**(5): p. 627-638.
124. Gao, S., et al., *Structural basis of oligomerization in the stalk region of dynamin-like MxA.* Nature, 2010. **465**(7297): p. 502-506.
125. Haller, O. and G. Kochs, *Human MxA protein: an interferon-induced dynamin-like GTPase with broad antiviral activity.* Journal of Interferon & Cytokine Research, 2011. **31**(1): p. 79-87.
126. Kane, M., et al., *MX2 is an interferon-induced inhibitor of HIV-1 infection.* Nature, 2013. **502**(7472): p. 563-566.
127. Goujon, C., et al., *Human MX2 is an interferon-induced post-entry inhibitor of HIV-1 infection.* Nature, 2013. **502**(7472): p. 559-562.
128. Liu, Z., et al., *The interferon-inducible MxB protein inhibits HIV-1 infection.* Cell host & microbe, 2013. **14**(4): p. 398-410.
129. Crameri, M., et al., *MxB is an interferon-induced restriction factor of human herpesviruses.* Nature communications, 2018. **9**(1): p. 1-16.
130. Yi, D.-R., et al., *Human MxB inhibits the replication of hepatitis C virus.* Journal of virology, 2019. **93**(1): p. e01285-18.
131. Gao, S., et al., *Structure of myxovirus resistance protein a reveals intra-and intermolecular domain interactions required for the antiviral function.* Immunity, 2011. **35**(4): p. 514-525.
132. Reichelt, M., et al., *Missorting of LaCrosse virus nucleocapsid protein by the interferon-induced MxA GTPase involves smooth ER membranes.* Traffic, 2004. **5**(10): p. 772-784.
133. Melén, K., et al., *Human MxB protein, an interferon-α-inducible GTPase, contains a*

nuclear targeting signal and is localized in the heterochromatin region beneath the nuclear envelope. Journal of Biological Chemistry, 1996. **271**(38): p. 23478-23486.

134. King, M.C., G. Raposo, and M.A. Lemmon, *Inhibition of nuclear import and cell-cycle progression by mutated forms of the dynamin-like GTPase MxB.* Proceedings of the National Academy of Sciences, 2004. **101**(24): p. 8957-8962.
135. Liu, S.-Y., et al., *Systematic identification of type I and type II interferon-induced antiviral factors*. Proceedings of the National Academy of Sciences, 2012. **109**(11): p. 4239-4244.
136. Fricke, T., et al., *MxB binds to the HIV-1 core and prevents the uncoating process of HIV-1.* Retrovirology, 2014. **11**(1): p. 1-14.
137. Smaga, S.S., et al., *MxB restricts HIV-1 by targeting the tri-hexamer interface of the viral capsid.* Structure, 2019. **27**(8): p. 1234-1245.
138. Scholey, J.M., I. Brust-Mascher, and A. Mogilner, *Cell division.* Nature, 2003. **422**(6933): p. 746-752.
139. Israels, E.D. and L.G. Israels, *The cell cycle.* The oncologist, 2000. **5**(6): p. 510-513.
140. Lim, S. and P. Kaldis, *Cdks, cyclins and CKIs: roles beyond cell cycle regulation.* Development, 2013. **140**(15): p. 3079-3093.
141. Schafer, K.A., *The cell cycle: a review.* Veterinary pathology, 1998. **35**(6): p. 461-478.
142. Güttinger, S., E. Laurell, and U. Kutay, *Orchestrating nuclear envelope disassembly and reassembly during mitosis.* Nature reviews Molecular cell biology, 2009. **10**(3): p. 178-191.
143. Tame, M.A., et al., *Chromosome misalignments induce spindle-positioning defects.* EMBO Rep, 2016. **17**(3): p. 317-25.
144. Nigg, E.A., *Centrosome aberrations: cause or consequence of cancer progression?* Nature Reviews Cancer, 2002. **2**(11): p. 815-825.
145. Sluder, G. and J.J. Nordberg, *The good, the bad and the ugly: the practical consequences of centrosome amplification.* Current opinion in cell biology, 2004. **16**(1): p. 49-54.
146. Badano, J.L., T.M. Teslovich, and N. Katsanis, *The centrosome in human genetic disease.* Nature Reviews Genetics, 2005. **6**(3): p. 194-205.
147. Woodruff, J.B., O. Wueseke, and A.A. Hyman, *Pericentriolar material structure and dynamics.* Philos Trans R Soc Lond B Biol Sci, 2014. **369**(1650).
148. Paintrand, M., et al., *Centrosome organization and centriole architecture: their sensitivity to divalent cations.* Journal of structural biology, 1992. **108**(2): p. 107-128.
149. Mennella, V., et al., *Amorphous no more: subdiffraction view of the pericentriolar material architecture.* Trends in cell biology, 2014. **24**(3): p. 188-197.
150. Bornens, M., *The centrosome in cells and organisms.* Science, 2012. **335**(6067): p. 422-426.
151. Loncarek, J., et al., *Control of daughter centriole formation by the pericentriolar material.* Nature cell biology, 2008. **10**(3): p. 322-328.
152. Zheng, Y., et al., *Nucleation of microtubule assembly by a γ-tubulin-containing ring complex.* Nature, 1995. **378**(6557): p. 578-583.
153. Wilkinson, C.J., et al., *A proteomic approach to the inventory of the human centrosome.* Centrosomes in development and disease, 2004: p. 123-142.
154. Bettencourt-Dias, M. and D.M. Glover, *Centrosome biogenesis and function: centrosomics brings new understanding.* Nature reviews Molecular cell biology, 2007. **8**(6): p. 451-463.

155. Doxsey, S., W. Zimmerman, and K. Mikule, *Centrosome control of the cell cycle.* Trends in cell biology, 2005. **15**(6): p. 303-311.
156. Kim, Y.H., et al., *Acentriolar microtubule organization centers and Ran-mediated microtubule formation pathways are both required in porcine oocytes.* Mol Reprod Dev, 2019. **86**(8): p. 972-983.
157. Khodjakov, A., et al., *De novo formation of centrosomes in vertebrate cells arrested during S phase.* The Journal of cell biology, 2002. **158**(7): p. 1171-1181.
158. Johnson, D.G. and C.L. Walker, *Cyclins and cell cycle checkpoints.* Annual review of pharmacology and toxicology, 1999. **39**.
159. Tyson, J.J., A. Csikasz-Nagy, and B. Novak, *The dynamics of cell cycle regulation.* Bioessays, 2002. **24**(12): p. 1095-1109.
160. Pascreau, G., M.E. Churchill, and J.L. Maller, *Centrosomal localization of cyclins E and A: structural similarities and functional differences.* Cell Cycle, 2011. **10**(2): p. 199-205.
161. Matsumoto, Y. and J.L. Maller, *A centrosomal localization signal in cyclin E required for Cdk2-independent S phase entry.* Science, 2004. **306**(5697): p. 885-888.
162. Ferguson, R.L., G. Pascreau, and J.L. Maller, *The cyclin A centrosomal localization sequence recruits MCM5 and Orc1 to regulate centrosome reduplication.* Journal of cell science, 2010. **123**(16): p. 2743-2749.
163. Wagner, N. and G. Krohne, *LEM-domain proteins: new insights into lamin-interacting proteins.* International review of cytology, 2007. **261**: p. 1-46.
164. Terasaki, M., et al., *A new model for nuclear envelope breakdown.* Molecular biology of the cell, 2001. **12**(2): p. 503-510.
165. Katsani, K.R., et al., *In vivo dynamics of Drosophila nuclear envelope components.* Molecular biology of the cell, 2008. **19**(9): p. 3652-3666.
166. Dultz, E., et al., *Systematic kinetic analysis of mitotic dis-and reassembly of the nuclear pore in living cells.* The Journal of cell biology, 2008. **180**(5): p. 857-865.
167. Blower, M.D., et al., *A Rae1-Containing Ribonucleoprotein Complex Is Required for Mitotic Spindle Assembly.* Cell, 2005. **121**(2): p. 223-234.
168. Orjalo, A.V., et al., *The Nup107-160 nucleoporin complex is required for correct bipolar spindle assembly.* Molecular biology of the cell, 2006. **17**(9): p. 3806-3818.
169. Hashizume, C., A. Kobayashi, and R.W. Wong, *Down-modulation of nucleoporin RanBP2/Nup358 impaired chromosomal alignment and induced mitotic catastrophe.* Cell death & disease, 2013. **4**(10): p. e854-e854.
170. Hazawa, M., et al., *Nucleoporin Nup58 localizes to centrosomes and mid-bodies during mitosis.* Cell division, 2019. **14**(1): p. 1-13.
171. Hashizume, C., et al., *Nucleoporin Nup62 maintains centrosome homeostasis.* Cell cycle (Georgetown, Tex.), 2013. **12**(24): p. 3804-3816.
172. Itoh, G., et al., *Nucleoporin Nup188 is required for chromosome alignment in mitosis.* Cancer science, 2013. **104**(7): p. 871-879.
173. Weis, K.J.C., *Regulating access to the genome: nucleocytoplasmic transport throughout the cell cycle.* 2003. **112**(4): p. 441-451.
174. Fahrenkrog, B., J. Köser, and U. Aebi, *The nuclear pore complex: a jack of all trades?* Trends in biochemical sciences, 2004. **29**(4): p. 175-182.

175. Fahrenkrog, B. and U. Aebi, *The nuclear pore complex: nucleocytoplasmic transport and beyond.* Nature Reviews Molecular Cell Biology, 2003. **4**(10): p. 757-766.
176. D'Angelo, M.A. and M.W. Hetzer, *Structure, dynamics and function of nuclear pore complexes.* Trends in cell biology, 2008. **18**(10): p. 456-466.
177. Hoelz, A., E.W. Debler, and G. Blobel, *The structure of the nuclear pore complex.* Annual review of biochemistry, 2011. **80**: p. 613-643.
178. Ibarra, A. and M.W. Hetzer, *Nuclear pore proteins and the control of genome functions.* Genes & development, 2015. **29**(4): p. 337-349.
179. Melén, K., et al., *Human MxB protein, an interferon-alpha-inducible GTPase, contains a nuclear targeting signal and is localized in the heterochromatin region beneath the nuclear envelope.* J Biol Chem, 1996. **271**(38): p. 23478-86.
180. Schulte, B., et al., *Restriction of HIV-1 Requires the N-Terminal Region of MxB as a Capsid-Binding Motif but Not as a Nuclear Localization Signal.* J Virol, 2015. **89**(16): p. 8599-610.
181. Cao, H., et al., *The anti-viral dynamin family member MxB participates in mitochondrial integrity.* Nature communications, 2020. **11**(1): p. 1-13.
182. Dicks, M.D.J., et al., *Multiple components of the nuclear pore complex interact with the amino-terminus of MX2 to facilitate HIV-1 restriction.* PLoS pathogens, 2018. **14**(11): p. e1007408.
183. Sabo, Y., et al., *HIV-1 induces the formation of stable microtubules to enhance early infection.* Cell Host Microbe, 2013. **14**(5): p. 535-46.
184. Wang, Z., et al., *HIV-1 resists MxB inhibition of viral Rev protein.* Emerging Microbes & Infections, 2020. **9**(1): p. 2030-2045.
185. Levy, D.N., et al., *Dynamics of HIV-1 recombination in its natural target cells.* Proceedings of the National Academy of Sciences, 2004. **101**(12): p. 4204-4209.
186. Juraleviciute, M., et al., *MX 2 is a novel regulator of cell cycle in melanoma cells.* Pigment cell & melanoma research, 2020. **33**(3): p. 446-457.
187. Guan, T., et al., *Structural analysis of the p62 complex, an assembly of O-linked glycoproteins that localizes near the central gated channel of the nuclear pore complex.* Molecular biology of the cell, 1995. **6**(11): p. 1591-1603.
188. Hashizume, C., et al., *Nucleoporin Nup62 maintains centrosome homeostasis.* Cell Cycle, 2013. **12**(24): p. 3804-3816.
189. Helmke, K.J., R. Heald, and J.D. Wilbur, *Interplay between spindle architecture and function.* International review of cell and molecular biology, 2013. **306**: p. 83-125.
190. Lai, C.-K., et al., *Association of hepatitis C virus replication complexes with microtubules and actin filaments is dependent on the interaction of NS3 and NS5A.* Journal of virology, 2008. **82**(17): p. 8838-8848.
191. Ploss, A. and J. Dubuisson, *New advances in the molecular biology of hepatitis C virus infection: towards the identification of new treatment targets.* Gut, 2012. **61**(Suppl 1): p. i25-i35.
192. Steiner, F. and J. Pavlovic, *Subcellular localization of MxB determines its antiviral potential against influenza A virus.* Journal of Virology, 2020. **94**(22): p. e00125-20.
193. Pascreau, G., M.E.A. Churchill, and J.L. Maller, *Centrosomal localization of cyclins E and A: structural similarities and functional differences.* Cell Cycle, 2011. **10**(2): p. 199-205.

194. Hemerly, A.S., et al., *Orc1 controls centriole and centrosome copy number in human cells.* Science, 2009. **323**(5915): p. 789-793.
195. Ferguson, R.L. and J.L. Maller, *Cyclin E-dependent localization of MCM5 regulates centrosome duplication.* Journal of cell science, 2008. **121**(19): p. 3224-3232.
196. Guo, Y., C. Kim, and Y. Mao, *New insights into the mechanism for chromosome alignment in metaphase.* International review of cell and molecular biology, 2013. **303**: p. 237-262.
197. Kops, G.J.P.L., A.T. Saurin, and P. Meraldi, *Finding the middle ground: how kinetochores power chromosome congression.* Cellular and molecular life sciences, 2010. **67**(13): p. 2145-2161.
198. Maiato, H., et al., *Mechanisms of chromosome congression during mitosis.* Biology, 2017. **6**(1): p. 13.
199. Fonseca, C.L., et al., *Mitotic chromosome alignment ensures mitotic fidelity by promoting interchromosomal compaction during anaphase*. Journal of Cell Biology, 2019. **218**(4): p. 1148-1163.
200. Aida, Y. and G. Matsuda, *Role of Vpr in HIV-1 nuclear import: therapeutic implications.* Current HIV research, 2009. **7**(2): p. 136-143.
201. Lüders, J. and T. Stearns, *Microtubule-organizing centres: a re-evaluation.* Nature Reviews Molecular Cell Biology, 2007. **8**(2): p. 161-167.
202. Sabo, Y., et al., *HIV-1 induces the formation of stable microtubules to enhance early infection.* Cell host & microbe, 2013. **14**(5): p. 535-546.
203. Dharan, A. and E.M. Campbell, *Role of microtubules and microtubule-associated proteins in HIV-1 infection.* Journal of virology, 2018. **92**(16): p. e00085-18.